QCD

Jan M. Pawlowski[1] and Tilman Plehn[1]
[1] *Institut für Theoretische Physik, Universität Heidelberg*

CONTENTS

I. Basics 2
A. Yang-Mills theory 2
1. Classical action 2
B. QCD 6
1. Classical action of the matter sector 6
2. Generating functional of QCD and perturbation theory 6

II. Divergences 8
A. Ultraviolet divergences 8
1. Counter terms 8
2. Running coupling 11
3. Resumming scaling logarithms 15
B. Infrared divergences 18
1. Single jet radiation 18
2. Parton splitting 19

III. Strong chiral symmetry breaking 23
A. Spontaneous symmetry breaking and the Goldstone theorem 24
B. Spontaneous symmetry breaking, quantum fluctuations and masses* 25
C. Little reminder on the Higgs mechanism 27
D. Low energy effective theories of QCD 29
E. Strong chiral symmetry breaking and quark-hadron effective theories 33
F. Chiral symmetry breaking in QCD 37
G. Low energy quantum fluctuations 38
1. Quark quantum fluctuations 38
2. Mesonic quantum fluctuations 41
3. RG equation for the effective potential * 43
4. EFT couplings and QCD 44

IV. Confinement in lattice gauge theory * 46
A. Scalar fields on the lattice 46
B. Non-Abelian gauge fields on the lattice 49
C. The Wegner-Wilson loop & the static quark potential 51
D. Continuum limit of lattice Yang-Mills theory 54

V. Parton densities 56
A. DGLAP equation 57
B. Solving the DGLAP equation 62
C. Resumming collinear logarithms 64

VI. Jet radiation 67
A. Jet ratios 67
B. Ordered emission 68

References 72

I. BASICS

The theory of strong interactions, quantum chromodynamics (QCD), has been developed on the basis of scattering experiments that showed an internal $SU(3)$-symmetry and related charges much the same way quantum-electrodynamics (QED) shows the $U(1)$-symmetry related to the electric charge. The corresponding gauge theory, $SU(3)$ Yang-Mills theory, is non-Abelian and hence self-interacting, i.e. the (quantized) pure gauge theory is already non-trivial, in contrast to the $U(1)$-based QED.

A. Yang-Mills theory

1. *Classical action*

We start by constructing the pure gauge part or Yang-Mills part of QCD as an $SU(3)$ gauge theory, fixing our conventions and repeating the main features known from the QFT II lecture. The weak $SU(2)$-theory turns out to have the same qualitative features as QCD (asymptotic freedom and confinement), but is technically simpler. On the other hand, the $SU(2)$ gauge bosons in the Standard Model are massive, leading to a major modification of this theory. Instead, we will assume massless gauge bosons throughout this lecture. As for QED, the classical action of QCD can be derived from the gauge-invariant (minimal) extension of the action of a free spin-one particle. The requirement of invariance of physics under local $SU(N_c)$ or color rotations with $\mathcal{U} \in SU(N_c)$, combined with a minimal coupling, leads us from partial to covariant derivatives,

$$\partial_\mu \to D_\mu(A) = \partial_\mu - i\, g\, A_\mu \,. \tag{I.1}$$

The gauge field A_μ in the adjoint representation is Lie-algebra–valued,

$$A_\mu = A_\mu^a\, t^a \,, \qquad \text{with} \qquad a = 1, ..., N_c^2 - 1 \,. \tag{I.2}$$

The matrices t^a are the generators of $SU(N_c)$. In physical QCD the gauge group has eight generators, $a = 1, ..., 8$, the Gell-Mann matrices. They are defined through

$$[t^a, t^b] = i\, f^{abc} t^c \,, \qquad \text{tr}_{\rm f}(t^a t^b) = \frac{1}{2}\delta^{ab} \,, \tag{I.3}$$

where the coefficients f^{abc} are the structure constants of the Lie algebra. and $\text{tr}_{\rm f}$ is the trace in the fundamental representation. The covariant derivative (I.1) does not carry any indices. In the adjoint representation it links to $SU(N_c)$ indices and reads

$$D_\mu^{ab}(A) = \partial_\mu \delta^{ab} - g\, f^{abc} A_\mu^c \,. \qquad \text{with} \qquad (t^c_{\rm ad})^{ab} = -i\, f^{abc}. \tag{I.4}$$

The covariant derivative D_μ with its two color indices then has to transform as a tensor under gauge transformations,

$$D_\mu(A) \to D_\mu(A^{\mathcal{U}}) = \mathcal{U}\, D_\mu\, \mathcal{U}^\dagger \,, \qquad \text{with} \qquad \mathcal{U} = e^{i\omega} \in SU(N_c) \,, \tag{I.5}$$

where $\omega \in su(N_c)$ is the corresponding Lie algebra element. The covariance of D under gauge transformations in (I.5) implies

$$A_\mu \to A_\mu^{\mathcal{U}} = \frac{i}{g} U\, (D_\mu U^\dagger) = \mathcal{U}\, A_\mu\, \mathcal{U}^\dagger + \frac{i}{g} \mathcal{U}\, (\partial_\mu \mathcal{U}^\dagger) \,. \tag{I.6}$$

From the first term we confirm that in a non-Abelian gauge theory the gauge boson A_μ carries the corresponding color charge. There are various notations on the market leading to factors i and $-$ in the Lie algebra relations above. In the present lecture notes we have chosen hermitian generators which leads to the factor $+1/2$ for the trace in (I.3). It also entails real structure constants f^{abc} in the Lie-algebra in (I.3).

In analogy to QED the field strength tensor is defined through the commutator of covariant derivatives, it is the curvature tensor of the gauge theory. Based on the definitions in (I.1) and (I.3) we find

$$F_{\mu\nu} = \frac{i}{g}[D_\mu \,,\, D_\nu] = F_{\mu\nu}^a t^a \qquad \text{with} \qquad F_{\mu\nu}^a = \partial_\mu A_\nu^a - \partial_\nu A_\mu^a + g\, f^{abc} A_\mu^b\, A_\nu^c. \tag{I.7}$$

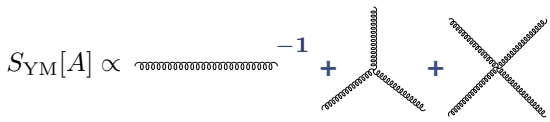

FIG. 1: Diagrammatic depiction of the Yang-Mills action.

Defined as in (I.7) the field strength $F_{\mu\nu}$ also transforms covariantly (as a tensor) under gauge transformations,

$$\begin{aligned} F_{\mu\nu}(A^{\mathcal{U}}) &= \frac{i}{g}\,[D_\mu(A^{\mathcal{U}}), D_\nu(A^{\mathcal{U}})] \\ &= \frac{i}{g}\,\mathcal{U}\,[D_\mu(A_\mu), D_\nu(A_\nu)]\,\mathcal{U}^\dagger = \mathcal{U}\,F_{\mu\nu}(A)\,\mathcal{U}^\dagger\,. \end{aligned} \tag{I.8}$$

This allows us to define a gauge-invariant Yang-Mills (YM) action,

$$S_{\rm YM}[A] = \frac{1}{2}\int_x \mathrm{tr_f}\;(F_{\mu\nu}\,F_{\mu\nu}) = \frac{1}{4}\int_x F^a_{\mu\nu}\,F^a_{\mu\nu}\,, \tag{I.9}$$

with $\int_x = \int d^dx$. Its gauge invariance follows from (I.8),

$$S_{\rm YM}[A^{\mathcal{U}}] = \frac{1}{2}\int_x \mathrm{tr_f}\;\left(\mathcal{U}\,F_{\mu\nu}(A)F_{\mu\nu}(A)\,\mathcal{U}^\dagger\right) = S_{\rm YM}[A]\,, \tag{I.10}$$

where the last equality holds due to cyclicity of the trace in color space. Clearly, the action (I.9) with the field strength (I.7) is a self-interacting theory with coupling constant g. It has a quadratic kinetic term and three-gluon and four-gluon vertices. This is illustrated diagrammatically as Figure 1.
This allows us to read off the Feynman rules for the purely gluonic vertices. The full Feynman rules of QCD in the general covariant gauge are summarized in **??**. As in QED we can identify color-electric and color-magnetic fields as the components in the field strength tensor,

$$\begin{aligned} E^a_i &= F^a_{0i} \\ B^a_i &= \frac{1}{2}\epsilon_{ijk}F^a_{jk}. \end{aligned} \tag{I.11}$$

In contrast to QED these color-electric and magnetic fields are no observables, they change under gauge transformations. Only $\mathrm{tr}\,\vec{E}^2, \mathrm{tr}\,\vec{B}^2$ are observables.

A Yang-Mills theory can most easily be quantized through the path integral. Naively, the generating functional of pure YM-theory would read

$$Z[J] = \int dA\;\exp\left(-S_{\rm YM}[A] + \int_x J^a_\mu\,A^a_\mu\right). \tag{I.12}$$

The fundamental problem is that it contains redundant integrations due to gauge invariance of the action, see I A 1. These redundant integrations are usually removed by introducing a gauge fixing condition

$$\mathcal{F}[A_{\rm gf}] = 0 \tag{I.13}$$

Commonly used gauge fixings are

$$\begin{aligned} \partial_\mu A_\mu &= 0\,, && \text{covariant or Lorenz gauge}\,, \\ \partial_i A_i &= 0\,, && \text{Coulomb gauge}\,, \\ n_\mu A_\mu &= 0\,, && \text{axial gauge}\,. \end{aligned} \tag{I.14}$$

The general covariant gauge has the technical advantage that it does not single out a space-time direction. This property reduces the possible tensor structure of correlation functions and hence simplifies computations. The Coulomb gauge and the axial gauge single out specific frames. At finite temperature (and density) this might be useful as the

temperature singles out the thermal rest frame. In that case the Coulomb gauge and the temporal or Weyl gauge ($n_\mu = \delta_{\mu 0}$) are used often.

Gauge fields that are connected by gauge transformations are physically equivalent, i.e. their actions agree. They lie in so-called gauge orbits, $\{A^{\mathcal{U}}, \mathcal{U} \in SU(N)\}$, and fixing a gauge is equivalent to choosing a representative of such an orbit $A \to A_{\rm gf}$, up to potential (Gribov) copies. The occurrence of Gribov copies and how to handle them is discussed in **??**. To keep things simple we ignore them for the time being and continue with the construction of the QCD Lagrangian.

The path integral measure $\mathrm{d}A$ introduced in I A 1 can be split into an integration over physically inequivalent configurations $A_{\rm gf}$ and the gauge transformations $\mathcal{U}$,

$$\mathrm{d}A = J\, \mathrm{d}A_{\rm gf}\, \mathrm{d}\mathcal{U} \tag{I.15}$$

In (I.15) J denotes the Jacobian of the transformation $A \to (A_{\rm gf}, \mathcal{U})$, and we include $\mathrm{d}\mathcal{U}$ as the Haar measure of the gauge group, see e.g. [1]. The coordinate transformation (I.15) and the computation of the Jacobian J are done using the Faddeev-Popov quantization, [2]. To separate the integral I A 1 into the two parts shown in (I.15) we insert a very convoluted unity into the path integral,

$$1 = \int \mathrm{d}\mathcal{U}\, \delta\left[\mathcal{F}[A^{\mathcal{U}}]\right]\, \Delta_{\mathcal{F}}[A] = \Delta_{\mathcal{F}}[A] \int \mathrm{d}\mathcal{U}\, \delta\left[\mathcal{F}[A^{\mathcal{U}}]\right] \quad \Leftrightarrow \quad \Delta_{\mathcal{F}}[A] = \left(\int \mathrm{d}\mathcal{U}\, \delta\left[\mathcal{F}[A^{\mathcal{U}}]\right]\right)^{-1}, \tag{I.16}$$

where $\Delta_{\mathcal{F}}[A]$ is gauge-invariant due to the property $\mathrm{d}(\mathcal{U}\mathcal{V}) = \mathrm{d}\mathcal{U}$ of the Haar measure. For the path integral this gives us

$$\int \mathrm{d}A\, e^{-S_{\rm YM}[A]} = \int \mathrm{d}A\, \mathrm{d}\mathcal{U}\, \delta\left[\mathcal{F}[A^{\mathcal{U}}]\right]\, \Delta_{\mathcal{F}}[A]\, e^{-S_{\rm YM}[A]}\,. \tag{I.17}$$

Let us now consider a general observable $\mathcal{O}$, like *e.g.* $\mathrm{tr}F^2(x)\,\mathrm{tr}F^2(0)$. Observables are necessarily gauge invariant and local. The expectation value of $\mathcal{O}$ is defined as

$$\langle\mathcal{O}\rangle = \frac{\int \mathrm{d}A\, \mathcal{O}[A]\, e^{-S_{\rm YM}[A]}}{\int \mathrm{d}A\, e^{-S_{\rm YM}[A]}} = \frac{\int \mathrm{d}A\, \mathrm{d}\mathcal{U}\, \delta\left[\mathcal{F}[A^{\mathcal{U}}]\right]\, \Delta_{\mathcal{F}}[A]\, \mathcal{O}[A]\, e^{-S_{\rm YM}[A]}}{\int \mathrm{d}A\, \mathrm{d}\mathcal{U}\, \delta\left[\mathcal{F}[A^{\mathcal{U}}]\right]\, \Delta_{\mathcal{F}}[A]\, e^{-S_{\rm YM}[A]}}\,, \tag{I.18}$$

where we have simply inserted (I.16) into the path integral. In (I.18) all terms are gauge invariant except for the δ-function. Hence we can absorb the $\mathcal{U}$-dependence via $A \to A^{\mathcal{U}^\dagger}$. Then the (infinite) integral over the Haar measure decouples in numerator and denominator, and we arrive at

$$\langle\mathcal{O}\rangle = \frac{\int \mathrm{d}A\, \delta\left[\mathcal{F}[A]\right]\, \Delta_{\mathcal{F}}[A]\, \mathcal{O}[A]\, e^{-S_{\rm YM}[A_{\rm gf}]}}{\int \mathrm{d}A\, \delta\left[\mathcal{F}[A]\right]\, \Delta_{\mathcal{F}}[A]\, e^{-S_{\rm YM}[A_{\rm gf}]}}\,. \tag{I.19}$$

To compute the Jacobian $\Delta_{\mathcal{F}}[A]$ we apply a coordinate transformation to the δ-distribution

$$\delta[\mathcal{F}[A^{\mathcal{U}}]] = \frac{\delta[\omega - \omega_1]}{|\det \frac{\delta\mathcal{F}}{\delta\omega}|} \equiv \frac{\delta[\omega - \omega_1]}{|\det \mathcal{M}_{\mathcal{F}}[A]|} \quad \text{with} \quad \mathcal{U} = e^{i\omega}\,, \tag{I.20}$$

combined with a gauge fixing condition in the form (I.13)

$$\mathcal{F}[A_{\rm gf} = A^{\mathcal{U}(\omega_1)}] = 0\,. \tag{I.21}$$

Using the definition (I.16) this leads to

$$\Delta_{\mathcal{F}}[A] = |\det \mathcal{M}_{\mathcal{F}}[A_{\rm gf}]| \qquad \text{with} \qquad \mathcal{M}_{\mathcal{F}}[A] = \left.\frac{\delta\mathcal{F}}{\delta\omega}\right|_{\omega=0}[A]\,. \tag{I.22}$$

Here $A_{\rm gf}$ is the solution with the minimal distance to $A = 0$. The inverse Jacobian $\det\mathcal{M}_{\mathcal{F}}$ of the ansatz (I.15) is called the Faddeev-Popov determinant. For its computation we consider an infinitesimal gauge transformation $\mathcal{U} = 1 + i\,g\,\omega$ where we have rescaled the transformation with the strong coupling g for convenience. Such a rescaling gives global factors of powers of $1/g$ that drop out in normalized expectation values. Then, the infinitesimal variation of the

covariant gauge $\partial_\mu A_\mu = 0$ follows as

$$\mathcal{F}[A^{\mathcal{U}}] = \partial_\mu A^{\mathcal{U}}_\mu = \partial_\mu A_\mu - \partial_\mu D_\mu \omega + O(\omega^2) \stackrel{!}{=} 0\,. \tag{I.23}$$

This gives us the Faddeev-Popov matrix

$$\mathcal{M}_{\mathcal{F}}[A] = -\frac{\delta \partial_\mu D_\mu \omega}{\delta \omega} = -\partial_\mu D_\mu \frac{\delta \omega}{\delta \omega} = -\partial_\mu D_\mu \mathbb{1}. \tag{I.24}$$

We assume that $-\partial^\mu D_\mu$ is a positive definite operator and we arrive at

$$\Delta_{\mathcal{F}}[A] = \det \mathcal{M}[A] = \det\left(-\partial_\mu D_\mu\right)\,. \tag{I.25}$$

A useful observation is that determinants can be represented by a Gaussian integral. In regular space such a Gaussian integral reads

$$\int_x e^{-\frac{1}{2}x^T M x} = \frac{(2\pi)^n}{\sqrt{\det M}}\,. \tag{I.26}$$

We want to use this relation to replace the Faddeev-Popov determinant (I.25) in the Lagrangian. It turns out that the usual form does not give a useful action or Lagrangian. However, we can instead use two anti-commuting Grassmann fields C and switch the sign in the exponent to

$$\det \mathcal{M}_{\mathcal{F}}[A] = \int \mathrm{d}c\,\mathrm{d}\bar{c}\,\exp\left\{\int d^dx\, d^dy\, \bar{c}^a(x)\mathcal{M}^{ab}_{\mathcal{F}}(x,y)c^b(y)\right\}\,. \tag{I.27}$$

Finally we slightly modify the gauge by introducing a Gaußian average over the gauges

$$\delta[\mathcal{F}[A^{\mathcal{U}}]] \to \int \mathrm{d}\mathcal{C}\,\delta[\mathcal{F}[A^{\mathcal{U}} - \mathcal{C}]]\exp\left\{-\frac{1}{2\xi}\int_x \mathcal{C}^a\mathcal{C}^a\right\}\,. \tag{I.28}$$

In summary, and restricting ourselves to the covariant gauge we then arrive at the generating functional for our Yang-Mills theory

$$Z[J_A, J_c, \bar{J}_c] = \int \mathrm{d}A\,\mathrm{d}c\,\mathrm{d}\bar{c}\,e^{-S_A[A,c,\bar{c}] + \int_x \left(J_A\cdot A + \bar{J}_c\cdot c - \bar{c}\cdot J_c\right)}\,. \tag{I.29}$$

The action including a general gauge fixing term and the Faddeev-Popov ghosts c^a is

$$S_A[A,c,\bar{c}] = \frac{1}{4}\int_x F^a_{\mu\nu}F^a_{\mu\nu} + \frac{1}{2\xi}\int_x \left(\partial_\mu A^a_\mu\right)^2 + \int_x \bar{c}^a \partial_\mu D^{ab}_\mu c^b\,, \tag{I.30}$$

where $\int_x = \int d^dx$ and the Landau gauge is achieved for $\xi = 0$. Note that the ghost action implies a negative dispersion for the ghost, related to the determinant of the positive operator $\mathcal{M}_{\mathcal{F}} = -\partial_\mu D_\mu$. However, this is a matter of convention, we might as well use a positive dispersion, the minus sign drops out for all correlation functions which do not involve ghosts, and only those are related to scattering amplitudes. The source term with all indices reads

$$\int_x \left(J_A\cdot A + \bar{J}_c\cdot c - \bar{c}\cdot J_c\right) \equiv \int_x \left(J^a_{A,\mu}A^a_\mu + \bar{J}^a_c c^a - \bar{c}^a J^a_c\right)\,. \tag{I.31}$$

The Feynman rules derived from (I.30) are summarized in **??**.

B. QCD

1. Classical action of the matter sector

After briefly sketching the gauge part of QCD we now add fermionic matter fields. As before we start with the classical action, now given by the Dirac action of a quark doublet,

$$S_{\rm Dirac}[\psi,\bar\psi,A] = \int_x \bar\psi \ (\not{D} + m_\psi - \gamma_0\,\mu) \ \psi\,, \tag{I.32}$$

where the Dirac matrices are defined through

$$\{\gamma_\mu\,,\,\gamma_\nu\} = 2\,\delta_{\mu\nu} \qquad \text{and} \quad \not{D} = \gamma_\mu D_\mu\,. \tag{I.33}$$

In (I.32), the fermions carry a Dirac index defining the 4-component spinor, gauge group indices in the fundamental representation of $SU(3)$, as well flavor indices. The latter we will ignore as long as we only talk about QCD and neglect the doublet nature of the matter fields in the Standard Model. The Dirac operator $\not{D}$ is diagonal in the flavor space as is the chemical potential term. The mass term depends on the current quark masses related to spontaneous symmetry breaking of the Higgs sector of the Standard Model. The up and down current quark masses are of the order $2-5$ MeV whereas the current quark mass of the strange quark is of the order 10^2 MeV. The other quark masses are of order $1-200$ GeV. In low energy QCD this has to be compared with the scale of strong chiral symmetry breaking $\Delta m \approx 300$ MeV. This mass scales are summarized in Table I.

Generation	first	second	third	Charge
Mass [MeV]	1.5-4	1150-1350	170×10^3	
Quark	u	c	t	$\frac{2}{3}$
Quark	d	s	b	$-\frac{1}{3}$
Mass [MeV]	4-8	80-130	$(4.1\text{-}4.4)\times10^3$	

TABLE I: Quark masses and charges. The scale of strong chiral symmetry breaking is $\Delta m \approx 300$ MeV as is $\Lambda_{\rm QCD}$. This entails that only $2+1$ flavours have to be considered for most applications to the phase diagram of QCD.

Evidently, for most applications of the QCD phase diagram we only have to consider the three lightest quark flavors, that is up, down and strange quark, to be dynamical. The current quark masses of up and down quarks are two order of magnitude smaller than all QCD infrared scales related to $\Lambda_{\rm QCD}$. Hence, the up and down quarks can be considered to be massless. This leads to the important observation that the physical masses of neutrons and protons — and hence the masses of the world around us — comes about from strong chiral symmetry breaking and has nothing to do with the Higgs sector.

In turn, the mass of the strange quark is of the order of $\Lambda_{\rm QCD}$ and has to be considered heavy for application in low energy QCD. The three heavier flavors, charm, bottom and top, are essentially static they do not contribute to the QCD dynamics relevant for its phase structure even though in particular the c-quark properties and bound states are much influenced by the infrared dynamics of QCD. In summary we will consider the $N_f = 2$ and $N_f = 2+1$ flavor cases for the phase structure of QCD, while for LHC physics all flavors are relevant.

2. Generating functional of QCD and perturbation theory

Again in analogy to the Yang-Mills action we describe the quantized theory using its generating functional. The full generating functional of QCD is the straightforward extension of the Yang-Mills version in I A 1. The quark fields are Grassmann fields because of their fermionic nature and we are led to the generating functional

$$Z[J] = \int {\rm d}\Phi\, e^{-S_{\rm QCD}[\Phi]+\int_x J\cdot\phi}\,, \tag{I.34}$$

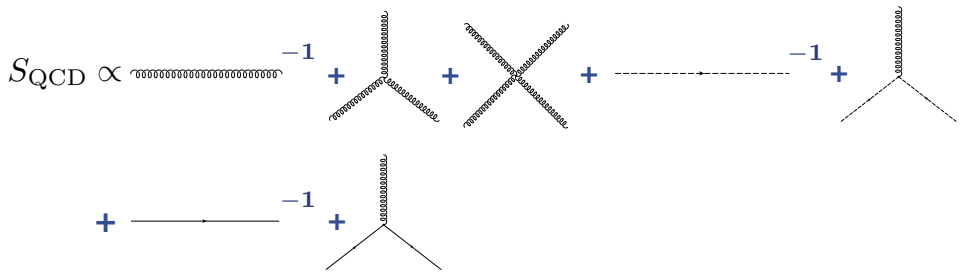

FIG. 2: Diagrammatic depiction of the gauge fixed QCD action.

As a notation we have introduced super-fields and super-currents

$$\Phi = (A, c, \bar{c}, \psi, \bar{\psi}) \qquad J = (J_A, J_c, \bar{J}_c, J_\psi, \bar{J}_\psi)$$
$$\mathrm{d}\Phi = \int \mathrm{d}A\, \mathrm{d}c\, \mathrm{d}\bar{c}\, \mathrm{d}\psi\, \mathrm{d}\bar{\psi} \qquad J \cdot \Phi = J_A \cdot A + \bar{J}_c \cdot c - \bar{c} \cdot J_c + \bar{J}_\psi \cdot \psi - \bar{\psi} \cdot J_\psi \,. \tag{I.35}$$

The gauge-fixed action $S_{\rm QCD}$ in (I.34) in the Landau gauge is given by

$$S_{\rm QCD}[\Phi] = \frac{1}{4}\int_x F^a_{\mu\nu} F^a_{\mu\nu} + \frac{1}{2\xi}\int_x \left(\partial_\mu A^a_\mu\right)^2 + \int_x \bar{c}^a \partial_\mu D^{ab}_\mu c^b + \int_x \bar{\psi}\left(\not{D} + m_\psi - \gamma_0\,\mu\right)\psi \,. \tag{I.36}$$

The action in (I.36) is illustrated diagrammatically in Figure 2. For physical observables the gauge dependence entering through the last two graphs in the first line, the ghost terms, is cancelled by the hidden gauge fixing dependence of the inverse gluon propagator. The Feynman rules are summarized in **??**.

The two equations (I.34), (I.36) define the fundamental quantum theory of strong interactions and have, apart from the mass matrix m_q of the quarks one input parameter, the strong coupling. In the full quantum theory we have a running coupling

$$\alpha_s(p) = \frac{g^2}{4\pi}\,, \tag{I.37}$$

where p is the relevant momentum/energy scale of a given process. The scale-dependence of $\alpha_s(p)$ is inflicted by quantum corrections. For perturbation theory being applicable the expansion parameter $\alpha_s/(4\pi)$ should be small. Moreover, the perturbative expansion is an asymptotic series (with convergence radius $\alpha_{s,\max} = 0$). The gluon self-coupling in QCD, depicted in Figure 2 leads to a running coupling which decreases with the momentum scale, i.e. ,

$$\beta_g = \frac{1}{2} p\partial_p \alpha_s = -\beta_0 \alpha^2 + O(\alpha_s^3) \qquad \text{with} \qquad \beta_0 = \frac{\alpha_s^2}{12\pi}\left(11N_c + 2N_f\right) . \tag{I.38}$$

Integrating the β-function (I.38) at one loop leads to the running coupling

$$\alpha_s(p) = \frac{\alpha_s(\mu)}{1 + \beta_0 \alpha_s(\mu) \log \frac{p^2}{\mu^2}} + O(\alpha_s^2)\,, \tag{I.39}$$

with some reference (momentum) scale μ^2. The running coupling in (I.39) tends to zero logarithmically for $p \to \infty$. This property is called asymptotic freedom (Nobel prize 2004) and guarantees the existence of the the perturbative expansion of QCD. Its validity for large energies and momenta is by now impressively proven in various scattering experiments, see e.g. [3]. These experiments can also be used to define a running coupling (which is not unique beyond two loop, see e.g. [4]) and the related plot of $\alpha_s(p^2)$ in Figure 3 has been taken from [3].

In turn, in the infrared regime of QCD at low momentum scales, perturbation theory is not applicable any more. The coupling grows and the failure of perturbation theory is finally signaled by the so-called Landau pole with $\alpha_s(\Lambda_{\rm QCD}) = \infty$. We emphasise that a large or diverging coupling does *not* imply confinement, the theory could still be QEDsS-like showing a Coulomb-potential with a large coupling. The latter would not lead to the absence of colored asymptotic states but rather to so-called color charge superselection sectors as in QED. There, we have asymptotic charged states and no physics process can change the charge.

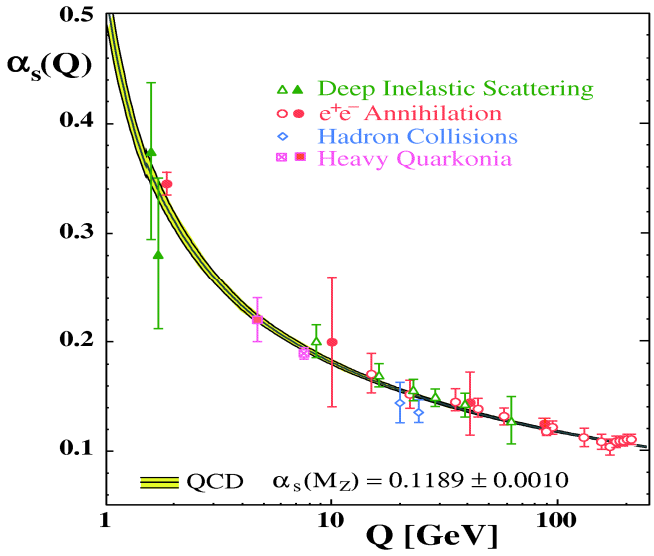

FIG. 3: Experimental tests of the running coupling, figure taken from [3].

II. DIVERGENCES

A. Ultraviolet divergences

From general field theory we know that when we are interested for example in cross section prediction with higher precision we need to compute further terms in its perturbative series in α_s. This computation will lead to ultraviolet divergences which can be absorbed into counter terms for any parameter in the Lagrangian. The crucial feature is that for a renormalizable theory like our Standard Model the number of counter terms is finite, which means once we know all parameters including their counter terms our theory becomes predictive.

In Section II B we will see that in QCD processes we also encounter another kind of divergences. They arise from the infrared momentum regime. Infrared divergences is what this lecture is really going to be about, but before dealing with them it is very instructive to see what happens to the much better understood ultraviolet divergences. In Section II A 1 we will review how such ultraviolet divergences arise and how they are removed. In Section II A 2 we will review how running parameters appear in this procedure, *i.e.* how scale dependence is linked to the appearance of divergences. Finally, in Section II A 3 we will interpret the use of running parameters physically and see that in perturbation theory they resum classes of logarithms to all orders in perturbation theory. Later in Section II B we will follow exactly the same steps for infrared divergences and develop some crucial features of hadron collider physics.

1. *Counter terms*

Renormalization as the proper treatment of ultraviolet divergences is one of the most important things to understand about field theories; you can find more detailed discussions in any book on advanced field theory. The particular aspect of renormalization which will guide us through this section is the appearance of the renormalization scale.

In perturbation theory, scales automatically arise from the regularization of infrared or ultraviolet divergences. We can see this by writing down a simple scalar loop integral, with to two virtual scalar propagators with masses $m_{1,2}$ and an external momentum p flowing through a diagram,

$$B(p^2; m_1, m_2) \equiv \int \frac{d^4q}{16\pi^2} \frac{1}{q^2 - m_1^2} \frac{1}{(q+p)^2 - m_2^2} \,. \tag{II.1}$$

Such two-point functions appear for example in the gluon self energy with virtual gluons, with massless ghost scalars, with a Dirac trace in the numerator for quarks, and with massive scalars for supersymmetric scalar quarks. In those cases the two masses are identical $m_1 = m_2$. The integration measure $1/(16\pi^2)$ is dictated by the Feynman rule for the integration over loop momenta. Counting powers of q in Eq.(II.1) we see that the integrand is not suppressed by powers of $1/q$ in the ultraviolet, so it is logarithmically divergent and we have to regularize it. Regularizing means

expressing the divergence in a well–defined manner or scheme, allowing us to get rid of it by renormalization.

One regularization scheme is to introduce a cutoff into the momentum integral Λ, for example through the so-called Pauli—Villars regularization. Because the ultraviolet behavior of the integrand or integral cannot depend on any parameter living at a small energy scales, the parameterization of the ultraviolet divergence in Eq.(II.1) cannot involve the mass m or the external momentum p^2. The scalar two-point function has mass dimension zero, so its divergence has to be proportional to $\log(\Lambda/\mu_R)$ with a dimensionless prefactor and some scale μ_R^2 which is an artifact of the regularization of such a Feynman diagram. Because it is an artifact, this scale μ_R has to eventually vanish from our theory prediction.

A more elegant regularization scheme is dimensional regularization. It is designed not to break gauge invariance and naively seems to not introduce a mass scale μ_R. When we shift the momentum integration from 4 to $4-2\epsilon$ dimensions and use analytic continuation in the number of space–time dimensions to renormalize the theory, a renormalization scale μ_R nevertheless appears once we ensure the two-point function and with it observables like cross sections keep their correct mass dimension

$$\int \frac{d^4q}{16\pi^2}\cdots \longrightarrow \mu_R^{2\epsilon} \int \frac{d^{4-2\epsilon}q}{16\pi^2}\cdots = \frac{i\mu_R^{2\epsilon}}{(4\pi)^2}\left[\frac{C_{-1}}{\epsilon}+C_0+C_1\,\epsilon+\mathcal{O}(\epsilon^2)\right] . \tag{II.2}$$

At the end, the scale μ_R might drop out after renormalization and analytic continuation, but to be on the safe side we keep it. The constants C_i in the series in $1/\epsilon$ depend on the loop integral we are considering. To regularize the ultraviolet divergence we have to assume $\epsilon > 0$, to find mathematically well defined poles $1/\epsilon$. Defining scalar integrals with the integration measure $1/(i\pi^2)$ will make for example C_{-1} come out as of the order $\mathcal{O}(1)$. This is the reason we usually find factors $1/(4\pi)^2 = \pi^2/(2\pi)^4$ in front of the loop integrals.

The poles in $1/\epsilon$ will cancel with the universal counter terms once we renormalize the theory. Counter terms we include by shifting parameters in the Lagrangian and the leading order matrix element. They cancel the poles in the combined leading order and virtual one-loop prediction

$$\begin{aligned} |\mathcal{M}_{\text{LO}}(g)+\mathcal{M}_{\text{virt}}|^2 &= |\mathcal{M}_{\text{LO}}(g)|^2 + 2\,\text{Re}\,\mathcal{M}_{\text{LO}}(g)\mathcal{M}_{\text{virt}}+\cdots \\ &\to |\mathcal{M}_{\text{LO}}(g+\delta g)|^2 + 2\,\text{Re}\,\mathcal{M}_{\text{LO}}(g)\mathcal{M}_{\text{virt}}+\cdots \\ \text{with}\qquad g \to g^{\text{bare}} &= g+\delta g \qquad \text{and} \quad \delta g \propto \alpha_s/\epsilon\,. \end{aligned} \tag{II.3}$$

The dots indicate higher orders in α_s, for example absorbing the δg corrections in the leading order and virtual interference. As we can see in Eq.(II.3) the counter terms do not come with a factor $\mu_R^{2\epsilon}$ in front. Therefore, while the poles $1/\epsilon$ cancel just fine, the scale factor $\mu_R^{2\epsilon}$ will not be matched between the actual ultraviolet divergence and the counter term.

We can keep track of the renormalization scale best by expanding the prefactor of the regularized but not yet renormalized integral in Eq.(II.2) in a Taylor series in ϵ, no question asked about convergence radii

$$\begin{aligned} \mu_R^{2\epsilon}\left[\frac{C_{-1}}{\epsilon}+C_0+\mathcal{O}(\epsilon)\right] &= e^{2\epsilon\log\mu_R}\left[\frac{C_{-1}}{\epsilon}+C_0+\mathcal{O}(\epsilon)\right] \\ &= \left[1+2\epsilon\log\mu_R+\mathcal{O}(\epsilon^2)\right]\left[\frac{C_{-1}}{\epsilon}+C_0+\mathcal{O}(\epsilon)\right] \\ &= \frac{C_{-1}}{\epsilon}+C_0+C_{-1}\,\log\mu_R^2+\mathcal{O}(\epsilon) \\ &\to \frac{C_{-1}}{\epsilon}+C_0+C_{-1}\,\log\frac{\mu_R^2}{M^2}+\mathcal{O}(\epsilon)\,. \end{aligned} \tag{II.4}$$

In the last step we correct by hand for the fact that $\log\mu_R^2$ with a mass dimension inside the logarithm cannot appear in our calculations. From somewhere else in our calculation the logarithm will be matched with a $\log M^2$ where M^2 is the typical mass or energy scale in our process. This little argument shows that also in dimensional regularization we introduce a mass scale μ_R which appears as $\log(\mu_R^2/M^2)$ in the renormalized expression for our observables. There is no way of removing ultraviolet divergences without introducing some kind of renormalization scale.

In Eq.(II.4) there appear two finite contributions to a given observable, the expected C_0 and the renormalization–induced C_{-1}. Because the factors C_{-1} are linked to the counter terms in the theory we can often guess them without actually computing the complete loop integral, which is very useful in cases where they numerically dominate.

Counter terms as they schematically appear in Eq.(II.3) are not uniquely defined. They need to include a given divergence to return finite observables, but we are free to add any finite contribution we want. This opens many ways to define a counter term for example based on physical processes where counter terms do not only cancel the pole but

also finite contributions at a given order in perturbation theory. Needless to say, such schemes do not automatically work universally. An example for such a physical renormalization scheme is the on–shell scheme for masses, where we define a counter term such that external on–shell particles do not receive any corrections to their masses. For the top mass this means that we replace the leading order mass with the bare mass, for which we then insert the expression in terms of the renormalized mass and the counter term

$$\begin{aligned} m_t^{\text{bare}} &= m_t + \delta m_t \\ &= m_t + m_t \frac{\alpha_s C_F}{4\pi} \left(3 \left(-\frac{1}{\epsilon} + \gamma_E - \log(4\pi) - \log \frac{\mu_R^2}{M^2} \right) - 4 + 3 \log \frac{m_t^2}{M^2} \right) \\ &\equiv m_t + m_t \frac{\alpha_s C_F}{4\pi} \left(-\frac{3}{\tilde{\epsilon}} - 4 + 3 \log \frac{m_t^2}{M^2} \right) \qquad \Leftrightarrow \qquad \frac{1}{\tilde{\epsilon}\left(\frac{\mu_R}{M}\right)} \equiv \frac{1}{\epsilon} - \gamma_E + \log \frac{4\pi\mu_R^2}{M^2} \,, \end{aligned} \tag{II.5}$$

with the color factor $C_F = (N^2-1)/(2N)$ and the Euler constant $\gamma_E \approx 0.577$ coming from the evaluation of the Gamma function $\Gamma(\epsilon) = 1/\epsilon + \gamma_E + \mathcal{O}(\epsilon)$. The convenient scale dependent pole $1/\tilde{\epsilon}$ includes the universal additional terms like the Euler gamma function and the scaling logarithm. This logarithm is the big problem in this universality argument, since we need to introduce the arbitrary energy scale M to separate the universal logarithm of the renormalization scale and the parameter-dependent logarithm of the physical process.

A theoretical problem with this on–shell renormalization scheme is that it is not gauge invariant. On the other hand, it describes for example the kinematic features of top pair production at hadron colliders in a stable perturbation series. This means that once we define a more appropriate scheme for heavy particle masses in collider production mechanisms it better be numerically close to the pole mass. For the computation of total cross sections at hadron colliders or the production thresholds at e^+e^- colliders the pole mass is not well suited at all, but since this is not where we expect to measure particle masses at the LHC we should do fine with something very similar to the pole mass.

Another example for a process dependent renormalization scheme is the mixing of γ and Z propagators. There we choose the counter term of the weak mixing angle such that an on–shell Z boson cannot oscillate into a photon, and vice versa. We can generalize this scheme for mixing scalars as they for example appear in supersymmetry, but it is not gauge invariant with respect to the weak gauge symmetries of the Standard Model either. For QCD corrections, on the other hand, it is the most convenient scheme keeping all exchange symmetries of the two scalars.

To finalize this discussion of process dependent mass renormalization we quote the result for a scalar supersymmetric quark, a squark, where in the on–shell scheme we find

$$\begin{aligned} m_{\tilde{q}}^{\text{bare}} &= m_{\tilde{q}} + \delta m_{\tilde{q}} \\ &= m_{\tilde{q}} + m_{\tilde{q}} \frac{\alpha_s C_F}{4\pi} \left(-\frac{2r}{\tilde{\epsilon}} - 1 - 3r - (1-2r) \log r - (1-r)^2 \log \left| \frac{1}{r} - 1 \right| - 2r \log \frac{m_{\tilde{q}}^2}{M^2} \right) . \end{aligned} \tag{II.6}$$

with $r = m_{\tilde{g}}^2/m_{\tilde{q}}^2$. The interesting aspect of this squark mass counter term is that it also depends on the gluino mass, not just the squark mass itself. The reason why QCD counter terms tend to depend only on the renormalized quantity itself is that the gluon is massless. In the limit of vanishing gluino contribution the squark mass counter term is again only proportional to the squark mass itself

$$m_{\tilde{q}}^{\text{bare}} \Big|_{m_{\tilde{g}}=0} = m_{\tilde{q}} + \delta m_{\tilde{q}} = m_{\tilde{q}} + m_{\tilde{q}} \frac{\alpha_s C_F}{4\pi} \left(-\frac{1}{\tilde{\epsilon}} - 3 + \log \frac{m_{\tilde{q}}^2}{M^2} \right) . \tag{II.7}$$

Taking the limit of Eq.(II.6) to derive Eq.(II.7) is computationally not trivial, though.

One common feature of all mass counter terms listed above is $\delta m \propto m$, which means that our renormalization is actually multiplicative,

$$m^{\text{bare}} = Z_m \, m = (1 + \delta Z_m) \, m = \left(1 + \frac{\delta m}{m} \right) m = m + \delta m \qquad \text{with} \qquad \delta Z_m = \frac{\delta m}{m} \,, \tag{II.8}$$

linking the two ways of writing the mass counter term. This form implies that particles with zero mass will not obtain a finite mass through renormalization. If we remember that chiral symmetry protects a Lagrangian from acquiring fermion masses this means that on–shell renormalization does not break this symmetry. A massless theory cannot become massive by mass renormalization. Regularization and renormalization schemes which do not break symmetries

of the Lagrangian are ideal.

When we introduce counter terms in general field theory we usually choose a slightly more model independent scheme — we define a renormalization point. This is the energy scale at which the counter terms cancels all higher order contributions, divergent as well as finite. The best known example is the electric charge which we renormalize in the Thomson limit of zero momentum transfer through the photon propagator

$$e \to e^{\text{bare}} = e + \delta e \; . \tag{II.9}$$

Looking back at δm_t as defined in Eq.(II.5) we also see a way to define a completely general counter term: if dimensional regularization, *i.e.* the introduction of $4 - 2\epsilon$ dimensions does not break any of the symmetries of our Lagrangian, like Lorentz symmetry or gauge symmetries, we can simply subtract the ultraviolet pole and nothing else. The only question is: do we subtract $1/\epsilon$ in the MS scheme or do we subtract $1/\tilde{\epsilon}$ in the $\overline{\text{MS}}$ scheme. In the $\overline{\text{MS}}$ scheme the counter term is then scale dependent.

Carefully counting, there are three scales present in such a scheme. First, there is the physical scale in the process. In our case of a top self energy this is for example the top mass m_t appearing in the matrix element for the process $pp \to t\bar{t}$. Next, there is the renormalization scale μ_R, a reference scale which is part of the definition of any counter term. And last but not least, there is the scale M separating the counter term from the process dependent result, which we can choose however we want, but which as we will see implies a running of the counter term. The role of this scale M will become clear when we go through the example of the running strong coupling α_s. Of course, we would prefer to choose all three scales the same, but in a complex physical process this might not always be possible. For example, any massive $(2 \to 3)$ production process naturally involves several external physical scales.

Just a side remark for completeness: a one loop integral which has no intrinsic mass scale is the two-point function with zero mass in the loop and zero momentum flowing through the integral: $B(p^2 = 0; 0, 0)$. It appears for example in the self energy corrections of external quarks and gluons. Based on dimensional arguments this integral has to vanish altogether. On the other hand, we know that like any massive two-point function it has to be ultraviolet divergent $B \sim 1/\epsilon_{\text{UV}}$ because setting all internal and external mass scales to zero is nothing special from an ultraviolet point of view. This can only work if the scalar integral also has an infrared divergence appearing in dimensional regularization. We can then write the entire massless two-point function as

$$B(p^2 = 0; 0, 0) = \int \frac{d^4q}{16\pi^2} \, \frac{1}{q^2} \frac{1}{(q+p)^2} = \frac{i\pi^2}{16\pi^2} \left(\frac{1}{\epsilon_{\text{UV}}} - \frac{1}{\epsilon_{\text{IR}}} \right) \; , \tag{II.10}$$

keeping track of the divergent contributions from the infrared and the ultraviolet regimes. For this particular integral they precisely cancel, so the result for $B(0; 0, 0)$ is zero, but setting it to zero too early will spoil any ultraviolet and infrared finiteness test. Treating the two divergences strictly separately and dealing with them one after the other also ensures that for ultraviolet divergences we can choose $\epsilon > 0$ while for infrared divergences we require $\epsilon < 0$.

2. *Running coupling*

To get an idea what these different scales which appear in the process of renormalization mean let us compute such a scale dependent parameter, namely the running strong coupling $\alpha_s(\mu_R^2)$. The Drell–Yan process is one of the very few relevant processes at hadron colliders where the strong coupling does not appear at tree level, so we cannot use it as our toy process this time. Another simple process where we can study this coupling is bottom pair production at the LHC, where at some energy range we will be dominated by valence quarks: $q\bar{q} \to b\bar{b}$. The only Feynman diagram is an s-channel off–shell gluon with a momentum flow $p^2 \equiv s$.

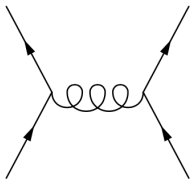

At next–to–leading order this gluon propagator will be corrected by self energy loops, where the gluon splits into two quarks or gluons and re-combines before it produces the two final–state bottoms. Let us for now assume that all quarks are massless. The Feynman diagrams for the gluon self energy include a quark look, a gluon loop, and the ghost loop which removes the unphysical degrees of freedom of the gluon inside the loop.

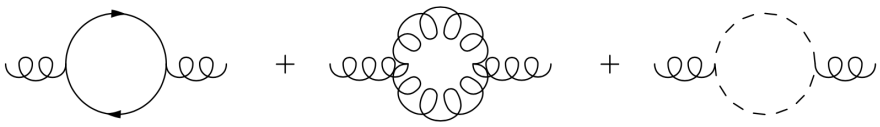

The gluon self energy correction or vacuum polarization, as propagator corrections to gauge bosons are usually labelled, will be a scalar. This way, all fermion lines close in the Feynman diagram and the Dirac trace is computed inside the loop. In color space the self energy will (hopefully) be diagonal, just like the gluon propagator itself, so we can ignore the color indices for now. In unitary gauge the gluon propagator is proportional to the transverse tensor $T^{\mu\nu} = g^{\mu\nu} - p^\nu p^\mu / p^2$. As mentioned in the context of the effective gluon–Higgs coupling, the same should be true for the gluon self energy, which we therefore write as $\Pi^{\mu\nu} \equiv \Pi\, T^{\mu\nu}$. The case with only one external momentum gives us the useful simple relations

$$\begin{aligned} T^{\mu\nu} g^\rho_\nu &= \left(g^{\mu\nu} - \frac{p^\mu p^\nu}{p^2} \right) g^\rho_\nu = T^{\mu\rho} \\ T^{\mu\nu} T^\rho_\nu &= \left(g^{\mu\nu} - \frac{p^\mu p^\nu}{p^2} \right) \left(g^\rho_\nu - \frac{p_\nu p^\rho}{p^2} \right) = g^{\mu\rho} - 2\frac{p^\mu p^\rho}{p^2} + p^2 \frac{p^\mu p^\rho}{p^4} = T^{\mu\rho} \,. \end{aligned} \tag{II.11}$$

Including the gluon, quark, and ghost loops the regularized gluon self energy with a momentum flow p^2 through the propagator reads

$$\begin{aligned} -\frac{1}{p^2}\,\Pi\left(\frac{\mu_R^2}{p^2}\right) &= \frac{\alpha_s}{4\pi} \left(-\frac{1}{\tilde\epsilon} + \log\frac{p^2}{M^2} \right) \left(\frac{13}{6} N_c - \frac{2}{3} n_f \right) + \mathcal{O}(\log m_t^2) \\ &\equiv \alpha_s \left(-\frac{1}{\tilde\epsilon} + \log\frac{p^2}{M^2} \right) b_0 + \mathcal{O}(\log m_t^2) \\ &\text{with} \qquad b_0 = \frac{1}{4\pi} \left(\frac{13}{6} N_c - \frac{2}{3} n_f \right) \\ &\text{and better} \qquad \boxed{b_0 = \frac{1}{4\pi} \left(\frac{11}{3} N_c - \frac{2}{3} n_f \right) \overset{\text{SM}}{>} 0} \,. \end{aligned} \tag{II.12}$$

The minus sign arises from the factors i in the propagators. The number of fermions coupling to the gluons is n_f. From the comments on $B(p^2;0,0)$ we understand how the loop integrals will give a logarithm $\log p^2$ which is then matched by a process-dependent logarithm $\log M^2$ implicitly included in the definition of $\tilde\epsilon$.

The factor b_0 arises from one-loop corrections, *i.e.* from diagrams which include one additional power of α_s. Strictly speaking, it gives the first term in a perturbative series in the strong coupling $\alpha_s = g_s^2/(4\pi)$. Later on, we will indicate where additional higher order corrections would enter.

In the last step of Eq.(II.12) we have snuck in additional contributions to the renormalization of the strong coupling from the other one-loop diagrams in the process, replacing the factor 13/6 by a factor 11/3. This is related to the fact that there are actually three types of divergent virtual gluon diagrams in the physical process $q\bar q \to b\bar b$: the external quark self energies with renormalization factors $Z_f^{1/2}$, the internal gluon self energy Z_A, and the vertex corrections Z_{Aff}. The only physical parameters we can renormalize in this process are the strong coupling and, if finite, the bottom mass. Wave function renormalization constants are not physical, but vertex renormalization terms are. The entire divergence in our $q\bar q \to b\bar b$ process which needs to be absorbed in the strong coupling Z_g is given by the combination

$$Z_{Aff} = Z_g Z_A^{1/2} Z_f \qquad \Leftrightarrow \qquad \frac{Z_{Aff}}{Z_A^{1/2} Z_f} \equiv Z_g \,. \tag{II.13}$$

The additional contributions change the above factor from 13/6 to 11/3 in the running of the strong coupling.

We can check this definition of Z_g by comparing all vertices in which the strong coupling g_s appears, namely the gluon coupling to quarks and ghosts, as well as the triple and quartic gluon vertex. All of them need to have the same divergence structure

$$\frac{Z_{Aff}}{Z_A^{1/2} Z_f} \overset{!}{=} \frac{Z_{A\eta\eta}}{Z_A^{1/2} Z_\eta} \overset{!}{=} \frac{Z_{3A}}{Z_A^{3/2}} \overset{!}{=} \sqrt{\frac{Z_{4A}}{Z_A^2}} \,. \tag{II.14}$$

If we had done the same calculation in QED and looked for a running electric charge, we would have found that the vacuum polarization diagrams for the photon do account for the entire counter term of the electric charge. The other two renormalization constants Z_{Aff} and Z_f cancel because of gauge invariance.

In contrast to QED, the strong coupling diverges in the Thomson limit because QCD is confined towards large distances and weakly coupled at small distances. Lacking a well enough motivated reference point we are lead to renormalize α_s in the $\overline{\text{MS}}$ scheme. From Eq.(II.12) we know that the ultraviolet pole which needs to be cancelled by the counter term is proportional to the function b_0

$$\begin{aligned}
& g_s^{\text{bare}} = Z_g g_s = (1+\delta Z_g)\, g_s = \left(1+\frac{\delta g_s}{g_s}\right) g_s \\
\Rightarrow \qquad & (g_s^2)^{\text{bare}} = (Z_g g_s)^2 = \left(1+\frac{\delta g_s}{g_s}\right)^2 g_s^2 = \left(1+2\frac{\delta g_s}{g_s}+\dots\right) g_s^2 = \left(1+\frac{\delta(g_s^2)}{g_s^2}\right) g_s^2 \\
\Rightarrow \qquad & \alpha_s^{\text{bare}} = \left(1+\frac{\delta\alpha_s}{\alpha_s}\right)\alpha_s \overset{\overline{\text{MS}}}{=} \left(1-\frac{\Pi}{p^2}\bigg|_{\text{pole}}\right)\alpha_s(M^2) \overset{\text{Eq.(II.12)}}{=} \left(1-\frac{\alpha_s}{\tilde\epsilon\left(\frac{\mu_R}{M}\right)}\, b_0\right)\alpha_s(M^2)\,. \qquad \text{(II.15)}
\end{aligned}$$

In the last step we have explicitly included the scale dependence of the counter term. Because the bare coupling does not depend on any scales, this means that α_s depends on the unphysical scale M. Similar to the top mass renormalization scheme we can switch to a more physical scheme for the strong coupling as well: we can absorb also the finite contributions of $\Pi(\mu_R^2/p^2)$ into the strong coupling by simply identifying $M^2 = p^2$. Based again on Eq.(II.12) this implies

$$\alpha_s^{\text{bare}} = \alpha_s(p^2)\left(1-\frac{\alpha_s(p^2)b_0}{\tilde\epsilon}+\alpha_s(p^2)b_0\log\frac{p^2}{M^2}\right)\,. \qquad \text{(II.16)}$$

On the right hand side α_s is consistently evaluated as a function of the physical scale p^2. The lograrithm just shifts the argument of $\tilde\epsilon$ from M^2 to p^2. This formula defines a running coupling $\alpha_s(p^2)$, because the definition of the coupling now has to account for a possible shift between the original argument p^2 and the scale M^2 coming out of the $\overline{\text{MS}}$ scheme. Combining Eqs.(II.15) and (II.16) the bare strong coupling can be expressed in terms of $\alpha_s(M^2)$ or in terms of $\alpha_s(p^2)$, and we can link the two scales through

$$\begin{aligned}
& \alpha_s(M^2) = \alpha_s(p^2) + \alpha_s^2(p^2) b_0 \log\frac{p^2}{M^2} = \alpha_s(p^2)\left(1+\alpha_s(p^2)b_0\log\frac{p^2}{M^2}\right) \\
\Leftrightarrow \qquad & \frac{d\alpha_s(p^2)}{d\log p^2} = -\alpha_s^2(p^2)b_0 + \mathcal{O}(\alpha_s^3)\,. \qquad \text{(II.17)}
\end{aligned}$$

To the given loop order the argument of the strong coupling squared on the right side can be neglected — its effect is of higher order. We nevertheless keep the argument as a higher order effect to later distinguish different approaches to the running coupling. From Eq.(II.12) we know that $b_0 > 0$, which means that towards larger scales the strong coupling has a negative slope. The ultraviolet limit of the strong coupling is zero. This makes QCD an asymptotically free theory. We can compute the function b_0 in general models by simply adding all contributions of strongly interacting particles in this loop

$$b_0 = -\frac{1}{12\pi}\sum_{\text{colored states}} D_j\, T_{R,j}\,, \qquad \text{(II.18)}$$

where we need to know some kind of counting factor D_j which is -11 for a vector boson (gluon), +4 for a Dirac fermion (quark), +2 for a Majorana fermion (gluino), +1 for a complex scalar (squark) and +1/2 for a real scalar. Note that this sign is not given by the fermionic or bosonic nature of the particle in the loop. The color charges are $T_R = 1/2$ for the fundamental representation of $SU(3)$ and $C_A = N_c$ for the adjoint representation. The masses of the loop particles are not relevant in this approximation because we are only interested in the ultraviolet regime of QCD where all particles can be regarded massless. When we really model the running of α_s we need to take into account threshold effects of heavy particles, because particles can only contribute to the running of α_s at scales above their mass scale.

We can do even better than this fixed order in perturbation theory: while the correction to α_s in Eq.(II.16) is perturbatively suppressed by the usual factor $\alpha_s/(4\pi)$ it includes a logarithm of a ratio of scales which does not need to be small. Instead of simply including these gluon self energy corrections at a given order in perturbation theory

we can instead include chains of one-loop diagrams with Π appearing many times in the off–shell gluon propagator. It means we replace the off–shell gluon propagator by

$$\begin{aligned}\frac{T^{\mu\nu}}{p^2} \to & \frac{T^{\mu\nu}}{p^2} + \left(\frac{T}{p^2}\cdot(-T\,\Pi)\cdot\frac{T}{p^2}\right)^{\mu\nu} \\ & + \left(\frac{T}{p^2}\cdot(-T\,\Pi)\cdot\frac{T}{p^2}\cdot(-T\,\Pi)\cdot\frac{T}{p^2}\right)^{\mu\nu} + \cdots \\ = & \frac{T^{\mu\nu}}{p^2}\sum_{j=0}^{\infty}\left(-\frac{\Pi}{p^2}\right)^j = \frac{T^{\mu\nu}}{p^2}\,\frac{1}{1+\Pi/p^2}\,, \end{aligned} \tag{II.19}$$

schematically written without the factors i. To avoid indices we abbreviate $T^{\mu\nu}T^{\rho}_{\nu} = T\cdot T$ which make sense because according to Eq.(II.11)

$$(T\cdot T\cdot T)^{\mu\nu} = T^{\mu\rho}T^{\sigma}_{\rho}T^{\nu}_{\sigma} = T^{\mu\sigma}T^{\nu}_{\sigma} = T^{\mu\nu}\,. \tag{II.20}$$

This resummation of the logarithm which appears in the next–to–leading order corrections to α_s moves the finite shift in α_s shown in Eqs.(II.12) and (II.16) into the denominator, while we assume that the pole will be properly taken care off in any of the schemes we discuss

$$\alpha_s^{\text{bare}} = \alpha_s(M^2) - \frac{\alpha_s^2 b_0}{\tilde{\epsilon}} \equiv \frac{\alpha_s(p^2)}{1-\alpha_s(p^2)\,b_0\,\log\dfrac{p^2}{M^2}} - \frac{\alpha_s^2 b_0}{\tilde{\epsilon}}\,. \tag{II.21}$$

Just as in the case without resummation, we can use this complete formula to relate the values of α_s at two reference points, *i.e.* we consider it a renormalization group equation (RGE) which evolves physical parameters from one scale to another in analogy to the fixed order version in Eq.(II.17)

$$\frac{1}{\alpha_s(M^2)} = \frac{1}{\alpha_s(p^2)}\left(1-\alpha_s(p^2)\,b_0\,\log\frac{p^2}{M^2}\right) = \frac{1}{\alpha_s(p^2)} - b_0\,\log\frac{p^2}{M^2} + \mathcal{O}(\alpha_s)\,. \tag{II.22}$$

The factor α_s inside the parentheses we can again evaluate at either of the two scales, the difference is a higher order effect. If we keep it at p^2 we see that the expression in Eq.(II.22) is different from the un-resummed version in Eq.(II.16). If we ignore this higher order effect the two formulas become equivalent after switching p^2 and M^2. Resumming the vacuum expectation bubbles only differs from the un-resummed result once we include some next–to–leading order contribution. When we differentiate $\alpha_s(p^2)$ with respect to the momentum transfer p^2 we find, using the relation $d/dx(1/\alpha_s) = -1/\alpha_s^2\; d\alpha_s/dx$

$$\frac{1}{\alpha_s}\,\frac{d\alpha_s}{d\log p^2} = -\alpha_s\frac{d}{d\log p^2}\,\frac{1}{\alpha_s} = -\alpha_s\,b_0 + \mathcal{O}(\alpha_s^2) \qquad \text{or} \qquad \boxed{p^2\frac{d\alpha_s}{dp^2} \equiv \frac{d\alpha_s}{d\log p^2} = \beta = -\alpha_s^2\sum_{n=0} b_n\alpha_s^n}\,. \tag{II.23}$$

This is the famous running of the strong coupling constant including all higher order terms b_n.

In the running of the strong coupling constant we relate the different values of α_s through multiplicative factors of the kind

$$\left(1 \pm \alpha_s b_0 \log\frac{p^2}{M^2}\right)\,. \tag{II.24}$$

Such factors appear in the un-resummed computation of Eq.(II.17) as well as in Eq.(II.21) after resummation. Because they are multiplicative, these factors can move into the denominator, where we need to ensure that they do not vanish. Dependent on the sign of b_0 this becomes a problem for large scale ratios $|\alpha_s \log p^2/M^2| > 1$, where it leads to the Landau pole. For $b_0 > 0$ and large coupling values at small scales $p^2 \ll M^2$ the combination $(1+\alpha_s b_0 \log p^2/M^2)$ can indeed vanish and become a problem.

It is customary to replace the renormalization point of α_s in Eq.(II.21) with a reference scale defined by the Landau

pole. At one loop order we first define the reference scale Λ_{QCD}

$$1 + \alpha_s(M^2)\, b_0\, \log \frac{\Lambda^2_{\text{QCD}}}{M^2} \stackrel{!}{=} 0 \qquad \Leftrightarrow \qquad \log \frac{\Lambda^2_{\text{QCD}}}{M^2} = -\frac{1}{\alpha_s(M^2) b_0} \qquad \Leftrightarrow \qquad \log \frac{p^2}{M^2} = \log \frac{p^2}{\Lambda^2_{\text{QCD}}} - \frac{1}{\alpha_s(M^2) b_0}\,, \tag{II.25}$$

and then include it in the running

$$\begin{aligned} \frac{1}{\alpha_s(p^2)} &\stackrel{\text{Eq.(II.22)}}{=} \frac{1}{\alpha_s(M^2)} + b_0\, \log \frac{p^2}{M^2} \\ &= \frac{1}{\alpha_s(M^2)} + b_0 \log \frac{p^2}{\Lambda^2_{\text{QCD}}} - \frac{1}{\alpha_s(M^2)} = b_0 \log \frac{p^2}{\Lambda^2_{\text{QCD}}} \qquad \Leftrightarrow \qquad \boxed{\alpha_s(p^2) = \frac{1}{b_0 \log \dfrac{p^2}{\Lambda^2_{\text{QCD}}}}}\,. \end{aligned} \tag{II.26}$$

This scheme can be generalized to any order in perturbative QCD and is not that different from the Thomson limit renormalization scheme of QED, except that with the introduction of Λ_{QCD} we are choosing a reference point which is particularly hard to compute perturbatively. One thing that is interesting in the way we introduce Λ_{QCD} is the fact that we introduce a scale into our theory without ever setting it. All we did was renormalize a coupling which becomes strong at large energies and search for the mass scale of this strong interaction. This trick is called dimensional transmutation.

In terms of language, there is a little bit of confusion between field theorists and phenomenologists: up to now we have introduced the renormalization scale μ_R as the renormalization point, for example of the strong coupling constant. In the $\overline{\text{MS}}$ scheme, the subtraction of $1/\tilde{\epsilon}$ shifts the scale dependence of the strong coupling to M^2 and moves the logarithm $\log M^2/\Lambda^2_{\text{QCD}}$ into the definition of the renormalized parameter. This is what we will from now on call the renormalization scale in the phenomenological sense, *i.e.* the argument we evaluate α_s at. Throughout this section we will keep the symbol M for this renormalization scale in the $\overline{\text{MS}}$ scheme, but from Section II B on we will shift back to μ_R instead of M as the argument of the running coupling, to be consistent with the literature.

3. *Resumming scaling logarithms*

In the last Section II A 2 we have introduced the running strong coupling in a fairly abstract manner. For example, we did not link the resummation of diagrams and the running of α_s in Eqs.(II.17) and (II.23) to physics. In what way does the resummation of the one-loop diagrams for the s-channel gluon improve our prediction of the bottom pair production rate at the LHC?

To illustrate those effects we best look at a simple observable which depends on just one physical energy scale p^2. The first observable coming to mind is again the Drell–Yan cross section $\sigma(q\bar{q} \to \mu^+\mu^-)$, but since we are not really sure what to do with the parton densities which are included in the actual hadronic observable, we better use an observable at an e^+e^- collider. Something that will work and includes α_s at least in the one-loop corrections is the R parameter

$$R = \frac{\sigma(e^+e^- \to \text{hadrons})}{\sigma(e^+e^- \to \mu^+\mu^-)} = N_c \sum_{\text{quarks}} Q_q^2 = \frac{11 N_c}{9}\,. \tag{II.27}$$

The numerical value at leading order assumes five quarks. Including higher order corrections we can express the result in a power series in the renormalized strong coupling α_s. In the $\overline{\text{MS}}$ scheme we subtract $1/\tilde{\epsilon}(\mu_R/M)$ and in general include an unphysical scale dependence on M in the individual prefactors r_n

$$R\left(\frac{p^2}{M^2}, \alpha_s\right) = \sum_{n=0} r_n\left(\frac{p^2}{M^2}\right) \alpha_s^n(M^2) \qquad\qquad r_0 = \frac{11 N_c}{9}\,. \tag{II.28}$$

The r_n we can assume to be dimensionless — if they are not, we can scale R appropriately using p^2. This implies that the r_n only depend on ratios of two scales, the externally fixed p^2 on the one hand and the artificial M^2 on the other.

At the same time we know that R is an observable, which means that including all orders in perturbation theory it cannot depend on any artificial scale choice M. Writing this dependence as a total derivative and setting it to zero

we find an equation which would be called a Callan–Symanzik equation if instead of the running coupling we had included a running mass

$$\begin{aligned}
0 &\stackrel{!}{=} M^2 \frac{d}{dM^2} R\left(\frac{p^2}{M^2}, \alpha_s(M^2)\right) \\
&= \left[M^2 \frac{\partial}{\partial M^2} + \beta \frac{\partial}{\partial \alpha_s}\right] \sum_{n=0} r_n \left(\frac{p^2}{M^2}\right) \alpha_s^n \\
&= \sum_{n=1} M^2 \frac{\partial r_n}{\partial M^2} \alpha_s^n + \sum_{n=1} \beta\, r_n\, n \alpha_s^{n-1} && \text{with} \quad r_0 = \frac{11 N_c}{9} = \text{const} \\
&= M^2 \sum_{n=1} \frac{\partial r_n}{\partial M^2} \alpha_s^n - \sum_{n=1} \sum_{m=0} n r_n\, \alpha_s^{n+m+1} b_m && \text{with} \quad \beta = -\alpha_s^2 \sum_{m=0} b_m \alpha_s^m \\
&= M^2 \frac{\partial r_1}{\partial M^2} \alpha_s + \left(M^2 \frac{\partial r_2}{\partial M^2} - r_1 b_0\right) \alpha_s^2 + \left(M^2 \frac{\partial r_3}{\partial M^2} - 2 r_2 b_0 - r_1 b_1\right) \alpha_s^3 + \mathcal{O}(\alpha_s^4) \,. && \text{(II.29)}
\end{aligned}$$

In the second line we have to remember that the M dependence of α_s is already included in the appearance of β, so α_s should be considered a variable by itself. This perturbative series in α_s has to vanish in each order of perturbation theory. Our kind–of–Callan–Symanzik equation requires

$$\begin{aligned}
\frac{\partial r_1}{\partial \log M^2} &= 0 \\
\frac{\partial r_2}{\partial \log M^2} &= r_1 b_0 \\
\frac{\partial r_3}{\partial \log M^2} &= r_1 b_1 + 2 r_2(M^2) b_0 \\
&\vdots
\end{aligned} \qquad \text{(II.30)}$$

The mix of r_n derivatives and the perturbative terms in the β function we can read off the α_s^3 term: first, we have the appropriate NNNLO corrections r_3; next, we have one loop in the gluon propagator b_0 and two loops for example in the vertex r_2; and finally, we need the two-loop diagram for the gluon propagator b_1 and a one-loop vertex correction r_1. The dependence on the argument M^2 vanishes for r_0 and r_1. Keeping in mind that there will be integration constants c_n and that another, in our case, unique momentum scale p^2 has to cancel the mass units inside $\log M^2$ we find

$$\begin{aligned}
r_0 &= c_0 = \frac{11 N_c}{9} \\
r_1 &= c_1 \\
r_2 &= c_2 + r_1 b_0 \log \frac{M^2}{p^2} = c_2 + c_1 b_0 \log \frac{M^2}{p^2} \\
r_3 &= \int d \log \frac{M'^2}{p^2} \left(c_1 b_1 + 2\left(c_2 + c_1 b_0 \log \frac{M'^2}{p^2}\right) b_0\right) = c_3 + (c_1 b_1 + 2 c_2 b_0) \log \frac{M^2}{p^2} + c_1 b_0^2 \log^2 \frac{M^2}{p^2} \\
&\vdots
\end{aligned} \qquad \text{(II.31)}$$

This chain of r_n values looks like we should interpret the apparent fixed-order perturbative series for R in Eq.(II.28) as a series which implicitly includes terms of the order $\log^{n-1} M^2/p^2$ in each r_n. They can become problematic if this logarithm becomes large enough to spoil the fast convergence in terms of $\alpha_s \sim 0.1$, evaluating the observable R at scales far away from the scale choice for the strong coupling constant M.

Instead of the series in r_n we can use Eq.(II.31) to express R in terms of the c_n and collect the logarithms appearing

with each c_n,

$$R = \sum_n r_n \left(\frac{p^2}{M^2}\right) \; \alpha_s^n(M^2) = c_0 + c_1 \left(1 + \alpha_s(M^2) b_0 \log\frac{M^2}{p^2} + \alpha_s^2(M^2) b_0^2 \log^2\frac{M^2}{p^2} + \cdots\right) \alpha_s(M^2) + c_2 \left(1 + 2\alpha_s(M^2) b_0 \log\frac{M^2}{p^2} + \cdots\right) \alpha_s^2(M^2) + \cdots \tag{II.32}$$

We encounter geometric series, which we resum as

$$R = c_0 + c_1 \frac{\alpha_s(M^2)}{1 - \alpha_s(M^2) b_0 \log\frac{M^2}{p^2}} + c_2 \left(\frac{\alpha_s(M^2)}{1 - \alpha_s(M^2) b_0 \log\frac{M^2}{p^2}}\right)^2 + \cdots \equiv \sum c_n \; \alpha_s^n(p^2) \; . \tag{II.33}$$

In the original ansatz α_s is always evaluated at the scale M^2. In the last step we use Eq.(II.22) with flipped arguments p^2 and M^2, derived from the resummation of the vacuum polarization bubbles. In contrast to the r_n integration constants the c_n are by definition independent of p^2/M^2 and therefore more suitable as a perturbative series in the presence of potentially large logarithms. Note that the un-resummed version of the running coupling in Eq.(II.16) would not give the correct result, so Eq.(II.33) only holds for resummed vacuum polarization bubbles.

This re-organization of the perturbation series for R can be interpreted as resumming all logarithms of the kind $\log M^2/p^2$ in the new organization of the perturbative series and absorbing them into the running strong coupling evaluated at the scale p^2. All scale dependence in the perturbative series for the dimensionless observable R is moved into α_s, so possibly large logarithms $\log M^2/p^2$ have disappeared. In Eq.(II.33) we also see that this series in c_n will never lead to a scale-invariant result when we include a finite order in perturbation theory. Some higher–order factors c_n are known, for example inserting $N_c = 3$ and five quark flavors just as we assume in Eq.(II.27)

$$R = \frac{11}{3} \left(1 + \frac{\alpha_s(p^2)}{\pi} + 1.4 \left(\frac{\alpha_s(p^2)}{\pi}\right)^2 - 12 \left(\frac{\alpha_s(p^2)}{\pi}\right)^3 + \mathcal{O}\left(\frac{\alpha_s(p^2)}{\pi}\right)^4\right) \; . \tag{II.34}$$

This alternating series with increasing perturbative prefactors seems to indicate the asymptotic instead of convergent behavior of perturbative QCD. At the bottom mass scale the relevant coupling factor is only $\alpha_s(m_b^2)/\pi \sim 1/14$, so a further increase of the c_n would become dangerous. However, a detailed look into the calculation shows that the dominant contributions to c_n arise from the analytic continuation of logarithms, which are large finite terms for example from $\mathrm{Re}(\log^2(-E^2)) = \log^2 E^2 + \pi^2$. In the literature such π^2 terms arising from the analytic continuation of loop integrals are often phrased in terms of $\zeta_2 = \pi^2/6$.

Before moving on we collect the logic of the argument given in this section: when we regularize an ultraviolet divergence we automatically introduce a reference scale μ_R. Naively, this could be an ultraviolet cutoff scale, but even the seemingly scale invariant dimensional regularization in the conformal limit of our field theory cannot avoid the introduction of a scale. There are several ways of dealing with such a scale: first, we can renormalize our parameter at a reference point. Secondly, we can define a running parameter and this way absorb the scale logarithm into the $\overline{\mathrm{MS}}$ counter term. In that case introducing Λ_{QCD} leaves us with a compact form of the running coupling $\alpha_s(M^2; \Lambda_{\mathrm{QCD}})$.

Strictly speaking, at each order in perturbation theory the scale dependence should vanish together with the ultraviolet poles, as long as there is only one scale affecting a given observable. However, defining the running strong coupling we sum one-loop vacuum polarization graphs. Even when we compute an observable at a given loop order, we implicitly include higher order contributions. They lead to a dependence of our perturbative result on the artificial scale M^2, which phenomenologists refer to as renormalization scale dependence.

Using the R ratio we see what our definition of the running coupling means in terms of resumming logarithms: reorganizing our perturbative series to get rid of the ultraviolet divergence $\alpha_s(p^2)$ resums the scale logarithms $\log p^2/M^2$ to all orders in perturbation theory. We will need this picture once we introduce infrared divergences in the following section.

B. Infrared divergences

After this brief excursion into ultraviolet divergences and renormalization we can return to the original example, the Drell–Yan process, written in the low-energy QED limit as

$$\sigma(pp \to \ell^+\ell^-)\Big|_{\text{QED}} = \frac{4\pi\alpha^2 Q_\ell^2}{3N_c} \int_0^1 dx_1 dx_2 \sum_j Q_j^2 \, f_j(x_1) \, f_{\bar{j}}(x_2) \, \frac{1}{q^2} \,, \tag{II.35}$$

At this stage the parton distributions (pdfs) $f_j(x)$ in the proton are only functions of the collinear momentum fraction of the partons inside the proton about which from a theory point of view we only know a set of sum rules.

The perturbative question we need to ask for $\mu^+\mu^-$ production at the LHC is: what happens if together with the two leptons we produce additional jets which for one reason or another we do not observe in the detector. Such jets could for example come from the radiation of a gluon from the initial–state quarks. In Section II B 1 we will study the kinematics of radiating such jets and specify the infrared divergences this leads to. In Sections II B 2 and V A we will show that these divergences have a generic structure and can be absorbed into a re-definition of the parton densities, similar to an ultraviolet renormalization of a Lagrangian parameter. In Sections V B and V C we will again follow the example of the ultraviolet divergences and specify what absorbing these divergences means in terms logarithms appearing in QCD calculations.

Throughout this writeup we will use the terms jets and final state partons synonymously. This is not really correct once we include jet algorithms and hadronization. On the other hand, the purpose of a jet algorithm is to take us from some kind of energy deposition in the calorimeter to the parton radiated in the hard process. The two should therefore be closely related.

1. *Single jet radiation*

Let us look at the radiation of additional partons in the Drell–Yan process. We can start for example by computing the cross section for the partonic process $q\bar{q} \to Zg$. However, this partonic process involves renormalization of ultraviolet divergences as well as loop diagrams which we have to include before we can say anything reasonable, *i.e.* ultraviolet and infrared finite.

To make life easier and still learn about the structure of collinear infrared divergences we instead look at the crossed process

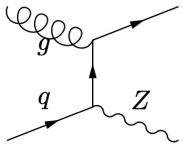

It should behave similar to any other $(2 \to 2)$ jet radiation, except that it has a different incoming state than the leading order Drell–Yan process and hence does not involve virtual corrections. This means we do not have to deal with ultraviolet divergences and renormalization, and can concentrate on parton or jet radiation from the initial state. Moreover, let us go back to Z production instead of a photon, to avoid confusion with additional massless particles in the final state.

The amplitude for this $(2 \to 2)$ process is — modulo charges and averaging factors, but including all Mandelstam variables

$$|\mathcal{M}|^2 \sim -\frac{t}{s} - \frac{s^2 - 2m_Z^2(s+t-m_Z^2)}{st} \,. \tag{II.36}$$

The Mandelstam variable t for one massless final–state particle can be expressed in terms of the rescaled gluon emission angle

$$t = -s(1-\tau)y \qquad \text{with} \qquad y = \frac{1-\cos\theta}{2} \qquad \text{and} \qquad \tau = \frac{m_Z^2}{s} \,. \tag{II.37}$$

Similarly, we obtain $u = -s(1-\tau)(1-y)$, so as a first check we can confirm that $t + u = -s(1-\tau) = -s + m_Z^2$. The

collinear limit when the gluon is radiated in the beam direction is given by

$$y \to 0 \qquad \Leftrightarrow \qquad t \to 0 \qquad \Leftrightarrow \qquad u = -s + m_Z^2 < 0$$
$$|\mathcal{M}|^2 \to \frac{s^2 - 2sm_Z^2 + 2m_Z^4}{s(s-m_Z^2)} \, \frac{1}{y} + \mathcal{O}(y^0) \; . \tag{II.38}$$

This expression is divergent for collinear gluon radiation or gluon splitting, *i.e.* for small angles y. We can translate this $1/y$ divergence for example into the transverse momentum of the gluon or Z

$$sp_T^2 = tu = s^2(1-\tau)^2 \; y(1-y) = (s-m_Z^2)^2 y + \mathcal{O}(y^2) \tag{II.39}$$

In terms of p_T, the collinear limit our matrix element squared in Eq.(II.38) becomes

$$|\mathcal{M}|^2 \sim \frac{s^2 - 2sm_Z^2 + 2m_Z^4}{s^2} \; \frac{s-m_Z^2}{p_T^2} + \mathcal{O}(p_T^0) \; . \tag{II.40}$$

The matrix element for the tree level process $qg \to Zq$ has a leading divergence proportional to $1/p_T^2$. To compute the total cross section for this process we need to integrate the matrix element over the entire two-particle phase space. Approximating the matrix element as C'/y or C/p_T^2, we then integrate

$$\int_{y^{\min}}^{y^{\max}} dy \frac{C'}{y} = \int_{p_T^{\min}}^{p_T^{\max}} dp_T^2 \frac{C}{p_T^2} = \; 2 \int_{p_T^{\min}}^{p_T^{\max}} dp_T \; p_T \; \frac{C}{p_T^2} \simeq 2C \int_{p_T^{\min}}^{p_T^{\max}} dp_T \frac{1}{p_T} = 2C \; \log \frac{p_T^{\max}}{p_T^{\min}} \tag{II.41}$$

The form C/p_T^2 for the matrix element is of course only valid in the collinear limit; in the non–collinear phase space C is not a constant.

Next, we follow the same strategy as for the ultraviolet divergence. First, we regularize the divergence for example using dimensional regularization. Then, we find a well–defined way to get rid of it. Dimensional regularization means writing the two-particle phase space in $n = 4 - 2\epsilon$ dimensions. Just for reference, the complete formula for the y-distribuion reads

$$s \, \frac{d\sigma}{dy} = \frac{\pi (4\pi)^{-2+\epsilon}}{\Gamma(1-\epsilon)} \left(\frac{\mu_F^2}{m_Z^2} \right)^\epsilon \; \frac{\tau^\epsilon (1-\tau)^{1-2\epsilon}}{y^\epsilon (1-y)^\epsilon} \, |\mathcal{M}|^2 \sim \left(\frac{\mu_F^2}{m_Z^2} \right)^\epsilon \; \frac{|\mathcal{M}|^2}{y^\epsilon (1-y)^\epsilon} \; . \tag{II.42}$$

In the second step we only keep the factors we are interested in. The additional factor $1/y^\epsilon$ regularizes the integral at $y \to 0$, as long as $\epsilon < 0$ by slightly increasing the suppression of the integrand in the infrared regime. This means that for infrared divergences we can as well choose $n = 4 + 2\epsilon$ space–time dimensions with $\epsilon > 0$. After integrating the leading collinear divergence $1/y^{1+\epsilon}$ we are left with a pole $1/(-\epsilon)$. This regularization procedure is symmetric in $y \leftrightarrow (1-y)$. What is important to notice is again the appearance of a scale $\mu_F^{2\epsilon}$ with the n-dimensional integral. This scale arises from the infrared regularization of the phase space integral and is referred to as factorization scale. The actual removal of the infrared pole — corresponding to the renormalization in the ultraviolet case — is called mass factorization and works exactly the same way as renormalizing a parameter: in a well–defined scheme we simply subtract the pole from the fixed-order matrix element squared.

2. Parton splitting

In this section we will show that we can indeed write all collinear divergences in a universal form, independent of the hard process which we choose as the Drell–Yan process. In the collinear limit, the radiation of additional partons or the splitting into additional partons will be described by universal splitting functions.

Infrared divergences occur for massless particles in the initial or final state, so we need to go through all ways incoming or outgoing gluons and quark can split into each other. The description of the factorized phase space, with which we will start, is common to all these different channels. The first and at the LHC most important case is the splitting of one gluon into two, shown in Figure 4. The two daughter gluons are close to mass shell while the mother has to have a finite positive invariant mass $p_a^2 \gg p_b^2, p_c^2$. We again assign the direction of the momenta as $p_a = -p_b - p_c$, which means we have to take care of minus signs in the particle energies. We can describe the

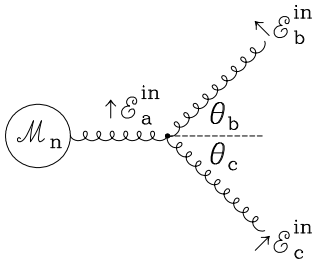

FIG. 4: Splitting of one gluon into two gluons. Figure from Ref. [5].

kinematics of this approximately collinear process in terms of the energy fractions z and $1-z$ defined as

$$z = \frac{|E_b|}{|E_a|} = 1 - \frac{|E_c|}{|E_a|} \qquad p_a^2 = (-p_b - p_c)^2 = 2(p_b p_c) = 2z(1-z)(1-\cos\theta)E_a^2 = z(1-z)E_a^2\theta^2 + \mathcal{O}(\theta^4)$$
$$\Leftrightarrow \qquad \theta \equiv \theta_b + \theta_c \simeq \frac{1}{|E_a|}\sqrt{\frac{p_a^2}{z(1-z)}}\,, \tag{II.43}$$

in the collinear limit and in terms of the opening angle θ between $\vec{p}_b$ and $\vec{p}_c$. Because $p_a^2 > 0$ we call this final–state splitting configuration time–like branching. For this configuration we can write down the so-called Sudakov decomposition of the four-momenta

$$-p_a = p_b + p_c = (-zp_a + \beta n + p_T) \;+\; (-(1-z)p_a - \beta n - p_T)\;. \tag{II.44}$$

It defines an arbitrary unit four-vector n, a p_T component orthogonal to the mother momentum and to n and p_a,

$$(p_a p_T) = 0 = (n p_T)\,, \tag{II.45}$$

and a free factor β. We can specify n such that it defines the direction of the p_b–p_c decay plane. In this decomposition we can set only one invariant mass to zero, for example that of a radiated gluon $p_c^2 = 0$. The second final state will have a finite invariant mass $p_b^2 \neq 0$.

As specific choice for the three reference four-vectors is

$$p_a = \begin{pmatrix} |E_a| \\ 0 \\ 0 \\ p_{a,3} \end{pmatrix} = |E_a| \begin{pmatrix} 1 \\ 0 \\ 0 \\ 1+\mathcal{O}(\theta) \end{pmatrix} \qquad n = \begin{pmatrix} 1 \\ 0 \\ 0 \\ -1 \end{pmatrix} \qquad p_T = \begin{pmatrix} 0 \\ p_{T,1} \\ p_{T,2} \\ 0 \end{pmatrix}\,. \tag{II.46}$$

Relative to $\vec{p}_a$ we can split the opening angle θ for massless partons according to Figure 4

$$\theta = \theta_b + \theta_c \qquad \text{and} \qquad \frac{\theta_b}{\theta_c} = \frac{\frac{p_T}{|E_b|}}{\frac{p_T}{|E_c|}} = \frac{1-z}{z} \qquad \Leftrightarrow \qquad \theta = \frac{\theta_b}{1-z} = \frac{\theta_c}{z}\,. \tag{II.47}$$

The momentum choice in Eq.(II.46) has the additional feature that $n^2 = 0$, which allows us to extract β from the momentum parameterization shown in Eq.(II.44) and the additional condition $p_c^2 = 0$

$$\begin{aligned} p_c^2 &= (-(1-z)p_a - \beta n - p_T)^2 \\ &= (1-z)^2 p_a^2 + p_T^2 + 2\beta(1-z)(np_a) \\ &= (1-z)^2 p_a^2 + p_T^2 + 4\beta(1-z)|E_a|(1+\mathcal{O}(\theta)) \stackrel{!}{=} 0 \end{aligned} \qquad \Leftrightarrow \qquad \beta \simeq -\frac{p_T^2 + (1-z)^2 p_a^2}{4(1-z)|E_a|}\,. \tag{II.48}$$

Using this phase space parameterization we divide an $(n+1)$-particle process into an n-particle process and a splitting process of quarks and gluons. First, this requires us to split the $(n+1)$-particle phase space alone into

an n-particle phase space and the collinear splitting. The general $(n+1)$-particle phase space separating off the n-particle contribution

$$\begin{aligned} d\Phi_{n+1} &= \cdots \frac{d^3\vec{p}_b}{2(2\pi)^3|E_b|}\,\frac{d^3\vec{p}_c}{2(2\pi)^3|E_c|} = \cdots \frac{d^3\vec{p}_a}{2(2\pi)^3|E_a|}\,\frac{d^3\vec{p}_c}{2(2\pi)^3|E_c|}\,\frac{|E_a|}{|E_b|} \\ &\equiv d\Phi_n\,\frac{dp_{c,3}dp_T p_T d\phi}{2(2\pi)^3|E_c|}\,\frac{1}{z} \\ &= d\Phi_n\,\frac{dp_{c,3}dp_T^2 d\phi}{4(2\pi)^3|E_c|}\,\frac{1}{z} \end{aligned} \tag{II.49}$$

azimuthal angle ϕ. In other words, separating the $(n+1)$-particle space into an n-particle phase space and a $(1\to 2)$ splitting phase space is possible without any approximation, and all we have to take care of is the correct prefactors in the new parameterization.

Our next task is to translate $p_{c,3}$ and p_T^2 into z and p_a^2. Starting from Eq.(II.44) for $p_{c,3}$ with the third components of p_a and p_T given by Eq.(II.46) we insert β from Eq.(II.48) and obtain

$$\begin{aligned} \frac{dp_{c,3}}{dz} &= \frac{d}{dz}\left[-(1-z)|E_a|(1+\mathcal{O}(\theta))+\beta\right] = \frac{d}{dz}\left[-(1-z)|E_a|(1+\mathcal{O}(\theta)) - \frac{p_T^2+(1-z)^2p_a^2}{4(1-z)|E_a|}\right] \\ &= |E_a|(1+\mathcal{O}(\theta)) - \frac{p_T^2}{4(1-z)^2E_a} + \frac{p_a^2}{4|E_a|} \\ &= \frac{|E_c|}{1-z}(1+\mathcal{O}(\theta)) - \frac{\theta^2z^2E_c^2}{4(1-z)^2E_a} + \frac{z(1-z)E_a^2\theta^2+\mathcal{O}(\theta^4)}{4|E_a|} \qquad \text{using Eq.(II.43) and Eq.(II.47)} \\ &= \frac{|E_c|}{1-z}+\mathcal{O}(\theta) \qquad \Leftrightarrow \qquad \frac{dp_{c,3}}{|E_c|} \simeq \frac{dz}{1-z}\,. \end{aligned} \tag{II.50}$$

Next, we replace dp_T^2 with dp_a^2 according to

$$\frac{p_T^2}{p_a^2} = \frac{E_b^2\theta_b^2}{z(1-z)E_a^2\theta^2} = \frac{z^2E_a^2\,(1-z)^2\theta^2}{z(1-z)E_a^2\theta^2} = z(1-z) \quad \Leftrightarrow \quad dp_T^2 = z(1-z)dp_a^2\,. \tag{II.51}$$

This gives us the final result for the separated collinear phase space

$$\boxed{d\Phi_{n+1} = d\Phi_n\,\frac{dz\,dp_a^2\,d\phi}{4(2\pi)^3} = d\Phi_n\,\frac{dz\,dp_a^2}{4(2\pi)^2}}\,, \tag{II.52}$$

where in the second step we assume an azimuthal symmetry.

Adding the transition matrix elements to this factorization of the phase space and ignoring the initial–state flux factor which is common to both processes we can now postulate a full factorization for one emission and in the collinear approximation

$$\begin{aligned} d\sigma_{n+1} &= \overline{|\mathcal{M}_{n+1}|^2}\;d\Phi_{n+1} \\ &= \overline{|\mathcal{M}_{n+1}|^2}\;d\Phi_n\frac{dp_a^2\,dz}{4(2\pi)^2}\;(1+\mathcal{O}(\theta)) \\ &\simeq \frac{2g_s^2}{p_a^2}\;\hat{P}(z)\;\overline{|\mathcal{M}_n|^2}\;d\Phi_n\frac{dp_a^2\,dz}{16\pi^2} \qquad \text{assuming} \quad \boxed{\overline{|\mathcal{M}_{n+1}|^2} \simeq \frac{2g_s^2}{p_a^2}\;\hat{P}(z)\;\overline{|\mathcal{M}_n|^2}}\,. \end{aligned} \tag{II.53}$$

This last step is an assumption. We will proceed to show it step by step by constructing the appropriate splitting kernels $\hat{P}(z)$ for all different quark and gluon configurations. If Eq.(II.53) holds true this means that we can compute the $(n+1)$ particle amplitude squared from the n-particle case convoluted with the appropriate splitting kernel. Using $d\sigma_n \sim \overline{|\mathcal{M}_n|^2}\,d\Phi_n$ and $g_s^2 = 4\pi\alpha_s$ we can write this relation in its most common form

$$\sigma_{n+1} \simeq \int \sigma_n\,\frac{dp_a^2}{p_a^2}dz\,\frac{\alpha_s}{2\pi}\,\hat{P}(z)\,. \tag{II.54}$$

Reminding ourselves that relations of the kind $\overline{|\mathcal{M}_{n+1}|^2} = p\overline{|\mathcal{M}_n|^2}$ can typically be summed, for example for the case of successive soft photon radiation in QED, we see that Eq.(II.54) is not the final answer. It does not include the necessary phase space factor $1/n!$ from identical bosons in the final state which leads to the simple exponentiation.

As the first parton splitting in QCD we study a gluon splitting into two gluons, shown in Figure 4. To compute its transition amplitude we need to write down all gluon momenta and polarizations in a specific frame. We skip the derivation and just quote the result

$$\begin{aligned}
\overline{|\mathcal{M}_{n+1}|^2} &= \frac{2g_s^2}{p_a^2}\,\frac{N_c}{2}\,2\left[\frac{z}{1-z}+z(1-z)+\frac{1-z}{z}\right]\,\overline{|\mathcal{M}_n|^2} \\
&\equiv \frac{2g_s^2}{p_a^2}\,\hat{P}_{g\leftarrow g}(z)\,\overline{|\mathcal{M}_n|^2} \\
\Leftrightarrow \qquad \hat{P}_{g\leftarrow g}(z) &= C_A\left[\frac{z}{1-z}+\frac{1-z}{z}+z(1-z)\right] ,
\end{aligned} \tag{II.55}$$

using $C_A = N_c$. The form of the splitting kernel is symmetric when we exchange the two gluons z and $(1-z)$. It diverges if either of the gluons become soft. The notation $\hat{P}_{i\leftarrow j} \sim \hat{P}_{ij}$ is inspired by a matrix notation which we can use to multiply the splitting matrix from the right with the incoming parton vector to get the final parton vector. Following the logic described above, with this calculation we prove that the factorized form of the $(n+1)$-particle matrix element squared in Eq.(II.53) holds for gluons only.

The same kind of splitting kernel we can compute for the splitting of a gluon into two quarks and the splitting of a quark into a quark and a gluon

$$g(p_a) \to q(p_b) + \bar{q}(p_c) \qquad \text{and} \qquad q(p_a) \to q(p_b) + g(p_c) . \tag{II.56}$$

Both splittings include the quark–quark–gluon vertex, coupling the gluon current to the quark and antiquark spinors. Again, we omit the calculation and quote the result

$$\begin{aligned}
\overline{|\mathcal{M}_{n+1}|^2} &= \frac{2g_s^2}{p_a^2}\,T_R\,\left[z^2+(1-z)^2\right]\,\overline{|\mathcal{M}_n|^2} \\
&\equiv \frac{2g_s^2}{p_a^2}\hat{P}_{q\leftarrow g}(z)\,\overline{|\mathcal{M}_n|^2} \\
\Leftrightarrow \qquad \hat{P}_{q\leftarrow g}(z) &= T_R\left[z^2+(1-z)^2\right] ,
\end{aligned} \tag{II.57}$$

with $T_R = 1/2$. In the first line we implicitly assume that the internal quark propagator can be written as something like $u\bar{u}/p_a^2$ and we only need to consider the denominator. This splitting kernel is again symmetric in z and $(1-z)$ because QCD does not distinguish between the outgoing quark and the outgoing antiquark.

The third splitting we compute is gluon radiation off a quark,

$$q(p_a) \to q(p_b) + g(p_c) , \tag{II.58}$$

sandwiching the qqg vertex between an outgoing quark $\bar{u}_\pm(p_b)$ and an incoming quark $u_\pm(p_a)$. The result is

$$\begin{aligned}
\overline{|\mathcal{M}_{n+1}|^2} &= \frac{2g_s^2}{p_a^2}\,C_F\,\frac{1+z^2}{1-z}\,\overline{|\mathcal{M}_n|^2} \\
&\equiv \frac{2g_s^2}{p_a^2}\hat{P}_{q\leftarrow g}(z)\,\overline{|\mathcal{M}_n|^2} \\
\Leftrightarrow \qquad \hat{P}_{q\leftarrow q}(z) &= C_F\frac{1+z^2}{1-z} .
\end{aligned} \tag{II.59}$$

The color factor for gluon radiation off a quark is $C_F = (N^2-1)/(2N)$. The averaging factor $1/N_a = 2$ now is the number of quark spins in the intermediate state. Just switching $z \leftrightarrow (1-z)$ we can read off the kernel for a quark splitting written in terms of the final–state gluon

$$\hat{P}_{g\leftarrow q}(z) = C_F\frac{1+(1-z)^2}{z} . \tag{II.60}$$

This result finalizes our calculation of all QCD splitting kernels $\hat{P}_{i\leftarrow j}(z)$ between quarks and gluons. As alluded to earlier, similar to ultraviolet divergences which get removed by counter terms these splitting kernels are universal. They do not depend on the hard n-particle matrix element which is part of the original $(n+1)$-particle process. In Eqs.(II.55), (II.57), (II.59), and (II.60) we have shown by construction that the collinear factorization Eq.(II.54) holds at this level in perturbation theory.

Before using this splitting property to describe QCD effects at the LHC we need to look at the splitting of partons in the initial state, meaning $|p_a^2|, p_c^2 \ll |p_b^2|$ where p_b is the momentum entering the hard interaction. The difference to the final–state splitting is that now we can consider the split parton momentum $p_b = p_a - p_c$ as a t-channel diagram, so we already know $p_b^2 = t < 0$ from our usual Mandelstam variables argument. This space–like splitting version of Eq.(II.44) for p_b^2 gives us

$$\begin{aligned} t \equiv p_b^2 &= (-z p_a + \beta n + p_T)^2 \\ &= p_T^2 - 2z\beta(p_a n) \qquad\qquad \text{with } p_a^2 = n^2 = (p_a p_T) = (n p_T) = 0 \\ &= p_T^2 + \frac{p_T^2 z}{1-z} \qquad\qquad \text{using Eq.(II.48)} \\ &= \frac{p_T^2}{1-z} = -\frac{p_{T,1}^2 + p_{T,2}^2}{1-z} < 0 \,. \end{aligned} \tag{II.61}$$

The calculation of the splitting kernels and matrix elements is the same as for the time–like case, with the one exception that for splitting in the initial state the flow factor has to be evaluated at the reduced partonic energy $E_b = z E_a$ and that the energy fraction entering the parton density needs to be replaced by $x_b \to z x_b$. The factorized matrix element for initial–state splitting then reads just like Eq.(II.54)

$$\sigma_{n+1} = \int \sigma_n \, \frac{dt}{t} dz \, \frac{\alpha_s}{2\pi} \, \hat{P}(z) \,. \tag{II.62}$$

What we are missing for the infrared or better collinear divergences is the description of the scale dependence and the interpretation in terms of perturbation theory. That will lead us to the DGLAP equations in Sec. V.

III. STRONG CHIRAL SYMMETRY BREAKING

In the previous sections we discussed the ultraviolet renomalisation of QCD and its relation to the scale dependence of physics. This scale dependence is apparent in the momentum dependence of the strong running coupling $\alpha_s(p^2) = g^2(p^2)/(4\pi)$ defined in (I.39) and (II.23). Here p is the relevant momentum/energy scale of a given process. The running coupling in (I.39) tends to zero logarithmically for $p \to \infty$. This property is called asymptotic freedom (Nobel prize 2004) and guarantees the existence of the the perturbative expansion of QCD. Its validity for large energies and momenta is by now impressively proven in various scattering experiments, see e.g. Figure 3 from [3]. These experiments can also be used to define a running coupling (which is not unique beyond two loop, see e.g. [4]).

In turn, in the infrared regime of QCD at low momentum scales, perturbation theory is not applicable any more. The coupling grows and the failure of perturbation theory is finally signaled by the so-called Landau pole with $\alpha_s(\Lambda_{\rm QCD}) = \infty$. We infer from (I.39) that at one loop, $\Lambda_{\rm QCD}$ is given by

$$\Lambda_{\rm QCD} = \mu \, e^{-\frac{1}{2\beta_0 \alpha_s(\mu)}} \,, \qquad \text{with} \qquad \mu \frac{d\Lambda_{\rm QCD}}{d\mu} = 0 \,. \tag{III.1}$$

The RG-invariance of $\Lambda_{\rm QCD}$ is readily proven with the β-function (I.38) up to two-loop terms. This implies that $\Lambda_{\rm QCD}$ may be related to a physical scale and indeed it is (non-trivially) related to the mass gap in QCD. However, we emphasise that a large or diverging coupling does *not* imply confinement, the theory could still be QED-like showing a Coulomb-potential with a large coupling. The latter would not lead to the absence of coloured asymptotic states but rather to so-called color charge superselection sectors as in QED. There, we have asymptotic charged states and no physics process can change the charge. For more details see e.g. [6].

A. Spontaneous symmetry breaking and the Goldstone theorem

In the Standard Model we have two phenomena involving spontaneous symmetry breaking. The first is the spontaneous symmetry breaking in the Higgs sector (Englert-Brout-Higgs-Guralnik-Hagen-Kibble) which provides (current) masses for the quarks and leptons as well as for the W, Z vector bosons, the gauge bosons of the weak interactions. The corresponding Goldstone boson manifest itself as the third polarisation of the massive vector bosons (Higgs-Kibble dinner).

The second phenomena is strong chiral symmetry breaking in the quark sector with a mass scale of ≈ 300 MeV. This mechanism, loosely speaking, lifts the current quark masses to constituent quark masses. For the up and down quarks the current quark mass is negligible, see Table I. The corresponding (pseudo-) Goldstone bosons, the pions $\vec{\pi}$, are composite (quark–anti-quark) states and do not appear in the QCD action.

In the following we discuss similarities of and differences between these two phenomena. Before we come to the Standard Model, let us recall some basic facts about spontaneous symmetry breaking. Further details can be found in the literature. As a basic, but important, example we consider a simple scalar field theory with N real scalars and action

$$S[\phi] = \frac{1}{2}\int_x (\partial_\mu \phi^a)^2 + \int_x V(\rho)\,, \qquad \text{with} \qquad a = 1, ..., N\,, \qquad \text{and} \qquad \rho = \frac{1}{2}\phi^a\phi^a\,, \tag{III.2}$$

and the ϕ^4-potential

$$V(\rho) = -\frac{1}{2}\mu_\phi^2(\phi^a\phi^a) + \frac{\lambda_\phi}{8}(\phi^a\phi^a)^2 = -\mu_\phi\rho + \frac{\lambda_\phi}{2}\rho^2\,. \tag{III.3}$$

In the following considerations we shall not need the specific form (III.3) but only its symmetries. Still, the simple potential (III.3) serves as a good showcase. The action (III.2) with the potential (III.3) has $O(N)$-symmetry. Moreover, the potential (III.3) has a manifold of non-trivial minima, each of which breaks $O(N)$-symmetry. This leads us to the vacuum manifold

$$V'(\rho_0) = 0\,, \qquad \text{with} \qquad \rho_0 = \frac{\mu_\phi^2}{\lambda_\phi}\,, \tag{III.4}$$

where the prime stands for the derivative w.r.t. ρ. In Figure 5 the potential is depicted for the $O(2)$-case with $N = 2$.

Without loss of generality we pick a specific point on the vacuum manifold (III.4), to wit

$$\phi_0 = \begin{pmatrix} 0 \\ \vdots \\ 0 \\ \sqrt{2\rho_0} \end{pmatrix}\,. \tag{III.5}$$

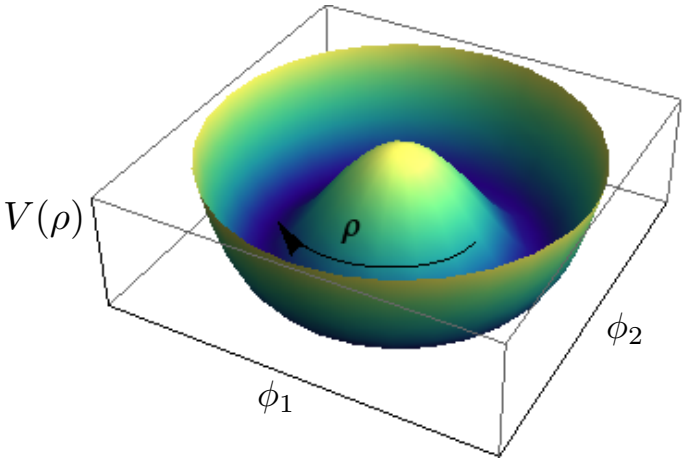

FIG. 5: Illustration of the Mexican hat potential for N = 2. The radial massive mode ρ is indicated by the arrow. The angular mode is the Goldstone mode.

The vacuum vector ϕ_0 in (III.5) is invariant under the subgroup (little group) $O(N-1)$ with the generators t^a, $a = N, N+1, ...N(N-1)/2$ of $O(N)$ that acts trivially on the Nth component field ϕ^N. This subgroup rotates the first $N-1$ component fields into each other. It leaves us with $N-1$ generators t^a, $a = 1, ..., N-1$ (of the quotient $O(N)/O(N-1)$) of the $N(N-1)/2$ generators of the group $O(N)$. In turn, a rotation of the vacuum vector within this quotient generates the full vacuum manifold. Applied to a vector $\phi^a = \delta^{Na}\sqrt{2\rho}$ with length it generates all fields,

$$\phi = e^{\frac{\theta^a}{\sqrt{2\rho_0}}t^a} \begin{pmatrix} 0 \\ \vdots \\ 0 \\ \sigma \end{pmatrix} , \tag{III.6}$$

where the denominator $1/\sqrt{2\rho_0}$ is chosen for convenience. Commonly, the Nth component field ϕ^N is expanded about the minimum $\sigma_0 = \sqrt{2\rho_0}$.

In the present lecture we choose a slightly different approach and stick to the Cartesian fields ϕ which we split into the radial mode σ and the rest, $\vec{\pi}$, i.e.

$$\phi = \begin{pmatrix} \vec{\pi} \\ \sigma \end{pmatrix} , \qquad \text{with} \qquad \phi_0 = \begin{pmatrix} 0 \\ \sigma \end{pmatrix} . \tag{III.7}$$

Note that in an expansion about the minimum ϕ_0 in the fields $\vec{\theta}$ and $\vec{\pi}$ agree in leading order. Using the representation (III.7) in the kinetic term in the action (III.2) we are led to

$$S_{\text{kinetic}}[\phi] = \frac{1}{2}\int_x \left[(\partial_\mu \sigma)^2 + (\partial_\mu \vec{\pi})^2\right] . \tag{III.8}$$

The mass term of the model is given by the quadratic term of the potential in an expansion about the minimum. It reads generally

$$\frac{1}{2}\int_x m^{2\,ab}(\phi_0)\phi^a\,\phi^b , \qquad \text{with} \qquad m^{2\,ab}(\phi_0) = \partial_{\phi^a}\partial_{\phi^b}V(\rho_0) = \delta^{ab}\,V'(\rho_0) + \phi_0^a\phi_0^b\,V''(\rho_0) . \tag{III.9}$$

Using the expansion point (III.5) leads to the mass matrix

$$m^{2\,ab}(\phi_0) = \delta^{ab}\,V'(\rho_0) + 2\,\delta^{Na}\delta^{Nb}\rho_0 V''(\rho_0) = \delta^{Na}\delta^{Nb}\rho_0\,\lambda . \tag{III.10}$$

Equation (III.10) entails that in the symmetry-broken phase of the model we have $N-1$ massless fields, the Goldstone fields. Note that we have not used the specific form (III.3) of the potential for this derivation.

The occurrence of the massless modes in (III.10) is a specific case/manifestation of the Goldstone theorem. It entails in general that in the case of a spontaneous symmetry breaking of a continuous symmetry massless modes, the Goldstone modes, occur. Their number is related to the number of generators in the Quotient G/H, where G is the symmetry group and H is the subgroup (little group) which leaves the vacuum invariant.

B. Spontaneous symmetry breaking, quantum fluctuations and masses*

The classical analysis done in chapter Section III A suffices to uncover the occurrence of massless modes in spontaneous symmetry breaking. However, it does not unravel the mechanism. The stability of the chosen vacuum, e.g. (III.5), necessitates, that an infinitesimal rotation on the vacuum manifold costs an infinite amount of energy. This does only happen (for continuous symmetries) in dimensions $d > 2$. In $d \leq 2$ no spontaneous symmetry breaking of a continuous symmetry occurs, which is covered by the Mermin-Wagner theorem (Mermin-Wagner-Hohenberg-Coleman). In $d = 2$ dimensions theories with discrete symmetry can exhibit spontaneous symmetry breaking, e.g. the Ising model.

Hence, the full analysis has to be done on the quantum level. A convenient way to address these questions is the quantum analogue of the classical action, the (quantum) effective action. Formally it is defined as the Legendre transform of the Schwinger functional, $W[J] = \log Z[J]$. In the present case this is

$$\Gamma[\phi] = \sup_J \left\{ \int_x J(x)\phi(x) - \log Z[J] \right\} , \qquad \text{where} \qquad Z[J] = \int D\varphi\, e^{-S[\varphi]+\int_x J\varphi} . \tag{III.11}$$

In the following we simply assume that (III.11) has a maximum and is differentiable w.r.t. J. Then the definition in (III.11) leads to

$$\phi = \frac{1}{Z[J]}\frac{\delta Z[J]}{\delta J} = \langle\varphi\rangle\,, \qquad \text{and} \qquad J = \frac{\delta\Gamma}{\delta\phi}\,. \tag{III.12}$$

The effective action also has a closed path integral representation in terms of a functional integro-differential equation, which we also quote for later use. For the derivation we substitute the current in (III.11) with (III.12) and use that $Z = \exp\{-\Gamma + \int_x J\phi\}$. This leads us to

$$e^{-\Gamma[\phi]} = \int D\varphi'\, e^{-S[\phi+\varphi']+\int_x \frac{\delta\Gamma}{\delta\phi}\varphi'}\,, \qquad \text{with} \qquad \langle\varphi'\rangle_c = 0\,, \tag{III.13}$$

where we also shifted the integration variable $\varphi = \varphi' + \varphi$. Equation (III.13) leads us immediately to the quantum equations of motion in general backgrounds ϕ, the Dyson-Schwinger equations. We simply take the ϕ-derivatives on both sides and arrive at

$$\frac{\delta\Gamma}{\delta\phi} = \left\langle\frac{\delta S}{\delta\varphi}\right\rangle\,, \tag{III.14}$$

the quantum eqautions of motion (EoM) in a given background $\phi = \langle\varphi\rangle$ triggered by the current J. Evaluated on the EoM with $J = 0$,

$$\left.\frac{\delta\Gamma}{\delta\phi}\right|_{\phi=\phi_{\rm EoM}} = 0\,, \tag{III.15}$$

The effective action $\Gamma[\phi_{\rm EoM}] = -\log Z[0]$ it is the free energy of the theory and implies $J[\phi_{\rm EoM}] = 0$. It is also a generating functional and generates the one-particle-irreducible (1PI) diagrams of the theory. As all diagrams can be constructed from 1PI diagrams, it contains the full information about the correlation functions of the theory. In the present context, the interesting feature is its relation to the free energy. It allows us to define the effective potential

$$V_{\rm eff}[\phi_c] = \Gamma[\phi_c]/{\rm vol}_4\,, \tag{III.16}$$

with constant fields ϕ_c and the four-volume ${\rm vol}_4 = \int d^4x$. If the effective potential shows the vacuum structure discussed above in the classical case, the theory exhibits spontaneous symmetry breaking. The Mermin-Wagner theorem simply entails that in lower dimensions the longe range nature of the quantum fluctuations washes out the non-trivial vacua.

The rôle of the effective action as the quantum analogue of the classical action is also very apparent in its relation to the propagator of the theory,

$$\langle\phi(p)\phi(-p)\rangle_c = \left.\frac{\delta^2\log Z[J]}{\delta J(p)\delta J(-P)}\right|_{J=0} = \left.\frac{1}{Z[0]}\frac{\delta^2 Z}{\delta J(p)\delta J(-P)}\right|_{J=0} - \langle\phi(p)\rangle\langle\phi(-p)\rangle\,, \qquad \text{with} \qquad \langle\phi\rangle = \frac{1}{Z[0]}\frac{\delta Z}{\delta J}\,, \tag{III.17}$$

where the subscript $_c$ stands for connected. Now we use the relation of $\log Z$ to the effective action defined in (III.11). We have

$$\delta(p-q) = \frac{\delta J(q)}{\delta J(p)} = \int_l \frac{\delta\phi(l)}{\delta J(p)}\cdot\frac{\delta J(q)}{\delta\phi(l)} = \int_l \frac{\delta^2\log Z}{\delta J(l)\delta J(p)}\cdot\frac{\delta^2\Gamma[\phi]}{\delta\phi(l)\delta(q)} \quad\Rightarrow\quad \langle\phi(p)\phi(q)\rangle_c = \frac{1}{\Gamma^{(2)}}(p,q)\,, \tag{III.18}$$

with the vertices

$$\frac{\delta^n\Gamma}{\delta\phi(p_1)\cdots\phi(p_n)} = \Gamma^{(n)}(p_1,...,p_n)\,, \qquad \text{with} \qquad \langle\varphi(p_1)\cdots\varphi(p_n)\rangle_{\rm 1PI} = \Gamma^{(n)}(p_1,...,p_n)\,. \tag{III.19}$$

The proof of the latter identity of the nth φ-derivatives with the 1PI n-point correlation functions we leave to the reader. Instead let us now come back to our simple example for spontaneous symmetry breaking. Let us assume for the moment that the full effective action resembles the classical action in (III.2). Then the ϕ^4-potential in (III.3) is the full quantum effective potential of the theory for $\rho \geq \rho_0$ (why is this not possible for smaller ρ?). The full

propagator of the theory is now given by

$$\langle\varphi(p)\varphi(-p)\rangle_c = \frac{1}{\Gamma^{(2)}[\phi_{\rm EoM}]}(p,-p) = \frac{1}{p^2}\left(\delta^{ab}-\delta^{aN}\delta^{bN}\right)+\frac{1}{p^2+8\rho_0\lambda}\delta^{ab}\,, \tag{III.20}$$

which describes the massless propagation of the $N-1$ Goldstone modes, and that of one massive one, the radial field σ, with mass $m_\sigma^2 = 8\rho_0\lambda$. This links the curvature of the effective potential to the masses of the propagating modes in the theory. Note however, that this is a Euclidean concept and finally we are interested in the pole masses of the physical excitations. They are defined via the respective (inverse) screening lengths in the spatial and temporal directions. The latter are defined by

$$\lim_{\|\vec{x}-\vec{y}\|\to\infty}\langle\phi(x)\phi(y)\rangle \sim e^{-\|\vec{x}-\vec{y}\|/\xi_{\rm spat}}\,, \qquad \text{and} \qquad \lim_{|x_0-y_0|\to\infty}\langle\phi(x)\phi(y)\rangle \sim e^{-|x_0-y_0|/\xi_{\rm temp}}\,. \tag{III.21}$$

The screening lengths $\xi_{\rm spat/temp}$ are inversely related to the pole mass $m_{\rm pol} = 1/\xi_{\rm temp}$ and screening mass $m_{\rm screen} = 1/\xi_{\rm spat}$ respectively. In the present example with the classical dispersion p^2 these masses are identical and also agree with the curvature masses $m_{\rm curv}$ derived from the effective potential. This is easily seen from (III.20). The screening lengths and masses are derived from the Fourier transform of the propagator in momentum space and we have e.g. for the radial mode φ^N at $\vec{p}=0$

$$\lim_{|x_0-y_0|\to\infty}\int\frac{dp_0}{(2\pi)}\langle\varphi^N(p_0,0)\varphi^N(-p_0,0)\rangle_c e^{ip_0\,(x_0-y_0)} \sim e^{-|x_0-y_0|8\rho_0\lambda}\,, \tag{III.22}$$

and hence $m_{\rm pol} = 1/\xi_{\rm temp} = m_{\rm curv}$. Here $\vec{p}=0$ has only be chosen for convenience. A similar computation can be made for the spatial screening length which agrees with the temporal one. In summary this leaves us with the definition of the pole mass as the smallest value for

$$\Gamma^{(2)}(p_0 = m_{\rm pol}, \vec{p}=0) = 0\,, \tag{III.23}$$

related to the pole (or cut) that is closest to the Euclidean frequency axis. A similar definition holds for the screening mass.

In principle this allows for the extraction of the pole and screening masses from the Euclidean propagators. In practice this quickly runs in an accuracy problem if the propagator is only known numerically. Moreover, this problem is tightly related to reconstruction problems of analyticity properties from numerical data which is an ill-posed problem without any further knowledge.

As a last remark we add that the above identity between screening lengths, and pole, screening and curvature masses fails in the full quantum theory:

- the coincidence of curvature and screening/pole masses hinges on the classical dispersion proportional to p^2, any non-trivial momentum dependence of the propagator leads to a violation.
- The coincidence of screening and pole mass hinges on the dispersion only being a function of p^2. While this is true in the vacuum (at vanishing temperature $T=0$ and density/chemical potential $n/\mu = 0$), finite temperature and density singles out a rest frame and the dispersion depends on $\vec{p}^2$ and p_0^2 separately.

Having said this, in the following we shall first use simple approximations to the full low energy effective action of QCD for extracting the physics of chiral symmetry breaking and confinement, as well as the mechanisms behind these phenomena.

C. Little reminder on the Higgs mechanism

Now we are in the position to discuss the Higgs mechanism in the Standard Model. Again we refer to the literature for the details. The Higgs mechanisms serves as an example, at which we can discuss similarities and differences for strong chiral symmetry breaking. Moreover, it is the combination of both mechanisms of mass generation that leads to the observed world. The action of the Standard Model is given by

$$S_{\rm SM}[\Phi] = \frac{1}{4}\int_x F^a_{\mu\nu}F^a_{\mu\nu} + \frac{1}{4}\int_x W^a_{\mu\nu}W^a_{\mu\nu} + \frac{1}{4}\int_x B_{\mu\nu}B_{\mu\nu} + (D\phi)^\dagger D\phi + V_H(\phi) + \int_x \bar\psi\cdot(i\not{D} + i\,m_\psi(\phi) + i\mu\gamma_0)\cdot\psi\,, \tag{III.24}$$

where we have introduced the electroweak gauge bosons W, B and the Higgs, a complex scalar $SU(2)$-doublet ϕ,

$$\phi = \begin{pmatrix} \phi_1 \\ \phi_2 \end{pmatrix} , \tag{III.25}$$

with complex components ϕ_1, ϕ_2. The Higgs potential V_H is a ϕ^4-potential as (III.3) with

$$V_H(\phi) = -\frac{1}{2}\mu_\phi^2 \phi^\dagger\phi + \frac{\lambda_\phi}{8}(\phi^\dagger\phi)^2 . \tag{III.26}$$

with non-trivial vacuum manifold

$$\rho_0 = \frac{\mu_\phi^2}{\lambda_\phi} \qquad \text{with} \qquad \rho = \frac{1}{2}\phi^\dagger\phi . \tag{III.27}$$

In the spirit of the discussion at the end of chapter Section III A we should interpret V_H as an approximation of the full effective potential of the theory. The Higgs field couples to the electroweak gauge group with the covariant derivative

$$D_\mu\phi = (\partial_\mu - ig_W W_\mu - ig_H B_\mu)\,\phi , \tag{III.28}$$

The mass term in (III.24) is linear in the Higgs field and vanishes for $\phi = 0$. The left-handed fermions ψ_L in the Standard Model, leptons and quarks, couple to the weak isospin (fundamental representation) with weak isospin $\pm - 1/2$, while the right-handed fermions ψ_R do not couple (trivial representation) with weak isospin 0, that is for example

$$W_\mu\psi_R = 0 . \tag{III.29}$$

The related covariant derivative of the fermions reads

$$D_\mu\psi = (\partial_\mu - igA_\mu - ig_W W_\mu - ig_H B_\mu)\,\psi . \tag{III.30}$$

The mass term $m(\phi)$ is linear in the Higgs field ϕ and hence constitues a Yukawa interaction. It relates to the Cabibbo-Kobayashi-Maskawa-Matrix (CKM) , and is not discussed in further details here. What is important in the present context, is, that a non-vanishing expectation value of the Higgs field, $\langle\phi\rangle = (0, \rho_0/\sqrt{2})$ provides mass terms for the weak gauge fields, the W, Z as well as for the (left-handed) quarks an leptons:

As in our $O(N)$-example in the previous section we expect spontaneous symmetry breaking in the scalar Higgs sector. The current masses of the leptons and quarks are then generated by the disappearance of the mass term for $\phi_0 \neq 0$. Since the structure of the full term is quite convoluted, we illustrate this at a simple example with one Dirac fermion ψ and a real scalar field σ. Then the Yukawa term reads in a mean field approximation

$$h\bar\psi\sigma\psi \xrightarrow{\text{mean field}} h\sigma_0\,\bar\psi\psi , \tag{III.31}$$

with mass $m = h\sigma_0$ which is proportional to the vacuum expectation value of the scalar field (vacuum expectation value of the Higgs) and the Yukawa coupling h.

For the masses of the gauge field we cut a long story short and simply note that in a mean field analysis as that done above for the fermion

$$(W_\mu\phi)^\dagger(W_\mu\phi) \xrightarrow{\text{mean field}} (W_\mu\phi_0)^\dagger(W_\mu\phi_0) , \tag{III.32}$$

leads to mass terms for the gauge fields. Since the vacuum field ϕ_0 has vanishing upper component ϕ_1 it is a combination of the generator $t^3 = \sigma_3/2$ of the weak $SU(2)$ and the generator $\mathbb{1}$ of the hypercharge $U(1)$ which remains massless: the photon. This also determines the subgroup which leaves the vacuum invariant. The superficial analysis here also reveals that the quotient involves three generators and hence we have three Goldstone bosons. In summary we hence start with three gauge bosons with two physical polarisations each together with three Goldstone bosons, which adds up to nine field degrees of freedom (dof). A convenient reparameterisation (including an appropriate gauge fixing, e.g. the unitary gauge) of the Standard Model leads us to three massive vector bosons with three polarisations each, that is again nine dofs.

D. Low energy effective theories of QCD

The Higgs mechanism in the electroweak sector of the Standard Model leads to (current) quark masses for the up and down quark of a couple of MeVs, $(m_{u/d})_{\rm cur} \approx$ 2-5 MeV, see Table I. However, the masses of the nucleons, the protons and neutrons, is about 1 GeV (proton (uud) $\approx$ 938 MeV , neutron (udd) $\approx$ 940 MeV), that is two orders of magnitude bigger. In other words, the three constituent quarks in the nucleons must have an effective mass of about $(m_{u/d})_{\rm con} \approx$ 300-400 MeV, the constituent quark masses. We already infer from this that there should be a further mechanism to generate this mass scale.

In low energy QCD with its mass scale $\Lambda_{\rm QCD} \approx 200 - 300\,$MeV, the electroweak sector of the Standard Model decouples as do the heavier quarks. We are left with two light (up and down) and one heavy quark (charm), Table I. Within fully quantitative computations of the QCD dynamics at low energies the strange quark with its current mass of about 1.2 GeV is also added. Still, its dynamics is very much suppressed at momentum scales of $\Lambda_{\rm QCD}$. For the present structural analysis we first resort to two flavour QCD ($N_f = 2$) with the Euclidean action

$$S_{\rm QCD}[\Phi] = \frac{1}{4}\int_x F^a_{\mu\nu}F^a_{\mu\nu} + \int_x \bar\psi\cdot(\not{D} + m_\psi - \mu\gamma_0)\cdot\psi\,, \tag{III.33}$$

where ψ is a Dirac spinor with two flavours and Φ is the two-flavour super field, see (I.35) and (I.36). The physics of the matter sector at low energies and temperatures, and not too large densities is well-described by quark-hadron models, the most prominent of which is the Nambu–Jona-Lasino model. From the perturbative point of view these models are seeded in the four-Fermi coupling already being generated from the propagators and couplings depicted in Figure 2 at tree level. The related one-loop diagram is depicted in Figure 6. It is built from one-gluon exchange tree level scatterings of quark–anti-quark pair into another one, which is highlighted in the red box in Figure 6. This t-channel process (in terms of the momentum routing the full one-loop diagram) has the structure

$$g^2\left(\bar\psi\gamma_\mu t^a\psi\right)(p)\left[\left(\delta_{\mu\nu} - (1-\xi)\frac{p_\mu p_\nu}{p^2}\right)\frac{1}{p^2}\right]\left(\bar\psi\gamma_\nu t^a\psi\right)(-p)\,, \tag{III.34}$$

with $t = p^2$. In (III.34) the t^a are generators of the color gauge group and the fermions are summed over the two flavours. The fermionic currents couple to each other via the exchange of a gluon with the classical gluon propagator in the square bracket, for the Feynman rules see **??**. In summary, (III.34) generates a four-Fermi interaction with a non-trivial momentum structure in the effective action of QCD.

The full momentum- and tensor structure is complicated even for the present simplified $N_f = 2$ case. As in the four-Fermi theory (Fermi theory) for weak interactions we resort to an approximation with point-like interactions (no momentum dependence). Then (III.34) can be rewritten in terms of an effective *local* (point-like) four-Fermi interaction. Such a rewriting in terms of local four-Fermi interactions holds for energies that are sufficiently low and do not resolve the large momentum structure of the scattering in (III.34). Moreover, the coupling is dimensionful and has the canonical momentum dimension -2 (related to the $1/p^2$ term in (III.34). In the Fermi theory of weak interactions this is the electroweak scale. In the present case it has to be related to the QCD mass gap proportional to $\Lambda_{\rm QCD}$.

We postpone the detailed analysis of this scale, and first concentrate on the tensor structure of (III.34). This is constrained by the symmetries of the theory, for a full discussion of the symmetry pattern we refer to the literature, e.g. [7, 8] and literature therein. Since the current masses of the light quarks are nearly vanishing we first work in the chiral limit. Then, any interaction that is generated by the dynamics of QCD carries chiral symmetry: the related four-Fermi interaction is chirally invariant, that is the invariance under the chiral transformations

$$\psi \to e^{i\frac{1\pm\gamma_5}{2}\alpha}\psi \quad\to\quad \bar\psi \to \bar\psi e^{i\frac{1\mp\gamma_5}{2}\alpha} \qquad \text{with} \qquad \gamma_5 = \gamma_0\gamma_1\gamma_2\gamma_3\,, \quad \text{and} \quad \{\gamma_5\,,\,\gamma_\mu\} = 0\,, \tag{III.35}$$

which holds separately for each vector current $\psi\gamma_\mu t^a\psi$. Furthermore, in the chiral limit QCD is invariant under flavour rotations $SU(N_f)$. For example, for $N_f = 2$ with up (u) and down (d) quarks and the flavour isospin group with $SU(2)$, the transformation reads

$$\psi = \begin{pmatrix} u \\ d \end{pmatrix} \to V \begin{pmatrix} u \\ d \end{pmatrix}, \qquad \text{with} \qquad V = e^{i\theta^a\tau^a} \in SU(2)\,, \tag{III.36}$$

with $a = 1, 2, 3$. For the 2+1 flavour case also considered here the respective symmetry is $SU(3)_F$. Chiral symmetry entails that the flavour rotations are a symmetry for the left- and right-handed quarks separately and the combined symmetry is $SU(2)_L \times SU(2)_R$ with symmetry transformations $V_{L/R} = e^{i\frac{1\pm\gamma_5}{2}\theta^a t^a}$. Including also the chiral $U(1)$

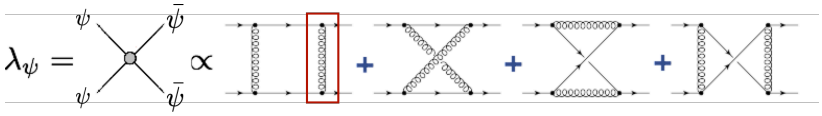

FIG. 6: One loop diagrams for the four-Fermi coupling λ_ψ in QCD.

rotations leads us to the full symmetry group

$$G_{\rm sym} = SU(N_c) \times SU(N_f)_V \times SU(N_f)_A \times U(1)_V \times U(1)_A \,, \tag{III.37}$$

where we have also taken into account the gauge group $SU(N_c)$. If we approximate (III.34) by a point-like four-Fermi interaction, one has to expand the tensor $\gamma_\mu \otimes \gamma_\nu$ multiplied by gauge group and flavour tensors. Then, the most general symmetric Ansatz is a combination of the tensor structures

$$\begin{aligned}
(V-A) &= (\bar\psi\gamma^\mu\psi)^2 + (\bar\psi\gamma^\mu\gamma^5\psi)^2 \\
(V+A) &= (\bar\psi\gamma^\mu\psi)^2 - (\bar\psi\gamma^\mu\gamma^5\psi)^2 \\
(S-P) &= (\bar\psi^f\psi^g)^2 - (\bar\psi^f\gamma^5\psi^g)^2 \\
(V-A)^{\rm adj} &= (\bar\psi\gamma^\mu t^a\psi)^2 + (\bar\psi\gamma^\mu\gamma^5 t^a\psi)^2 \,,
\end{aligned} \tag{III.38}$$

where f, g are flavour indices and $(\bar\psi^f\psi^g)^2 \equiv \bar\psi^f\psi^g\bar\psi^g\psi^f$. While each separate term in the tensors in (III.38) is invariant under gauge transformation, and under the flavour vector transformations, axial rotations in $SU(N_f)_A \times U(1)_A$ rotate the terms on the right hand side in (III.38) into each other. For a related full analysis we refer to the literature. However, below we shall exemplify these computations at the relevant example of the scalar–pseudo-scalar channel

The chiral invariants (III.38) can be rewritten using the Fierz transformations which relates different four-Fermi terms on the basis of the Grassmann natures of the fermions. These transformations are explained and detailed in the literature, see e.g. [7, 8]. Here we just concentrate on the scalar–pseudo-scalar channels in physical two-flavour QCD with $N_c = 3$ and $N_f = 2$. These channels are related to the scalar σ-meson and the pseudo-scalar pions $\vec\pi$. The $(S-P)$-channel is given by

$$(S-P) = \frac{1}{2}\left[(\bar\psi\psi)^2 + (\bar\psi\vec\tau\psi)^2 - (\bar\psi\gamma^5\psi)^2 - (\bar\psi\gamma^5\vec\tau\psi)^2\right] \,, \tag{III.39}$$

where $\vec\tau = (\sigma_1, \sigma_2, \sigma_3)$ with Pauli matrices

$$\sigma_1 = \begin{pmatrix} 0 & 1 \\ 1 & 0 \end{pmatrix} \,, \qquad \sigma_2 = \begin{pmatrix} 0 & -i \\ i & 0 \end{pmatrix} \,, \qquad \sigma_3 = \begin{pmatrix} 1 & 0 \\ 0 & -1 \end{pmatrix} \,, \tag{III.40}$$

The representation (III.39) simplifies the identification of the scalar mode $\bar\psi\psi$ related to the scalar σ-meson, and the pseudo-scalar modes $i\bar\psi\gamma_5\vec\tau\psi$ related to the pseudo-scalar (axial-scalar) pions $\vec\pi$.

We shall use the representation (III.39) in the following investigations of the chiral properties of low energy QCD. Hence we discuss its symmetry properties in more detail, and show explicitly its invariance under $G_{\rm sym}$. To begin with, the invariance of $(S-P)$ under gauge and flavour $U_V(1)$ transformation is apparent. The flavour $SU(2)_V$ transformations $\psi \to e^{i\theta^a\tau^a}\psi$ trivially leaves $\bar\psi\psi$ and $\bar\psi\gamma_5\psi$ invariant. For the vector and pseudo-vector bilinears we concentrate on infinitesimal transformations $e^{i\theta^a\tau^a} = 1 + i\theta^a\tau^a + O(\theta^2)$. Then the second term in (III.39) transforms as

$$(\bar\psi\vec\tau\psi)^2 \;\longrightarrow\; (\bar\psi\vec\tau\psi)^2 + 2i\,\theta^a(\bar\psi\vec\tau\psi)(\bar\psi[\vec\tau\,,\,\tau^a]\psi) = (\bar\psi\vec\tau\psi)^2 - 2\,\theta^a\epsilon^{bac}(\bar\psi\tau^b\psi)(\bar\psi\tau^c\psi) = (\bar\psi\vec\tau\psi)^2 \,. \tag{III.41}$$

The invariance of the last term in (III.39) under $SU(2)_V$ transformations follows analogously. Finally, axial transformations related the first two terms to the last two terms. We exemplify this property with the axial $U_A(1)$ rotations $\psi \to e^{i\gamma_5\alpha}\psi$, where we consider infinitesimal transformations with $e^{i\gamma_5\alpha} = 1\!\!1 + i\gamma_5\alpha + O(\alpha^2)$. Concentrating on the scalar and pseudo-scalar terms we have

$$(\bar\psi\psi)^2 - (\bar\psi\gamma^5\psi)^2 \;\longrightarrow\; (\bar\psi\psi)^2 - (\bar\psi\gamma^5\psi)^2 + 4i\,\alpha\Big[(\bar\psi\psi)(\bar\psi\gamma_5\psi) - (\bar\psi\gamma^5\psi)(\bar\psi\psi)\Big] = (\bar\psi\psi)^2 - (\bar\psi\gamma^5\psi)^2 \,, \tag{III.42}$$

The invariance for the full expression in (III.39) follows analogously. It is left to study $SU(2)_A$ transformations. Now we show that (III.39) also carries the $SU(2)_A$-invariance. To that end we consider infinitesimal $SU(2)_A$ transformations

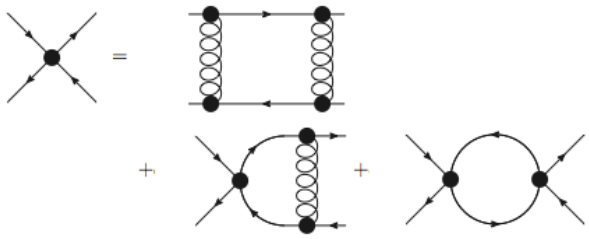

FIG. 7: One loop diagrams for the four-Fermi coupling λ_ψ from the action (III.50).

$e^{i\gamma_5\theta^a\tau^a} = 1 + i\gamma_5\theta^a\tau^a + O(\theta^2)$ of the combination $(\bar\psi\psi)^2 - (\bar\psi\gamma^5\vec\tau\psi)^2$, and use the Lie algebra identity

$$\tau^a\tau^b = \delta^{ab} + i\epsilon^{abc}\tau^c\,, \qquad \to \qquad \{\tau^a\,,\,\tau^b\} = 2\delta^{ab}\,. \tag{III.43}$$

Then we are led to

$$(\bar\psi\psi)^2 - (\bar\psi\gamma^5\vec\tau\psi)^2 \;\longrightarrow\; (\bar\psi\psi)^2 - (\bar\psi\gamma^5\vec\tau\psi)^2 + 2i\,\theta^a\Big[(\bar\psi\psi)(\bar\psi\gamma_5\tau^a\psi) - (\bar\psi\gamma^5\tau^b\psi)\,\big(\bar\psi\{\tau^a\,,\,\tau^b\}\psi\big)\Big] = (\bar\psi\psi)^2 - (\bar\psi\gamma^5\psi)^2\,. \tag{III.44}$$

The invariance of the combination $(\bar\psi\gamma_5\psi)^2 - (\bar\psi\vec\tau\psi)^2$ is shown along the same lines. Consequently (III.39) is invariant under $SU(2)_A$ transformation and hence under the full symmetry group G_{sym}.

In QCD, we have experimental evidence for the breaking of the axial $U_A(1)$-symmetry, i.e. the pseudo-scalar η'-meson (in $N_f = 2$ the η) is anomalously heavy. This mass-difference can be nicely explained by the anomalous breaking of axial $U_A(1)$ symmetry. Consequently, giving up axial $U_A(1)$-symmetry we have to consider more four-Fermi interactions as in (III.38) (altogether 10 invariants for $N_f = 2$), in particular

$$\frac{1}{2}\left[(\bar\psi\psi)^2 - (\bar\psi\vec\tau\psi)^2 + (\bar\psi\gamma^5\psi)^2 - (\bar\psi\gamma^5\vec\tau\psi)^2\right]\,. \tag{III.45}$$

It is the relative minus signs in the scalar and pseudo-scalar terms in comparison to (III.39) that leads to the breaking of $U_A(1)$-symmetry. This is easily seen by re-doing the infinitesimal analysis (III.42) in (III.45). If also follows easily that the other symmetries still hold, in particular the $SU(2)_V \times SU_A(2)_A$ invariance follows as (III.45) contains the same $SU(2)_V \times SU_A(2)_A$-invariant combinations of four-quark terms as (III.39). Hence we conclude that the combination (III.45) only breaks $U_A(1)$-symmetry, and adding up the two channels (III.39) and (III.45) leads to the $U_A(1)$-breaking combination

$$\frac{1}{2}\left[(\bar\psi\psi)^2 - (\bar\psi\gamma^5\vec\tau\psi)^2\right]\,. \tag{III.46}$$

Equation (III.46) is invariant under the remaining symmetries $SU(N_c)\times SU(N_f)_V \times SU(N_f)_A \times U(1)_V$. This concludes our brief discussion of the global symmetries of QCD in the chiral limit.

In summary the following picture emerges: assume we perform a chain of scattering experiments of QCD/Standard Model starting at the electroweak scale ≈ 90 Gev towards the strong QCD scale Λ_{QCD}. At each scale we can describe the quantum equations of motion and scattering experiments by a suitably chosen effective action $\Gamma[\phi]$. On the level of the path integral for QCD, (I.34), this is described by the Wilsonian idea of integrating out momentum modes above some momentum scale μ,

$$Z_\mu[J] = \int [\mathrm{d}\Phi]_{p^2\geq\mu^2}\, e^{-S_{\text{QCD}}[\Phi]+\int_x J\cdot\Phi} \qquad \Rightarrow \qquad \text{Effective Action } \Gamma_\mu[\Phi]\,, \tag{III.47}$$

where the path integral measure only contains an integration over fields Φ_μ that are non-vanishing for $p^2 \geq \mu^2$: $\Phi_\mu(p^2 < \mu^2) \equiv 0$. After Legendre transformation this leads us to an effective action $\Gamma_\mu[\Phi]$ that only contains the quantum effects of scales larger than the running (RG) scale μ and serves as a classical action for the quantum effects with momentum scales $p^2 < \mu^2$. This effective action also carries the symmetries of the fundamental QCD action, as long as these symmetries are not (anomalously broken by quantum effects.

We know already from the perturbative renormalisation programme that this amounts to adjusting the (running) coupling in the (classical) action with the sliding (experimental) momentum scale. In such a Wilsonian setting this is very apparent. The running of the coupling comes from the loop diagrams that are evaluated at the momentum scale

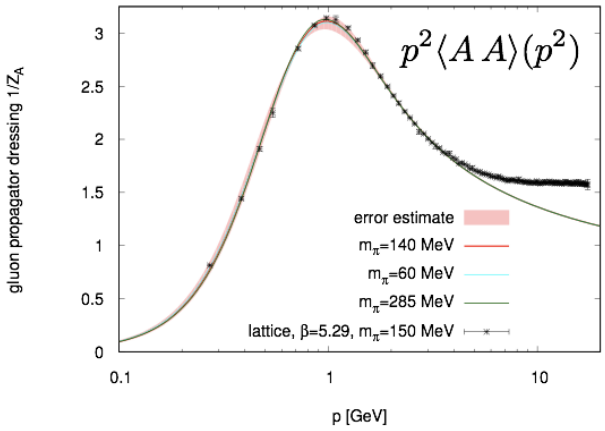

FIG. 8: Gluon propagator for $N_f = 2$ from the lattice and from non-perturbative diagrammatic methods, taken from [9].

μ. On top of this momentum adjustment of the fundamental parameters of the theory one also creates additional terms in the -effective- action. The one of importance for us is the four-Fermi terms argued for above. It is created at one-loop with the box diagrams depicted in depicted in Figure 6. This leads us finally to the following four-Fermi interaction in the effective action,

$$\Gamma_{4-\text{fermi}}[\phi]|_{1-\text{loop}} = -\frac{\lambda_\psi}{4}\int\left[(\bar\psi\psi)^2 - (\bar\psi\gamma^5\vec\tau\psi)^2\right] + \cdots \qquad \text{with} \qquad \lambda_\psi \propto \alpha_s^2\,, \tag{III.48}$$

where it is understood that the coupling λ_ψ carries the running momentum or RG scale μ introduced above. Together with the kinetic term of the quarks this is the classical action of the Nambu–Jona-Lasinio type model. Equation (III.48) holds for massless quarks and two flavours, $N_f = 2$. The two terms in (III.48) carry the same quantum number as the scalar and axial-scalar excitations in low energy QCD, the sigma-meson σ and pion $\vec\pi$ respectively. The one loop diagrams generating the four-Fermi coupling λ_ψ are depicted in Figure 6. In line with the picture outlined above the four-Fermi coupling λ_ψ at a given momentum scale $p = \mu$ should be computed with the loop momenta q in the box diagrams in Figure 6 being bigger than μ. Than the related diagram is peaked at this scale and we conclude by dimensional analysis that

$$\lambda_\psi(\mu) \simeq \alpha_s^2(\mu)\frac{1}{\mu^2}\,. \tag{III.49}$$

Note that this coupling feeds back into the loop expansion of other correlations functions such as the quark propagator and quark-gluon vertices. However, in comparison to other (one-loop) diagrams it is suppressed by additional orders of the strong coupling α_s. In turn, in the low momentum regime where α_s grows strong it gives potentially relevant contributions. Indeed, taking as a starting point for a loop analysis the sum of the QCD action (III.33) and the four-Fermi term (III.48)

$$\Gamma[\phi] \simeq S_{\text{QCD}}[\phi] + \Gamma_{4-\text{fermi}}[\phi]\,, \tag{III.50}$$

we get also self-interaction terms of the four-Fermi coupling proportional to λ_ψ^2 as well as terms proportional to $\alpha_s\lambda_\psi$. This is depicted in Figure 7.

The glue sector of QCD is expected to have a mass gap already present in the purely gluonic theory, related to the confinement property of Yang-Mills theory. Then this has to manifest itself in a decoupling of the gluonic contribution to the four-Fermi coupling in Figure 7. In the Landau gauge this mechanism is easily visible due to the mass gap in the gluon propagators, see Figure 8 for lattice results and results from non-perturbative diagrammatic methods.

Note that the gluon propagator is gauge dependent, and the careful statement is that the Landau gauge facilitates the access to the related physics. One should not confuse this with a massive gluon, as the gluon is no physical particle and shows positivity violation. Moreover, the gluonic sector is certainly relevant for the confining physics and hence the decoupling discussed above only takes place in the matter sector for the specific question under investigation, the mechanism of strong chiral symmetry breaking.

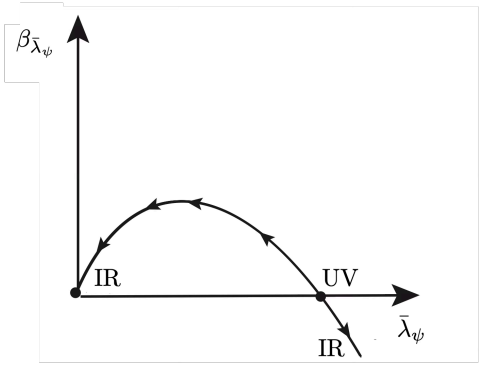

FIG. 9: Sketch of the β-function of the dimensionless four-quark coupling $\bar\lambda_\psi$ in NJL-type models.

E. Strong chiral symmetry breaking and quark-hadron effective theories

Assuming for the moment the gluonic decoupling we are left with a purely fermionic theory. The four-Fermi term (III.48) is the interaction part of the Nambu–Jona-Lasino model, one of the best-studied model for low energy QCD, see e.g. [7, 8, 10]. It is non-renormalisable as can be seen from the momentum dimension of the four-Fermi coupling which is -2. As shown above, in QCD it is generated by fluctuations with $\lambda_\psi(p) \propto \alpha_s(p)$ and tends to zero in the UV, that is for large momenta $p \to \infty$. Its momentum dependence is best extracted from the dimensionless coupling

$$\bar\lambda_\psi = \lambda_\psi(\mu)\mu^2\,, \tag{III.51}$$

where we have introduced the renormalisation group scale μ, here being identical with the momentum scale of the scattering process described, $\mu^2 = p^2$. The β-function of the dimensionless four-Fermi coupling in (III.51) is given by

$$\beta_{\bar\lambda_\psi} = \mu\partial_\mu\bar\lambda_\psi = 2\bar\lambda_\psi - A\,\bar\lambda_\psi^2 \qquad \text{with} \qquad A > 0\,, \tag{III.52}$$

and is depicted in Figure 9. The prefactor A depends on the RG-scale μ as well as other parameters of the theory such as the masses. The full RG equation for the four-quark coupling in QCD is depicted in Figure 11 and its analysis will be done in Section III F. Here we concentrate on the underlying mechanism of chiral symmetry breaking. The first term on the right hand side of (III.52) encodes the trivial dimensional running of $\bar\lambda_\psi$. The second term on the right hand side originates in the last diagram in Figure 7, the pure four-Fermi term. In the absense of other mass scales this loop has to be proportional to μ^2 leading to a factor two in the β-function in comparison to the loop itself. The key feature relevant for the description of chiral symmetry breaking is the sign of the diagram. It is negative, $-A\bar\lambda^2$, with a positive constant A leading to (III.52).

From the perspective of a one-loop investigation based on the classical fermionic action in (III.50) the coupling in the loop term on the right hand side of (III.52) is the classical one in this action. As we have done for the β-function of the strong coupling, e.g. (II.17), we can elevate this coupling to the full running coupling in terms of a one-loop RG-improvement. This accounts for a one-loop resummation of diagrams. In the present context the physics behind such an improvement is very apparent: As already indicated, the NJL-type action was derived within a successive integrating out of momentum modes, and constitutes an effective action for the UV physics with $p^2 \geq \mu^2$. Accordingly, its couplings depend on this RG-scale. In summary we end up with (III.52) with μ-dependen couplings on the right hand side. Note that this is only a one-loop RG improvement as we have discarded the μ-dependence of the couplings in the diagram when taking the μ-derivative. The related terms are proportional to $-A/2\,\bar\lambda_\psi\,\mu\partial_\mu\bar\lambda_\psi$ and can be shuffled to the left hand side. This accounts for a further resummation leading to (III.52) with a global factor $1/(1 + A/2\,\bar\lambda)$ on the right hand side. In the following qualitative analysis it is dropped and we strictly resort to the one-loop improvement.

The β-function of (III.52) is depicted in Figure 9. It divides the positive $\bar\lambda_\psi$-axis into two physically distinct regimes,

$$I_1 = [0, \bar\lambda_{\rm UV}) \qquad \text{and} \qquad I_2 = (\bar\lambda_{\rm UV}, \infty) \qquad \text{with} \qquad \beta_{\bar\lambda_\psi}(\bar\lambda_{\rm UV}) = 0 \qquad \text{with} \qquad \bar\lambda_{\rm UV} = \frac{2}{A}\,. \tag{III.53}$$

The zeroes of the β-function are fixed points of the renormalisation group flows, and $\bar\lambda_{\rm UV} \neq 0$ is a non-trivial fixed point FP of the β-function while $\bar\lambda_{\rm Gauß} = 0$ is the trivial Gaußian fixed point (related to the free Gaußian theory). Now

we initiate the RG-flow at an initial ultraviolet scale $\mu_{\rm in}$ with some value of the dimensionless four-quark coupling

$$\bar\lambda_\psi(\mu_{\rm in}) = \bar\lambda_{\psi,\,\rm in}\,. \tag{III.54}$$

If $\bar\lambda_{\psi,\,\rm in} < \bar\lambda_{\rm UV}$ and we lower the running momentum scale, the RG-flow lowers the four-Fermi coupling towards 0. Accordingly $\bar\lambda_\psi(\mu\to 0) = 0$. Since the regime of small couplings is governed by the linear term $2\bar\lambda_\psi$ in the β-function in (III.52) this entails $\lambda_\psi(\mu\to 0) = \lambda_0$. Here λ_0 is some finite value which is adjusted by the input $\bar\lambda_{\psi,\rm in}$ at the initial scale $\mu_{\rm in}$.

In turn, if $\bar\lambda_{\psi,\,\rm in} > \bar\lambda_{\rm UV}$, the RG-flow toward smaller μ drives $\bar\lambda_\psi$ towards ∞. Then the linear term can be neglected as it is sub-leading and the RG-flow reads

$$\mu\partial_\mu\bar\lambda_\psi = -A\,\bar\lambda_\psi^2\,, \qquad\longrightarrow\qquad \bar\lambda_\psi(\mu) = \frac{\bar\lambda(\mu_0)}{1+\bar\lambda_\psi(\mu_0)A\,\log\mu/\mu_0}\,, \tag{III.55}$$

where μ_0 is some reference scale at which the approximation in the RG-flow in (III.55) is already valid. We conclude from (III.55) diverges at

$$\mu = \mu_0\exp\left\{-\frac{1}{A\,\bar\lambda(\mu_0)}\right\}\,, \tag{III.56}$$

which signals a resonance in the four-quark scalar-pseudo–scalar channel with the quantum numbers of the σ- mode and the pion.

At this scale chiral symmetry breaking occurs. To make this more apparent we resort to a further rewriting of our low energy effective theory in terms of the scalar, σ, and pseudo-scalar, $\vec\pi$, degrees of freedom. This is suggestive already for the reason that the divergence in (III.55) entails that these resonance are relevant degrees of freedom for lower momentum scales. For the rewriting of the theory we use the Hubbard-Stratonovich transformation, see e.g. [7, 8, 10]. With this transformation we a four-Fermi interaction using a scalar auxiliary field. Concentrating on the scalar part of the four-Fermi interaction in (III.48) we write at some momentum scale μ,

$$-\frac{\lambda_\psi}{4}(\bar\psi\psi)^2 = \left[\frac{h}{2}(\bar\psi\psi)\sigma + \frac{m_\varphi^2}{2}\sigma^2\right]_{\rm EoM(\sigma)}\,, \qquad\text{with}\qquad \lambda_\psi = \frac{h^2}{m_\varphi^2}\,. \tag{III.57}$$

Accordingly we can extend the effective action $\Gamma[\phi]$ given in (III.50) by the right hand side of (III.57) while dropping the four-Fermi term. For the sake of simplicity we concentrate on the σ-meson first and reduce the four-Fermi term to its scalar part. Then

$$\Gamma[\phi]\to\Gamma[\phi,\sigma] = \Gamma[\phi]|_{\lambda_\psi\to 0} + \left[\frac{h}{2}(\bar\psi\psi)\sigma + \frac{m^2}{2}\sigma^2\right]_{h^2/m^2=\lambda_\psi}\,, \tag{III.58}$$

This new effective action agrees with the original one on the equation of motion of σ and hence carries the same physics. As a side remark, note that the 1PI correlation functions of quarks and gluon derived from $\Gamma[\phi,\sigma]$ at fixed σ do not agree with the quark and gluon correlation functions derived from $\Gamma[\phi] = \Gamma[\phi,\sigma_{\rm EoM}(\phi)]$, the implicit dependences also contribute.

A similar derivation can be done for the pion part of the four-Fermi interaction, and hence the whole four-Fermi interaction can be bosonised. The mesonic equations of motion can be summarised in

$$\sigma_{\rm EoM} = \frac{h}{2m_\varphi^2}\,\bar\psi\psi\,, \qquad\qquad \vec\pi_{\rm EoM} = \frac{h}{2m_\varphi^2}\,\bar\psi\,i\gamma_5\vec\tau\psi\,. \tag{III.59}$$

On the level of the generating functional of QCD, (III.57) and its extension to pions can be implemented by a Gaußian path integral with

$$\exp\left\{\frac{\lambda_\psi}{4}\int\left[(\bar\psi\psi)^2-(\bar\psi\gamma^5\vec\tau\psi)^2\right]\right\} = \int{\rm d}\sigma{\rm d}\vec\pi\,\exp\left\{-\int_x\left(\frac{1}{2}m^2(\sigma^2+\vec\pi^2)+\frac{h}{2}\bar\psi\left[\sigma+i\gamma_5\vec\tau\vec\pi\right]\psi\right)\right\}_{h^2/m^2=\lambda_\psi}\,. \tag{III.60}$$

We also remark that as shift in the σ-field,

$$\sigma \to -\frac{2}{h} m_\psi + \sigma \,, \tag{III.61}$$

eliminates the quark mass term at the expense of the linear term in σ that can be interpreted as a source term. Inserting this identity in the path integral for the low energy dofs including the currents for the fundamental fields, the quarks and gluons (and ghosts) as well as current for the mesonic dofs we have the full generating functional in this setting. Performing the Legendre transformation we are immediately led to (III.58). Kinetic terms as well as a potential for σ are generated by further quantum effects. In summary this leads us finally to a low energy effective theory with a classical action $S_{\rm eff} = \Gamma_{\rm UV}$, where $\Gamma_{\rm UV}$ is the full quantum effective action including quantum fluctuations above a given cutoff scale Λ. This also entails that $S_{\rm eff}$ carries a Λ-dependence. $S_{\rm eff}$ is given by

$$S_{\rm eff}[\psi,\bar\psi,\phi] \propto \int_x \bar\psi \cdot (\not\partial + m_\psi) \cdot \psi + \int_x \left[(\partial_\mu\sigma)^2 + (\partial_\mu\vec\pi)^2\right] + \int_x \frac{h}{2}\bar\psi\left[\sigma + i\gamma_5\vec\tau\vec\pi\right]\psi + \int_x V_{\rm UV}(\rho) \tag{III.62}$$

with $\phi = (\sigma,\vec\pi)$ and

$$V_{\rm UV}(\rho) = m_\varphi^2\rho + \frac{\lambda}{2}\rho^2 \,, \qquad \text{with} \qquad \rho = \frac{1}{2}\left(\sigma^2 + \vec\pi^2\right) . \tag{III.63}$$

As indicated above, the quark mass term can be eliminated at the expense of a linear term in σ by the shift of σ in (III.61). On the level of the quadratic quark-meson interaction (III.60) this triggers a linear term $c_\sigma\sigma$ and the full potential reads

$$V_{\rm UV}(\rho) = m_\varphi^2\rho + \frac{\lambda_\varphi}{2}\rho^2 - c_\sigma\,\sigma \,, \qquad \text{with} \qquad c_\sigma = \frac{2}{h} m_\varphi^2 m_\psi \,. \tag{III.64}$$

This concludes the derivation of the low energy effective theory with the action (III.62) from QCD by *integrating-out* QCD quantum fluctuations above the validity scale of the low energy effective theory. From the gluonic decoupling scale $\Lambda_{\rm dec} \lesssim 1$ GeV one concludes that (III.62) should be seen as a classical action for quantum fluctuations with momenta $p^2 \lesssim 1$ GeV, see Figure 8. A more detailed analysis reveals that the initial scale for low energy effective theories has to be taken far lower for quantitative computations. Nonetheless, for qualitative considerations it is sufficient, and, as a matter of fact, low energy effective theories even work well quantitatively at surprisingly large moment scale about 1 GeV.

In (III.62) we have introduced a self-interaction of the mesonic fields proportional to ρ^2 as well as an explicit breaking term linear in σ related to the quark mass term. The question arises, is this the most general ϕ^4-term one can generate from QCD? As mentioned before, the symmetries of this low energy effective field theory (EFT) are determined by those of the action of QCD. In the chiral limit the full symmetry group is (III.37). The axial $U_A(1)$ symmetry is anomalously broken, hence our restriction to the $U_A(1)$-breaking combination (III.46). In its bosonised quark-meson mode version the symmetry transformations with $G_{\rm sym}$ also involve transformations of the mesonic fields. Their transformation properties can be most easily accessed in the matrix notation for the field. To that end we introduce

$$\hat\phi = \mathbb{1}\,\sigma + i\gamma_5\vec\tau\vec\pi \qquad \text{with} \qquad \hat\phi_{\rm EoM} = \frac{h}{2m_\varphi^2}\left(\mathbb{1}\,\bar\psi\psi - \gamma_5\vec\tau\,\bar\psi\gamma_5\vec\tau\psi\right) , \tag{III.65}$$

where we have used (III.59) in the second equation. Now we can read-off the symmetry transformations under $V \in SU(N_c)\times SU(N_f)_V \times SU(N_f)_A \times U(1)_V$ from (III.65) by evoking the symmetry transformations of the quarks. One easily sees that axial $U(1)_A$-rotations do not close on σ and $\vec\pi$. For example, $\sigma_{\rm EoM}$ transforms into $\bar\psi\gamma_5\psi$. Furthermore, ϕ is invariant under vector $U_V(1)$ transformations. Similarly, σ is invariant under transformations with $e^{i\theta^a\tau^a} \in SU(2)_V$, while π is rotated, $\vec\pi \to V\vec\pi$ with $V = e^{\theta^a t^a} \in O(3)$ with $(t^a)^{bc} = \epsilon^{abc}$. This follows from

$$\bar\psi\gamma_5\vec\tau\psi \;\longrightarrow\; \bar\psi\gamma_5\vec\tau\psi + i\theta^a\bar\psi\gamma_5[\vec\tau\,,\,\tau^a]\psi = \bar\psi\gamma_5\vec\tau\psi - \theta^a\epsilon^{bac}\bar\psi\gamma_5\tau^c\psi \,. \tag{III.66}$$

Finally, transformations with $e^{i\gamma_5\theta^a\tau^a} \in SU(2)_A$ rotate $(\sigma,\vec\pi)$ into each other. This is read-off from the infinitesimal transformations of $\hat\phi_{\rm EoM}$ leading to

$$\sigma \to \sigma + 2\theta^a\pi^a \,, \qquad\qquad \pi^b \to \pi^b - \theta^b\sigma \,. \tag{III.67}$$

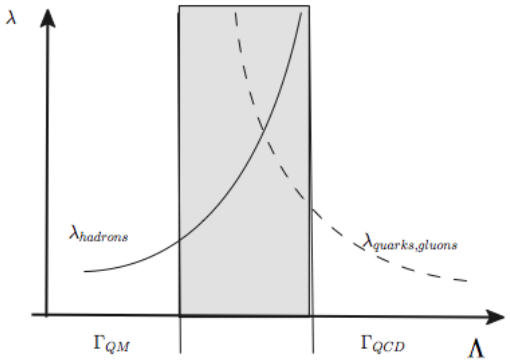

FIG. 10: Scale dependence of the effective four-Fermi coupling. The shaded area is the regime where the effective field theory is triggered.

Combining all the manifestations of the symmetry group we are led to an $O(4)$ invariance of our low energy effective field theory, sloppily written as

$$\psi \to V\psi \quad \text{with} \quad V \in G_{\text{sym}}/U_A(1)\,, \qquad \phi \to e^{\theta^a t^a}\phi\,, \qquad \text{with} \quad \phi = \begin{pmatrix} \vec{\pi} \\ \sigma \end{pmatrix} \quad \text{and} \quad e^{\theta^a t^a} \in O(4)\,. \tag{III.68}$$

In conclusion chiral symmetry breaking is in one-to-one correspondence to the breaking of the $O(4)$-symmetry. Moreover, the formulation with effective mesonic σ and pion degrees of freedom now allows us to discuss strong chiral symmetry breaking in complete analogy to the Higgs mechanism that served as an introductory example. Let us first consider the fully symmetric case with $c_\sigma = 0$. The mesonic sector of (III.62) simply is an $O(4)$-model, and the QCD four-Fermi coupling are related to the Yukawa coupling and the mesonic mass parameters via the relation (III.57) in the Hubbard-Stratonovich transformation. Accordingly, a diverging λ_ψ implies a vanishing m_φ if the Yukawa coupling is fixed. Hence, at the singularity of λ_ψ the mesonic mass parameter m_φ^2 changes sign. For $m_\varphi^2 < 0$ we are in the phase of -spontaneously- broken $O(4)$-symmetry. We choose the σ direction as our radial mode, and its expectation value is given by

$$\sigma_0 = \sqrt{\frac{-m_\varphi^2}{\lambda_\varphi}}\,, \tag{III.69}$$

in the chiral limit. This leads to an effective quark mass term with

$$m_\psi = \frac{h}{2}\sigma_0 = \frac{h}{2}\sqrt{\frac{-m_\varphi^2}{\lambda_\varphi}}\,, \tag{III.70}$$

which in QCD is of the order of 300 MeV.

In summary we have derivated low energy EFTs in QCD by successively integrating out momentum shells of quantum fluctuations in QCD. The first class of low energy EFTS we encountered are the *Nambu-Jona–Lasigno type four-quark models* (in short in a slight abuse of notation NJL-model), baptised after a seminal work of Nambu and Jona-Lasigno from 1961 introducing a four-Fermi model for Nucleons. NJL-type models are not renormalisable and requires a ultraviolet cutoff scale Λ_{UV} that cannot be removed.

In a second step we have bosonised the resonant scalar–pseudo-scalar channels of the four-quark interaction leading us to a Yukawa-type model, the *Quark-Meson Model* (QM-model). This model is renormalisable and its UV cutoff Λ_{UV} seemingly can be removed to infinity. However, we emphasise that the two models are equivalent on the level of the respective path integrals via the Hubbard-Stratonovich transformation. In other words, if one considers all quantum fluctuations in both models the physics results are the same, as must be the necessity of a ultraviolet cutoff scale Λ_{UV}. In the QM model this necessity is encoded in a UV-instability of the model. In other words, its renormalisability is of no help if it comes to the existence of the model at large scales.

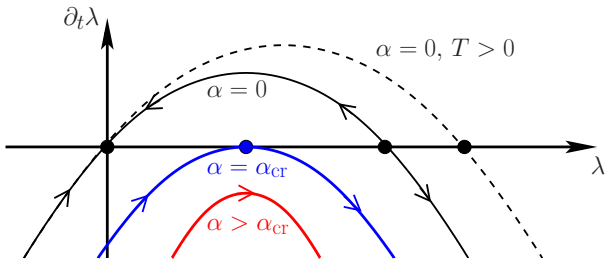

FIG. 11: Flow $\partial_t\bar{\lambda}_q$ of the dimensionless four-quark coupling $\bar{\lambda}_\psi = \lambda_\psi k^2$ in the scalar-pseudoscalar channel as a function of the four-quark coupling for different values of the strong couplings α_s. If the strong coupling is large enough, $\alpha_s > \alpha_{s,\rm cr}$ with the critical coupling $\alpha_{s,\rm cr}$, the flow is negative for all $\bar{\lambda}_q$. Then, chiral symmetry breaking happens for all initial values of $\bar{\lambda}_\psi$, for more details see the discussion below(III.71).

F. Chiral symmetry breaking in QCD

In the last Chapters we have derived low energy effective theories of QCD that capture chiral symmetry breaking in terms of the respective initial condition for the four-quark coupling at the UV-scale $\Lambda \propto 1\,\text{GeV}$ of these models. It is left to analyse how QCD triggers the respective symmetry-breaking four-quark couplings. For this analysis we extend the renormalisation group analysis of the four-quark coupling on the basis of (III.52) to that in full QCD. The respective RG-equation can be derived from the diagrammatic form of the four-quark coupling, its sketch has been provided in 7. In contradistinction to (III.52) the full β-function has two further terms, one is proportional to α_s^2 with $\alpha_s = g_s^2/(4\pi)$. It is given by $-C\,\alpha^2$ with a positive prefactor C and comprises the contributions of the quark-gluon box diagrams in (III.52), see also 6. These diagrams generate the four-quark coupling at large momentum scales in the first place. A further contribution comes from the mixed diagram in 7 with one gluon exchange and one four-quark coupling. Accordingly it is proportional to $\alpha_s\lambda_\psi$, and is given by -$B\,\alpha_s\bar{\lambda}_\psi$ with a positive prefactor B . In summary this leaves us with the full RG-equation for the dimensionless four-quark interaction $\bar{\lambda}_\psi$ in the scalar–pseudoscalar channel, schematically given by

$$\beta_{\bar{\lambda}_\psi} = 2\bar{\lambda}_\psi - A\,\bar{\lambda}_\psi^2 - B\bar{\lambda}_\psi\alpha_s - C\,\alpha_s^2 + \text{tadpole-terms}\,, \tag{III.71}$$

and the positive constants A, B, C depend on other parameters of the theory, and in particular on the mass scales. It is depicted in Figure 11. In (III.71), $2\bar{\lambda}_\psi$ is the canonical scaling term and the other terms are quantum corrections computed from the respective diagrams in the flow. For $\alpha_s = 0$, the β-function in(III.71) reduces to that of the four-quark coupling in an NJL-type model, (III.52). Then, for large enough initial coupling $\bar{\lambda}_\psi(\mu = \Lambda) > 2/A(\Lambda)$ at the UV cutoff scale Λ, the β-function $\partial_t\bar{\lambda}_\psi$ is negative and the coupling grows towards the infrared. It finally diverges at a pole that signals chiral symmetry breaking. In turn, for $\bar{\lambda}_\psi(\mu = \Lambda) < 2/A(\Lambda)$ the coupling weakens towards the infrared and runs into the Gaußian fixed point without chiral symmetry breaking.

When switching on the strong coupling, the β-function of the four-quark coupling in(III.71) is deformed: Firstly, the canonical running gets an anomalous part with $2\bar{\lambda}_\psi \to (2 - B\,\alpha_s)\bar{\lambda}_\psi$. More importantly the whole β-function is shifted down globally by $-C\,\alpha_s^2$, see Figure 11. This term originates from quark-gluon box diagrams and is negative. For large enough α_s the β-function $\beta_{\bar{\lambda}_\psi}$ is negative for all $\bar{\lambda}_\psi$,

$$\partial_t\bar{\lambda}_\psi < 0 \quad \forall\bar{\lambda} \quad \text{if} \quad \alpha_s > \alpha_{s,\rm cr}\,, \qquad \text{with} \qquad \alpha_{s,\rm cr} = \frac{2}{B + 2\sqrt{A\,C}}\,, \tag{III.72}$$

with the critical coupling $\alpha_{s,\rm cr}$, see Figure 11. Accordingly, if the growth of the strong coupling towards the infrared is unlimited, chiral symmetry breaking in QCD is always present, and is basically the converse of asymptotic freedom. More precisely it is the one-gluon exchange coupling in the quark-gluon box diagrams that has to satisfy(III.72) in the infrared. In this context it is important to mention that it is the gapping of the gluon depicted in Figure 8 related to confinement that stops the growth of the exchange couplings in the infrared and even leads to their decay for small momenta. In short, the glue dynamics decouples below momenta of one GeV, leaving us with the quark-hadron dynamics.

Moreover, the simple relation between the size of the strong coupling and chiral symmetry breaking also provides a simple explanation for the restoration at finite temperature, which we already add here as a sneak preview: the strong coupling melts down and finally we have $\alpha_s < \alpha_{s,\rm cr}$ for all frequencies and momenta, and spontaneous chiral

symmetry breaking cannot happen any more.

In summary, the analyses in the last Chapters have revealed, how dynamical chiral symmetry breaking occurs in QCD and the glue dynamic decouples in the infrared, and the dynamics of low energy QCD is well-described with the low energy effective theories introduced before. Despite being low energy EFTs, these models have a complicated dynamics reflecting the strongly-correlated nature of low energy QCD. Hence, typically one resorts to approximations within these models. In the reminder of this chapter we shall discuss different approximations to the Quark-Meson model ranging from a mean-field treatment to a full non-perturbative renormalisation group study.

G. Low energy quantum fluctuations

In the last chapter we have derived the action of the QM-model by integrating out quantum fluctuations above a momentum scale $\Lambda \approx 1$ GeV. We have argued that below this scale the gluonic degrees of freedom become less important and decouple from the theory below the mass gap of QCD. Practically, this can be seen from the results for gluonic correlation functions such as the gluon propagator displayed in Figure 8. This entails that the action (III.62) serves as a classical action for the quantum fluctuations with momenta $p^2 \leq \Lambda^2$. More explicitly we use the definition (III.47) with $\mu = \Lambda$ and arrive at the path integral

$$Z \approx \int [d\phi\, d\psi d\bar{\psi}]_{p^2\leq\Lambda^2} e^{-S_{\text{eff},\Lambda}[\psi_<,\bar{\psi}_<,\phi_<]} \qquad \text{with} \qquad Z_\Lambda \simeq e^{-S_{\text{eff},\Lambda}}\,, \tag{III.73}$$

where we have dropped the source terms. The fields $\psi_<, \bar{\psi}_<, \phi_<$ only carry low momentum modes with momenta $p^2 < \Lambda^2$. Then the full quark field $\psi = \psi_< + \psi_>$ is a sum of $\psi_< = \psi_{p^2\geq\mu^2}$ and $\psi_> = \psi_{p^2\geq\mu^2}$. Note also that the path integral of the large momentum modes in (III.47) is performed in the presence of fields that also carry low momentum contributions,

$$Z_\Lambda[\psi_<, \bar{\psi}_<, \phi_<] = \int [\mathrm{d}\Phi]_{p^2\geq\mu^2}\, e^{-S[\phi,\Phi]}\,. \tag{III.74}$$

where S is the QCD action with a bosonised scalar–pseudo-scalar channel. Equation (III.73) is approximate as we do not integrate out the low momentum gluons. Therefore low energy quantum effects with momentum scales $p^2 \leq \Lambda$ are encoded in loop diagrams with the classical action $S_{\text{eff},\Lambda} \simeq \Gamma_\Lambda$ defined in (III.62). Here, Γ_Λ is the effective action that originates in the integrating-out of QCD fluctuations with momenta $p^2 \geq \Lambda^2$. Henceforth we drop the supscripts $_{<,>}$ for the sake of readability.

As we have seen at the end of the last chapter, the coupling parameters in the mesonic potential play a crucial rôle for chiral symmetry breaking. Here we compute the one-loop correction to the 'classical' potential V in (III.64) as well as studying its the renormalisation group or flow equation.

1. *Quark quantum fluctuations*

First we note that the quark path integral in (III.73) with the action $S_{\text{eff},\Lambda}$ in (III.62) is Gaußian, and hence the one-loop computation is exact. This leads to the following representation of (III.73),

$$Z \approx \int \int [d\phi]_{p^2\leq\Lambda^2} e^{-S_{\phi,\text{eff},\Lambda}[\phi]}\,, \tag{III.75}$$

with

$$S_{\phi,\text{eff},\Lambda}[\phi] = \int_x \left[(\partial_\mu\sigma)^2 + (\partial_\mu\vec{\pi})^2\right] + \int_x V_{\text{UV}}(\rho) - \ln\left[\frac{1}{\mathcal{N}}\int [d\psi d\bar{\psi}]_{p^2\leq\Lambda^2} e^{-\int_x \bar{\psi}\cdot\left(\not{\partial}+m_\psi\right)\cdot\psi + \int_x \frac{h}{2}\bar{\psi}[\sigma+i\gamma_5\vec{\tau}\vec{\pi}]\psi}\right]\,, \tag{III.76}$$

where $1/\mathcal{N}$ is an appropriate, field-independent normalisation specified later. The quark path integral can be rewritten as follows,

$$\frac{1}{\mathcal{N}}\int [d\psi d\bar{\psi}]_{p^2\leq\Lambda^2}\, e^{-\int_x \bar{\psi}\cdot\left(\not{\partial}+\frac{h}{2}[\sigma+i\gamma_5\vec{\tau}\vec{\pi}]\right)\cdot\psi} = \frac{1}{\mathcal{N}}\det{}_\Lambda\left(\not{\partial} + \frac{h}{2}\left[\sigma + i\gamma_5\vec{\tau}\vec{\pi}\right]\right)\,, \tag{III.77}$$

where $\det_\Lambda$ is the determinant from momentum modes with $p^2 \leq \Lambda^2$. Expanded in powers of the field, the logarithm of (III.77) adds to the kinetic term in (III.76) as well as to the potential V. It also leads to terms with higher order derivatives or derivative couplings such as $Z(\rho)(\partial_\mu\phi)^2$, $(\phi\Delta\phi)^2$. As we work at low energies we drop these terms in the spirit of an expansion in $p^2/m^2_{\rm gap}$ where $m^2_{\rm gap}$ is the lowest mass scale in QCD. Evidently the pion plays a special role as is has a very small mass in comparison to the QCD mass scale $\Lambda_{\rm QCD}$ The mass scales $m_{\rm had}$ of all other hadronic low energy degrees of freedom in QCD satisfy $m_{\rm had} \gtrsim \Lambda_{\rm QCD}$. Accordingly the pion carries the quantum fluctuations in QCD for scales below $\Lambda_{\rm QCD}$. These scale considerations are also behind the impressively successful framework of chiral perturbation theory. In summary at leading order the low energy effective action $S_{\phi,\rm eff}$ only changes to $V_{\rm UV} \to V_{\phi,\rm eff}$,

$$V_{\phi,\rm eff}(\rho) = V_{\rm UV}(\rho) + \Delta V_q(\rho)\,, \tag{III.78}$$

with

$$\Delta V_q(\rho) = -{\rm Tr}_\Lambda \ln\left(\not{D} + \frac{h}{2}\left[\sigma + i\gamma_5\vec{\tau}\vec{\pi}\right]\right) + \ln\mathcal{N}\,, \qquad V_{\rm UV}(\rho) = m^2_\varphi\rho + \frac{\lambda_\varphi}{2}\rho^2\,. \tag{III.79}$$

In (III.79) we have used that for a given operator $\mathcal{O}$ we have $\ln\det_\Lambda\mathcal{O} = {\rm Tr}_\Lambda\ln\mathcal{O}$, where the trace sums over momenta with $p^2 \leq \Lambda^2$, as well as Dirac and internal indices, and the 'classical' potential V defined in (III.63). For the present considerations and scales the gluonic fluctuations and background are irrelevant. Thus we have dropped the gluonic fluctuations and we also put the gauge field to zero, $A_\mu = 0$. At finite temperature and density we also will consider constant temporal backgrounds $A_0 \neq 0$ which is related to so-called *statistical confinement*. Finally we introduce a convenient choice for the normalisation $\ln\mathcal{N}$: the quark determinant at vanishing background,

$$\ln\mathcal{N} \simeq \frac{1}{2}{\rm Tr}_\Lambda\ln\left(-\not{\partial}^2\right)\,, \tag{III.80}$$

where we have rewritten the determinant in terms of the positive semi-definite Laplace operator $-\not{\partial}^2 = -\partial^2_\mu$. Due to the symmetry analysis performed above the fermionic determinant can only depend on the $O(4)$-invariant combination $\rho = 1/2(\sigma^2 + \vec{\pi}^2)$, and we can simplify the computation by using $\vec{\pi} \equiv 0$. In momentum space we have

$$\begin{aligned} V_{\phi,\rm eff}(\sigma^2/2) &= V_{\rm UV}(\sigma^2/2) - N_f N_c \int\frac{d\Omega_4}{(2\pi)^4}\int_0^\Lambda dp\, p^3\,{\rm tr}_{\rm Dirac}\ln\frac{i\not{p} + \frac{h}{2}\sigma}{i\not{p}} \\ &= V_{\rm UV}(\sigma^2/2) - \frac{6}{\pi^2}\int_0^\Lambda dp\, p^3\ln\frac{p^2 + \frac{h^2}{4}\sigma^2}{p^2}\,, \end{aligned} \tag{III.81}$$

where $\int d\Omega_4 = 2\pi^2$ is the four-dimensional angular integration. The prefactor $N_f N_c = 6$ in the middle part in (III.81) results from the trace over flavour and colour space. The Dirac trace gives a factor 4, while the momentum symmetrisation with $p \to -p$ provides a factor 1/2. The denominators in (III.81) take care of the normalisation (III.80). Note also that up to these prefactors (III.81) is nothing but the Coleman-Weinberg potential of a φ^4-theory with interaction $\lambda/4!\,\varphi^2$ where we substitute $\lambda\varphi^2 \to h^2\rho$. We have an important relative minus sign due to the fermion loop and a symmetry factor $4N_fN_c = 24$ due to the number of degrees of freedom. We simply could take over this well-known result, for a detailed discussion see e.g. Chapter 11.2 in the QFT I+II lecture notes from 2022/23 .

For its importance we recall the computation here, and also discuss some particularities due to the embedding in QCD in the present low energy EFT context. The momentum integral in (III.81) is easily performed. We also restore the full mesonic field content, $\sigma^2/2 \to \rho$, and arrive at

$$V_{\phi,\rm eff}(\rho) = V_{\rm UV}(\rho) - \frac{3}{8\pi^2}\left[2\Lambda^2h^2\rho + h^4\rho^2\left[\ln\frac{h^2\rho}{2\Lambda^2} - \ln\left(1 + \frac{h^2\rho}{2\Lambda^2}\right)\right] + 4\Lambda^4\ln\left(1 + \frac{h^2\rho}{2\Lambda^2}\right)\right]\,. \tag{III.82}$$

As mentioned above, up to the symmetry factor -24 this is precisely the result of the Coleman-Weinberg computation performed originally in the context of the Higgs mechanism. We note that (III.82) seemingly depends on the momentum cutoff scale Λ. However, the potential $V_{\rm UV}(\rho)$ is the result of integrating-out quantum fluctuations up to the momentum scale Λ. Hence, it also carries a Λ-dependence. Now we use, that the full generating functional Z of QCD in (III.73) is Λ-independent: we only introduced Λ as an intermediate scale, splitting the path integral over momentum modes into a UV-part with $p^2 > \Lambda^2$ and an IR-part with $p^2 < \Lambda^2$. We conclude

$$\Lambda\frac{\partial Z}{\partial\Lambda} = 0\,. \tag{III.83}$$

Equation (III.83) is the (momentum cutoff) RG-equation for the generating functional of QCD. In the present context it is only approximately valid as we did not include the quantum fluctuations of gluons below the cutoff scale Λ. Accordingly, (III.83) only holds in our present EFT setting if the cutoff scale Λ is small enough. This will be aparent in the final, renormalised result, and we shall resume the discussion of the sufficient smallness of the cutoff scale there.

We start the analysis by first performing the integration over the quark fluctuations. This is a path integral with a bilinear action and can be readily performed. It leaves us with a purely mesonic low energy effective theory, and $V_{\phi,\mathrm{eff}}(\rho)$ is the full *effective* potential computed from the fermionic quantum fluctuations, but also has the interpretation of a *classical* potential of the mesonic low energy effective theory. Using (III.83) for the full effective potential (III.81) or (III.82), $\Lambda\partial_\Lambda V_{\mathrm{eff}} = 0$, leads us to scaling relations for the couplings in the potential V. As Λ only appears in the integration limit in (III.81), the integrand simply is the Λ-derivative and we obtain

$$\begin{aligned}\Lambda\partial_\Lambda V_{\mathrm{UV}} =& \frac{6}{\pi^2}\Lambda^4 \ln\left(1+\frac{h^2\rho}{2\Lambda^2}\right)\\ =& \frac{3}{\pi^2}\left(\Lambda^2 h^2\rho - \frac{h^4}{4}\rho^2\right) + O(\rho^3/\Lambda^2)\,,\end{aligned} \tag{III.84}$$

and

$$\Lambda\partial_\Lambda V_{\mathrm{UV}} = \Lambda\frac{\partial m_\varphi^2}{\partial\Lambda}\rho + \frac{1}{2}\Lambda\frac{\partial\lambda_\varphi}{\partial\Lambda}\rho^2\,. \tag{III.85}$$

The RG equation (III.85) signifies that the present quark-meson model is indeed renormalisable: the divergences can be absorbed in the couplings of the classical action. For the sake of completeness we remark that two further logarithmic singularities occur in a full analysis: the wave function renormalisations of quarks and mesons which also can be absorbed by wave functions in the classical action with e.g. $\partial_\mu\phi^2 \to Z_{\phi,\Lambda}\partial_\mu\phi^2$. The scale derivatives of m_φ^2 and λ_φ define the β-functions of meson mass and self-coupling respectively,

$$\beta_{m_\varphi^2} = \Lambda\frac{\partial(m_\varphi^2/\Lambda^2)}{\partial\Lambda}\,, \qquad \beta_{\lambda_\varphi} = \Lambda\frac{\partial\lambda_\varphi}{\partial\Lambda}\,, \tag{III.86}$$

in analogy to the β-function of the strong coupling in (I.38) and the four-Fermi coupling in (III.52) discussed before. Now we use $\Lambda\partial_\Lambda\Lambda^2 = 2\Lambda^2$ and $\Lambda\partial_\Lambda \ln\Lambda^2/\Lambda_{\mathrm{QCD}}^2 = 2$ for integrating the RG-equation (III.84). For the logarithmic term we have to introduce a reference scale which we choose to be the dynamical scale of QCD, Λ_{QCD}^2. Practically this scale is identified with the UV cutoff scale of the low energy EFT which is proportional to Λ_{QCD}^2, and is typically of the order of 1 GeV. In summary this leads us to

$$m_\varphi^2 = m_{\varphi,\mathrm{r}}^2 + \frac{3}{2\pi^2}\Lambda^2 h^2\,, \qquad \lambda_\varphi = \lambda_{\varphi,\mathrm{r}} - \frac{3}{4\pi^2}h^4\ln\frac{\Lambda^2}{\Lambda_{\mathrm{QCD}}^2}\,, \tag{III.87}$$

with the renormalised couplings $m_{\varphi,\mathrm{r}}^2, \lambda_{\varphi,\mathrm{r}}$. In the present approximation without the mesonic quantum fluctuations they directly carry the physics. The Λ-independent constant part in the subtraction is chosen such that the ρ^2-term in the effective potential has the coupling $\lambda_{\varphi,\mathrm{r}}$. It is evident from (III.87) that a variation of the reference scale in the logarithmic term can be absorbed in an according variation of $\lambda_{\varphi,\mathrm{r}}$,

$$\Lambda_{\mathrm{QCD}}\frac{\partial\lambda_\varphi}{\partial\Lambda_{\mathrm{QCD}}} = 0 \qquad\longrightarrow\qquad \Lambda_{\mathrm{QCD}}\frac{\partial\lambda_{\varphi,\mathrm{r}}}{\partial\Lambda_{\mathrm{QCD}}} = \beta_{\lambda_\varphi}\,, \tag{III.88}$$

where we have assumed the absense of other scales. This relation is again governed by the β-function β_{λ_φ}, and reflects the invariance observables do not depend on this choice. Inserting these results back into (III.82) leads us to the final, Λ-independent effective potential

$$V_{\phi,\mathrm{eff}}(\rho) = m_{\varphi,\mathrm{r}}^2\rho + \frac{\lambda_{\varphi,\mathrm{r}}}{2}\rho^2 - \frac{3}{8\pi^2}h^4\rho^2\left[\ln\frac{h^2\rho}{2\Lambda_{\mathrm{QCD}}^2} - \frac{1}{2}\right]\,. \tag{III.89}$$

As already discussed in the beginning of the derivation, (III.89) is the Coleman-Weinberg result in disguise. Multiplying with the symmetry factor $-4N_fN_c = -24$ gives precisely the same logarithmic term in the ρ^2 contribution. The missing constant term simply originates in the different renormalisation procedure: with the present one all corrections to the relevant couplings including the constant parts are absorbed, that is $m_\varphi^2 \to m_{\varphi,\mathrm{r}}^2$ and $\lambda_\varphi \to \lambda_{\varphi,\mathrm{r}}$.

As these couplings have to be fixed by appropriate infrared observables this is a convenient choice. In summary we have the following practical and consistent RG procedure:

(0) Regularisation: Sharp momentum cutoff with $p^2 \leq \Lambda^2$ in all loops.

(1) Renormalisation: Remove all divergent terms in the loop contributions. For the logarithmic term substitute $\ln \Lambda^2 \to \ln \Lambda^2_{\rm QCD}$.

(2) Renormalisation scheme: we demand $\partial_\rho V_{\phi,\rm eff} = \partial_\rho V_{\phi,\rm UV} + O(\rho^2) + \ln \rho$–terms. This is arranged by the $-1/2$ in the bracket in (III.89). It enforces that the ρ-dependent pion mass function $m_\pi(\rho) = \partial_\rho V_{\phi,\rm eff}(\rho)$ simply is $m^2_{\phi,\rm r}$ in the symmetric regime, that is for vanishing ρ. Moreover, the linear term in ρ of m^2_π is given by the UV coupling $\lambda_{\phi,\rm r}$. This cannot be expressed within a Taylor expansion at $\rho = 0$ due to the logarithmic term.

(3) Physics: The relevant parameters $h, m_{\varphi,\rm r}, \lambda_{\varphi,\rm r}$ and the explicit symmetry breaking scale c are fixed by the pion decay constant f_π, the physical pion and σ pole masses, $m_{\pi,\rm pol}, m_{\sigma,\rm pol}$ and the constituent quark mass $m_{q,\rm const}$.

Depending on the values of $m^2_{\varphi,\rm r}, \lambda_{\varphi,\rm r}$ the effective potential in (III.89) has non-trivial minima or describes the symmetric phase. The effect of the fermionic quantum fluctuations is most easily accessed via the scale-running of the parameters in the 'classical' potential $V(\rho)$. Concentrating on the scale-dependence of the mass parameter m^2_φ in (III.87) we conclude that lowering the cutoff scale Λ lowers the effective mass m^2_φ. This entails that the fermionic quantum fluctuation<s indeed lower the mass parameter. Put differently, the quark fluctuations trigger chiral symmetry breaking.

Moreover, deep in the symmetric phase, that is for large Λ, the mesonic quantum fluctuations are suppressed in comparison to the quark fluctuations. In the vicinity of the symmetry breaking scale Λ_χ the mesonic fluctuations are getting massless, $m_\varphi \to 0$ and the mesonic fluctuations kick in. In turn, the effective quark mass grows in the chirally broken regime with $m_\psi = h/2\sigma_0$, and eventually the quark fluctuations are switched off for Λ below the constituent quark mass. ...

2. *Mesonic quantum fluctuations*

The remaining mesonic fluctuations can be treated at one loop similarly to the fermionic computation done above. The result is a Coleman-Weinberg type potential without the relative minus sign. Accordingly, the mesonic fluctuations work against chiral symmetry breaking. Due to the different scales and coupling sizes this is a marginal effect even in the chiral limit. In the physical scale with explicit chiral symmetry breaking and a pion mass of about 140 MeV the mesonic quantum fluctuations also decouple for scales Λ below the pion mass.

It is left to integrate-out the quantum fluctuations of the mesonic degrees of freedom in (III.75). Again concentrating on the low energy effective potential in the spirit of the lowest order of a derivative expansion we have

$$V_{\rm eff}(\rho) = V_{\phi,\rm eff}(\rho) + \Delta V_\phi(\rho) + c_\sigma\,\sigma \qquad \text{with} \qquad \Delta V_\phi(\rho) = \frac{1}{2}\mathrm{Tr}_\Lambda \ln\left[-\partial_\mu^2 + m^2_\phi(\rho)\right] , \tag{III.90}$$

where ΔV_ϕ is the one loop approximation to the mesonic path integral (III.75) with the 'classical' potential $V_{\phi,\rm eff}(\rho)$, and Tr_Λ sums over all momenta $p^2 \leq \Lambda^2$. In (III.90) we have re-introduced the linear term in σ that triggers the explicit symmetry breaking. In the present case ΔV_ϕ boils down to

$$\Delta V_\phi(\rho) = \frac{1}{4\pi^2}\int_0^\Lambda dp\, p^3 \left[3\ln\left(p^2 + m^2_\pi(\rho)\right) + \ln\left(p^2 + m^2_\sigma(\rho)\right)\right] . \tag{III.91}$$

For (III.91) we have used that we can evaluate the expressions for vanishing $\vec\pi = 0$ as done in the quark case. Then the mass matrix is diagonal, see (III.10), and the meson loop splits into a sum of the pion and σ loops. The two diagonal mass functions read for a given potential V

$$m^2_\pi(\rho) = \partial_\rho V(\rho) , \qquad m^2_\sigma(\rho) = \left(\partial_\rho + 2\rho\partial^2_\rho\right)V(\rho) . \tag{III.92}$$

Accordingly, the factor three in front of the first term on the right hand side in (III.91) accounts for the $N_f^2 - 1 = 3$

pions. In the present case we have $V_{\phi,\text{eff}}(\rho)$ and we get

$$m_\pi^2(\rho) = m_{\varphi,\text{r}}^2 + \left(\lambda_{\varphi,\text{r}} - \frac{3}{4\pi^2}\, h^4 \ln \frac{h^2\rho}{2\Lambda_{\text{QCD}}^2}\right)\, \rho\,,$$

$$m_\sigma^2(\rho) = m_{\varphi,\text{r}}^2 + 3\left(\lambda_{\varphi,\text{r}} - \frac{1}{2\pi^2} - \frac{3}{4\pi^2}\, h^4 \ln \frac{h^2\rho}{2\Lambda_{\text{QCD}}^2}\right)\, \rho \tag{III.93}$$

The integration in (III.92) is the same as in the quark case and we arrive at

$$\begin{aligned}\Delta V_\phi(\rho) = \frac{3}{16\pi^2}\Bigg\{&\Lambda^2 m_\pi^2 + m_\pi^4\left[\ln\frac{m_\pi^2}{\Lambda^2} - \ln\left(1+\frac{m_\pi^2}{\Lambda^2}\right)\right] + \Lambda^4 \ln\left(1+\frac{m_\pi^2}{\Lambda^2}\right)\Bigg]\\ &+ \frac{1}{16\pi^2}\Bigg[\Lambda^2 m_\sigma^2 + m_\sigma^4\left[\ln\frac{m_\sigma^2}{\Lambda^2} - \ln\left(1+\frac{m_\sigma^2}{\Lambda^2}\right)\right] + \Lambda^4 \ln\left(1+\frac{m_\sigma^2}{\Lambda^2}\right)\Bigg\}\,,\end{aligned} \tag{III.94}$$

where m_π^2, m_σ^2 are the ρ-dependent masses defined in (III.92). Seemingly (III.94) introduces divergent terms that are neither proportional to ρ^0, ρ, ρ^2 due to ΔV_q in (III.92). However, (III.94) goes beyond one-loop (ΔV_q is already one-loop) and these terms are to be expected and can be removed within a consistent renormalisation procedure. Here, our simple renormalisation procedure discussed below (III.89) pays off. Then after renormalisation (III.94) turns into

$$\Delta V_\phi(\rho) = \frac{3}{16\pi^2} m_\pi^4\left[\ln\frac{m_\pi^2}{\Lambda_{\text{QCD}}^2} - \frac{1}{2}\right] + \frac{1}{16\pi^2} m_\sigma^4\left[\ln\frac{m_\sigma^2}{\Lambda_{\text{QCD}}^2} - \frac{1}{2}\right]\,, \tag{III.95}$$

where $m_\pi(\rho), m_\sigma(\rho)$ are derived from (III.92). In (III.95) we have applied to renormalisation scheme summarised in the points (1)-(4) below (III.89). The factor $-1/2$ in the brackets arrange for

$$m_{\text{eff},\pi}^2(\rho) = \partial_\rho V_{\text{eff}}(\rho) = m_{\varphi,\text{r}}^2 + \lambda_{\varphi,\text{r}}\rho - \frac{3}{8\pi^2}\rho \ln\frac{h^2\rho}{2\Lambda_{\text{QCD}}^2} + \frac{3}{8\pi^2} m_\pi^2 (\partial_\rho m_\pi^2) \ln\frac{m_\pi^2}{\Lambda_{\text{QCD}}^2}\,. \tag{III.96}$$

From (III.95) we can proceed in several ways:

(0) We drop ΔV_ϕ completely. As in (2) the missing quantum fluctuations are partially absorbed in the couplings $m_\varphi, \lambda_\varphi$. This approximation is also called 'extended mean field' in the literature. It is very close to the mean field approximation with $V_{\text{eff}}(\rho) = V(\rho)$, where we also drop ΔV_q.

(1) As ΔV_q already is a one loop expression we drop it in the computation of (III.95). This leads us to a consistent one-loop computation. This amounts to dropping some quantum contributions in comparison to (1). However, as in (1) we have to fix the parameters $h, m_\varphi, \lambda_\varphi$ in the effective potential with the low energy observables. This implicitly absorbes (part of the) dropped contributions in these couplings. Differences between (1) and (2) only occur due to missing contributions in (2) in the couplings $\lambda_{\varphi,n}$ of the ρ^n-terms in V_{eff} with $n \geq 3$.

(2) For the evaluation of (III.90) with $V + \Delta V_q$ in (III.89) and ΔV_ϕ in (III.95) we have to take into account that already the effective potential $V + \Delta V_q$ may not be convex. In non-convex regimes its second derivatives are not positive definite: $m_\pi < 0$ for $\rho < \rho_\pi$, where ρ_π is the solution of the reduced EoM: $V_{\text{cl}}'(\rho_\pi) + \Delta V_q'(\rho_\pi) = 0$. The σ mass also gets negative for even smaller ρ.

A simple resolution of this artefact of the approximation is to continue the result from larger $\rho \geq \rho_\pi$. The more consistent way is to resolve the related renormalisation group (RG) equation for the effective potential. The RG approach is able to deal consistently with the regimes with negative curvature which are indeed flattened out by quantum fluctuations. This effect cannot be seen in perturbation theory.

In any case the result of this computation is an effective potential $V_{\text{eff}}(\rho)$ which depends on the couplings $h, m_\varphi, \lambda_\varphi$. We either compute these couplings from QCD or we fix them with low energy observables such as the meson mass, the pion decay constant and the constituent quark mass. Here we use the latter way which is described in details below.

(3) We solve the full renormalisation group equation, (III.83), for the effective potential, that governs its scale-dependence, see (III.97) below. Integrating the RG equation provides an iterative and fully consistent inclusion

of the fluctuation effects. The RG is described in the chapter Section III G 3 below, where it is also detailed how it boils down to the procedures (0)-(2) described above.

In the following we will consider all of these approximations, in particular at finite temperature and density. This allows us to evaluate the importance of the quantum (and later thermal) fluctuations as well as the stability of the results.

3. *RG equation for the effective potential**

The present considerations are but one step away from a consistent treatment of the low energy effective theory with functional renormalisation group methods. For that purpose let us reconsider the RG equation for the ultraviolet potential $V_{\rm UV}$ derived from (III.83). Below (III.83) we have discussed the renormalisation group scaling that originates in the quark quantum fluctuations. In the general case the RG-scaling of the potential comes from both quark and meson fluctuations. This leads us to

$$\Lambda\partial_\Lambda V_{\rm UV} = -\Lambda\partial_\Lambda\left(\Delta V_q + \Delta V_\phi\right) . \tag{III.97}$$

Equation (III.97) entails how the UV effective potential $V_{\rm UV}$ at a large cutoff scale Λ changes with lowering or increasing the cutoff scale. In the discussion so far we have concentrated on the UV relevant terms that scale with positive powers of the cutoff Λ. Then we ensured the cutoff independence of the full effective potential $V_{\rm eff} = V_{\rm UV} + \Delta V_q + \Delta V_\phi$ by an appropriate renormalisation procedure. The low energy quark and meson fluctuation are encoded in the terms $\Delta V_q + \Delta V_\phi$. Such a treatment assumes an asymptotically large cutoff scale.

Here we take a different point of view: iteratively lowering to cutoff scale Λ from large values (w.r.t. the non-perturbative infrared pyhsics) leads to shifting more and more infrared fluctuations from $\Delta V_q + \Delta V_\phi$ to $V_{\rm UV}$. Indeed, at $\Lambda = 0$ we have

$$V_{\rm eff} = V_{\Lambda=0} , \qquad \text{with} \qquad V_\Lambda = V_{{\rm UV},\Lambda} , \tag{III.98}$$

the former 'UV' effective potential is the full quantum effective potential. Evidently, if the cutoff scale is not asymptotically large, also the UV-irrelevant terms cannot be neglected in (III.97). Note also that its right hand side has to be seen as a function of V_Λ, the one-loop computations done before indeed used V_Λ a a classical potential. Hence, it is only left to bring (III.97) in a form that only depends on V_Λ on both sides.

To that end we consider an infinitesimal RG step with $\Lambda^2 \to \Lambda^2(1-\epsilon)$. This is governed by the path integral

$$Z \approx \int_{\Lambda^2(1-\epsilon)}^{\Lambda^2} [d\phi\, d\psi d\bar\psi] e^{-S_{{\rm eff},\Lambda}[\psi,\bar\psi,\phi]} \qquad \text{with} \qquad e^{-S_{{\rm eff},\Lambda}} \simeq Z_\Lambda . \tag{III.99}$$

Now we exploit that each loop in a loop expansion of (III.99) is proportional to ϵ as it only takes into account momenta with $\Lambda^2(1-\epsilon) \le p^2 \le \Lambda^2$. Hence, for $\epsilon \to 0$ the one-loop contribution is leading, and the ϵ-derivative can be converted in the Λ-derivative of the momentum integration boundary of the one-loop expressions for ΔV_q and ΔV_ϕ, (III.79) and (III.90) respectively. This leads us to

$$\Lambda\partial_\Lambda V_\Lambda = -\frac{1}{4\pi^2}\Lambda^4\left[3\ln\left(1+\frac{m_\pi^2(\rho)}{\Lambda^2}\right)+\ln\left(1+\frac{m_\sigma^2(\rho)}{\Lambda^2}\right)\right]+\frac{6}{\pi^2}\Lambda^4\ln\left(1+\frac{h^2}{2}\frac{\rho}{\Lambda^2}\right) , \tag{III.100}$$

where

$$m_{\pi/\sigma}^2(\rho) = \Gamma^{(2)}_{\Lambda,\pi\pi/\sigma\sigma}(\rho, p=0) = V^{(2)}_{\Lambda,\pi\pi/\sigma\sigma}(\rho) , \qquad \frac{h^2}{2}\rho = \Gamma^{(2)}_{\Lambda,\psi\bar\psi}(\rho, p=0) , \qquad \text{with} \qquad \Gamma^{(2)}_\Lambda = \Gamma_{{\rm UV},\Lambda} , \tag{III.101}$$

are the second derivatives of the scale-dependent 'UV' effective action Γ_Λ. We emphasise that the implicit Λ-dependence in $\Gamma^{(2)}$ is not hit by the ϵ-derivative.

The approximations (0)-(2) now follow from respective approximations of (III.100): For (0) we drop the meson fluctuations, for (1) we do not feed back the RG-running of $V_{\rm UV}$ on the right hand side of (III.100), for (2) we integrate out the quarks first. This is done with introducing separate cutoffs for quarks, Λ_q and mesons, Λ_ϕ and take the limit $\Lambda_q/\Lambda_\phi \to 0$.

Equation (III.100) is the Wegner-Houghton equation [11] for the effective potential of the current Quark-Meson Model. For the sake of completeness we also quote the full Wegner-Houghton equation for the effective action: as the

derivation of (III.100) simply follows from the RG-invariance of the generating functional Z, it also applies to the full effective action. Hence we conclude

$$\Lambda\partial_\Lambda\Gamma_\Lambda[\psi,\bar\psi,\phi] = -\frac{1}{2}\mathrm{Tr}_{p^2=\Lambda^2}\ln\frac{\Gamma^{(2)}_{\phi\phi}}{\Lambda^2} + \mathrm{Tr}_{p^2=\Lambda^2}\ln\frac{\Gamma^{(2)}_{\psi\bar\psi}}{\Lambda^2}\,, \tag{III.102}$$

where the trace $\mathrm{Tr}_{p^2=\Lambda^2} = \mathrm{Tr}\,\delta(\sqrt{p^2}-\Lambda)$ only sums over the momentum shell with $p^2=\Lambda^2$. Equation (III.102) is, together with the Callan-Symanzik equation [12, 13], the first of many functional renormalisation group equations for the effective action. These continuum RG equations are based on continuum version [14, 15] of the Kadanoff block spinning procedure on the lattice, [16], for the first seminal work on the RG see [17, 18]. In particular the pioneering work [17] already emphasises and details the full power of the renormalisation group, and is still very much under-appreciated by the community.

4. *EFT couplings and QCD*

It is left to fix the couplings parameters in our low energy effective theory with the classical action $S_{\rm eff}$ defined (III.62). After integrating out the quarks and mesons we are led to the full low energy effective action $\Gamma_{\rm lowE}$ with

$$\Gamma_{\rm lowE}[\psi,\bar\psi,\phi] = \int_x \bar\psi\cdot(\not\partial + m_\psi)\cdot\psi + \int_x\left[(\partial_\mu\sigma)^2+\partial_\mu\vec\pi)^2\right] + \int_x\frac{h}{2}\bar\psi\left[\sigma+i\gamma_5\vec\tau\vec\pi\right]\psi + \int_x V_{\rm eff}(\rho)\,, \tag{III.103}$$

with the effective potential $V_{\rm eff} = V_{\phi,\rm eff}+\Delta V_\phi + c\sigma$ defined in (III.90) with $V_{\phi,\rm eff} = V_{\rm UV}+\Delta V_q$. In the best approximation discussed here, $V_{\phi,\rm eff}$ is given by (III.89) and ΔV_ϕ by (III.95). We have the fermion mass m_ψ or mesonic shift parameter c, the Yukawa coupling h, the mesonic mass parameter m_ϕ^2 and the mesonic self-coupling λ_ϕ. The fermion mass can be traded for the shift parameter c as argued before. The value of the latter determines the expectation value of the σ-field which is, in the present approximation, simply is the pion decay constant,

$$\sigma_0 = \langle\sigma\rangle = f_\pi\,, \qquad\qquad f_\pi \approx 93\,\mathrm{MeV}\,. \tag{III.104}$$

The latter value related to the physical f_π's $(f_\pi^\pm, f_\pi^0)$ measured in the experiment. Consequently c could be dropped, we simply evaluate the theory on this expectation value. Accordingly, h is determined by the constituent quark mass,

$$m_{\psi,\rm con} = \frac{1}{2}h\langle\sigma\rangle = \frac{1}{2}h\,f_\pi \qquad\longrightarrow\qquad h\approx 6.45 \quad\text{with}\quad m_{\psi,\rm con}\approx 300\,\mathrm{MeV}\,. \tag{III.105}$$

Note that the constituent quark masses of the quarks depend on the model and approximation used, typical values for up and down quark constituent masses are $m_{\psi,\rm con}\approx 350$ MeV in full QCD. A reduced value in (III.105) for two flavour QCD is common place in the $N_f=2$ quark-meson model. The related observable is the chiral condensate,

$$\langle\bar\psi(x)\psi(x)\rangle = -\int\frac{d^4p}{(2\pi)^4}\mathrm{tr}\,\langle\psi(p)\bar\psi(-p)\rangle\,, \tag{III.106}$$

where the trace sums over Dirac and flavour indices.

Finally we have to fix λ_ϕ and m_ϕ with the Yukawa coupling and σ-expectation value σ_0 deduced above, see also Table II. Note also, that a potential further input is the value of the pion decay constant in the chiral limit,

$$f_{\pi,\chi} = f_\pi(m_\pi=0)\approx 88\,\mathrm{MeV}\,, \tag{III.107}$$

which can be determined with chiral perturbation theory, functional continuum methods or from chiral extrapolations of lattice results at different finite pion masses. This leaves us with a triple of 'observables' $(m_\pi, m_\sigma, f_{\pi,\chi})$, see Table II, and a triple of EFT couplings $(m_\phi,\lambda_\phi,c_\sigma)$. Note that the inclusion of $f_{\pi,\chi}$ as an 'observable' relates to the correct chiral dynamics reflected in the curvature and four-meson interaction in the chiral limit. The pion and sigma masses are related to those found in the Particle Data Booklet (2016), [19] of the Particle Data Group (PDG). Here, the pion mass is taken between that of the charged pions $\pi^\pm$ with $m_{\pi^\pm}\approx 139.57$ MeV and the neutral pion π^0 with $m_{\pi^0}\approx 134.98$ MeV, and the mass of the sigma meson is taken to be that of the $f_0(500)$, see [20], that is $m_\sigma\approx 450\,\mathrm{MeV}$, despite the f_0 certainly not being a simple $q\bar q$ state. The unclear nature of the value of m_σ is one of the biggest uncertainties for low energy EFTs. Typically, its values range from 400–550 MeV, see PDG, [19].

Seemingly, this leaves us with as many unknowns as physics input. However, c can be determined from the pion

Observables	Value [MeV]	EFT couplings	Value
f_π	93	$\sigma_0 = f_\pi$	93 MeV
$m_{\rm con}$	300	$h = \frac{2m_{\rm con}}{f_\pi}$	6.45
m_π	138	m_ϕ	$m_\phi(m_\pi, m_\sigma)$
m_σ	450	λ_ϕ	$\lambda_\phi(m_\pi, m_\sigma)$
$f_{\pi,\chi}$	88	$c_\sigma = f_\pi m_\pi^2$	$1.77 * 10^6 \text{MeV}^3$

TABLE II: Low energy observables and related EFT couplings as used for the $N_f = 2$ computations. While the σ-expectation value σ_0 and the Yukawa coupling are directly related to pion decay constant and constituent quark masses in the present approximations, the other EFT couplings depend on the approximations (0)–(3) described below (III.96).

mass and the pion decay constant with $m_\pi^2 = \partial_\rho V_{\rm eff}(\rho_0)$ and $\rho_0 = \sigma_0^2/2 = f_\pi^2/2$. This follows from the EoM for σ,

$$\partial_\sigma V_{\rm eff}(\rho_0) = \sigma_0 m_\pi^2 = c_\sigma \qquad \longrightarrow \qquad c_\sigma = f_\pi m_\pi^2 \approx 1.77 * 10^6\,\text{MeV}^3\,. \tag{III.108}$$

We conclude that in the current approximation to the UV effective action, the pion decay constant in the chiral limit, $f_{\pi,\chi}$, is a prediction.

Here we present a crude (mean-field) estimate of its value based on the assumption of being close to the chiral limit. It is based on the expansion of the full effective potential about the unperturbed minimum in the broken phase,

$$V_{\rm eff} = \sum_{n=2}^{\infty} \frac{\lambda_n}{n!} (\rho - \kappa)^n + c_\sigma \sigma\,, \qquad \text{with} \qquad \kappa = \frac{f_{\pi,\chi}^2}{2}\,, \quad \lambda_2 = \lambda_{\phi,\rm eff}\,. \tag{III.109}$$

Close to the chiral limit the difference $(f_\pi - f_{\pi,\chi})/f_\pi \ll 1$ is small. In the vicinity of the unperturbed minimum κ the full effective potential can be written as

$$V_{\rm eff} = \frac{\lambda_{\phi,\rm eff}}{2} (\rho - \kappa)^2 + c_\sigma \sigma + O\left((\rho - \kappa)^2\right)\,. \tag{III.110}$$

Dropping the higher terms leads us to

$$m_\pi^2 = \lambda_{\phi,\rm eff} \frac{f_\pi^2 - f_{\pi,\chi}^2}{2}\,, \qquad m_\sigma^2 = \lambda_{\phi,\rm eff} \frac{3f_\pi^2 - f_{\pi,\chi}^2}{2}\,. \tag{III.111}$$

In this leading order, the mesonic self-coupling drops out of the ratio of m_π^2/m_σ^2 which can be used for determining the pion decay constant in the chiral limit. We get

$$f_{\pi,\chi} = f_\pi \sqrt{\frac{1 - 3\frac{m_\pi^2}{m_\sigma^2}}{1 - \frac{m_\pi^2}{m_\sigma^2}}} \approx 83\,\text{MeV}\,, \qquad \text{and} \qquad \lambda_{\phi,\rm eff} = \frac{m_\sigma^2 - m_\pi^2}{f_\pi^2} \approx 21.2\,. \tag{III.112}$$

This is a very good agreement with the theoretical prediction of $f_{\pi,\chi} \approx 88\,\text{MeV}$, in particular given the crude nature of the present estimate, which can be improved if going beyond the current mean field level.

The above analysis elucidates that the current EFT provides a prediction for either $f_{\pi,\chi}$ or m_σ, and the question arises which of them should be taken as a physics input: we first note that $f_{\pi,\chi} \approx 88\,\text{MeV}$ is under far better theoretical control than the mass of the σ-meson. Apart from the difficulties of identifying directly the σ-mesons in the EFT's at hand with a resonance in the particle spectrum, it has a large width. Hence it cannot be assumed that the curvature mass $m_{\sigma,\rm curv}$ we use here is in good agreement with the pole mass $m_{\sigma,\rm pol}$, see the discussion at the end of chapter Section III B. This is in stark contradistinction to the pion masses where the (non-trivial) identification $m_{\pi,\rm curv} \approx m_{\pi,\rm pol}$ holds true on the percent level. This suggests to adjust m_σ such that $f_{\pi,\chi} \approx 88$ MeV. In the mean field discussion done here this leads to $m_\sigma^2 \approx 600 - 650\,\text{MeV}$. Note that with a future better determination of the curvature mass $m_{\sigma,\rm curv}$ a semi-quantitative EFT might require higher oder mesonic UV-couplings such as $\lambda_{3,\rm UV} \neq 0$ in (III.110). This is related to the fact that the physical UV cutoff $\Lambda_{\rm UV} \approx 1$ GeV, at which the low energy EFT is initiated, is less than one order of magnitude larger than the physical scales.

This discussion completes our EFT picture of chiral symmetry breaking in QCD. In essence it also extends to the $N_f = 2+1$ flavour case and beyond, then, however, a consistent determination of the low energy couplings including

the correct chiral dynamics, e.g. $f_{\pi,\chi}$ is far more intricate.

IV. CONFINEMENT IN LATTICE GAUGE THEORY *

Before we proceed to the finite temperature situation we discuss confinement within the framework of lattice gauge theory, the standard approach to the strongly correlated sector of QCD. We shall mainly concentrate on Yang-Mills theory, the pure gluonic theory, as this suffices to discuss the phenomenon of confinement. Within the lattice setting confinement can be shown algebraically in the strong coupling limit, where the bare lattice coupling g_0 is taken to infinity, while the continuum limit requires the opposite limit $g_0 \to 0$. Despite the strong coupling limit not being the physics corner of the lattice theory (indeed it relates to an infinite coarse graining), it is a very illustrative and revealing study.

A. Scalar fields on the lattice

The lattice approach aims at a numerical computation of the full path integral of QCD, and is best explained at the example of the ϕ^4-theory, the working horse of quantum field theory. We consider the classical action of a free complex scalar field $\phi \in \mathbb{C}$,

$$S[\phi] = \int_x \phi^\dagger(x) \left(-\Delta + m^2\right) \phi(x)\,, \tag{IV.1}$$

with Laplace operator $\Delta = \partial_\mu^2$ and the Euclidean generating functional

$$Z[J] = \int d\phi \, \exp\left\{-S[\phi] + \int_x J(x)\phi(x)\right\}\,. \tag{IV.2}$$

The path integral measure

$$d\phi = \prod_{x\mathbb{R}^4} d\phi(x)\,, \tag{IV.3}$$

is the (infinite) product of integrations at all space-time points. This infinite product reflects the UV-singularities we have been discussing in the previous section. A simple way to remove these singularities is to consider a hyper-cubic space-time lattice with lattice spacing a instead $\mathbb{R}^4$,

$$d\phi = \prod_{\hat{n}\in\mathbb{Z}^4} d\phi(n\,a)\,, \qquad \text{with} \qquad n = \begin{pmatrix} n_0 \\ n_1 \\ n_2 \\ n_3 \end{pmatrix}\,, \qquad \text{and} \qquad n_\mu \in \mathbb{Z}\,. \tag{IV.4}$$

A two-dimensional lattice with lattice spacing a is depicted in Fig. 12.

On such a lattice with lattice spacing a and finite box size $L\mu = N_\mu\, a$ the infinite product is reduced to a finite one, resulting in $N_0N_1N_2N_3$ complex integrations. Usually the spatial lengths agree, $L_i = L$ for $i, j = 1, 2, 3$ and the ratio

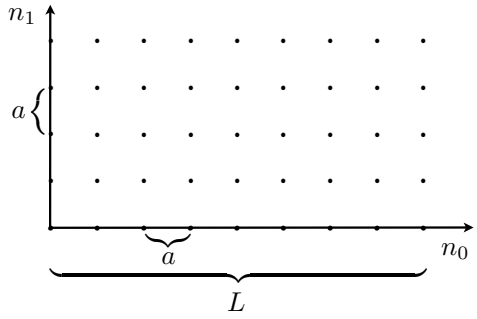

FIG. 12: two-dimensional space-time lattice with lattice spacing a.

L_0/L relates to finite temperature. At zero temperature all lengths agree and we have to perform N^4 integrations. Evidently, the numerical effort quickly increases with $N \to \infty$, and one has to resort to Monte-Carlo techniques. In the present lecture course we concentrate on the analytical aspects of the lattice theory, which allows us to show confinement analytically in the strong coupling limit. This is an elucidating albeit unphysical example.

It is left to define the lattice action in the lattice version of the generating functional (IV.2). To that end we rewrite everything in terms of dimensionless variables, to wit

$$\begin{aligned} x_\mu &\to n_\mu a \\ \phi(x) &\to \frac{1}{a}\hat{\phi}_n \\ \int d^4x &\to a^4 \sum_n \\ \phi^\dagger \Delta \phi &\to \frac{1}{a^4}\hat{\phi}^\dagger \hat{\Delta}\hat{\phi} \\ m^2 &\to \frac{1}{a^2}\hat{m}^2 \,, \end{aligned} \tag{IV.5}$$

with a symmetric discrete Laplacian

$$\hat{\Delta}\hat{\phi}_n = \sum_\mu \left[\hat{\phi}_{n+\hat{\mu}} + \hat{\phi}_{n-\hat{\mu}} - 2\hat{\phi}_n\right] , \tag{IV.6}$$

where $(\hat{\mu})_\nu = \delta_{\mu\nu}$, and the derivatives

$$\hat{\partial}^R_\mu \hat{\phi}_n = \hat{\phi}_{n+\hat{\mu}} - \hat{\phi}_n \,, \qquad \hat{\partial}^L_\mu \hat{\phi}_n = \hat{\phi}_{\hat{n}} - \hat{\phi}_{\hat{n}-\hat{\mu}} \,, \qquad \hat{\partial}^S_\mu \hat{\phi}_{\hat{n}} = \frac{1}{2}\left(\hat{\phi}_{\hat{n}+\mu} - \hat{\phi}_{\hat{n}-\mu}\right) . \tag{IV.7}$$

The Laplacian (IV.6) can be represented as $\hat{\Delta} = \hat{\partial}^R_\mu \hat{\partial}^L_\mu$. In the continuum limit, $a \to 0$, the derivativs defined above go to the continuum derivatives, i.e. $\hat{\Delta}/a^2 \to \Delta$, $\hat{\partial}^{R/L/S}_\mu / a \to \partial_\mu$. With these definitions we can transform the action (IV.1) into the discretised lattice action,

$$S[\hat{\phi}] = \sum_{n,m} \hat{\phi}^\dagger K_{nm} \hat{\phi}_m \,, \tag{IV.8}$$

with

$$K_{nm} = -\sum_\mu \left[\delta_{n+\hat{\mu},m} + \delta_{n-\hat{\mu},m} - 2\delta_{n,m}\right] + \hat{m}^2 \delta_{nm} \,, \tag{IV.9}$$

where we have assumed $L \to \infty$ ($N \to \infty$ at fixed lattice spacing a) for the sake of simplicity. This leads us finally to the generating functional of the free scalar lattice theory,

$$Z[\hat{J}] = \int \prod_n d\hat{\phi}_n e^{-S[\hat{\phi}] + \sum_n \left(\hat{J}_n \hat{\phi}_n + J^\dagger_n \hat{\phi}^\dagger_n\right)} = \frac{1}{\sqrt{\det K}} e^{\sum_{n,m} \hat{J}^\dagger_n {K^{-1}}_{nm} \hat{J}_m} . \tag{IV.10}$$

From (IV.10) we derived the propagator

$$\langle \hat{\phi}^\dagger_n \hat{\phi} \rangle = {K^{-1}}_{nm} \,, \qquad K_{nm} {K^{-1}}_{mn'} = \delta_{n,n'} \,. \tag{IV.11}$$

The momentum space representation of functions $f(n)$ n the lattice is defined as a sum over plane waves $e^{i\hat{p}n}$. This leads to a periodicity in $\hat{p} \to \hat{p} + 2\pi$, and we write

$$K_{nm} = \int_{-\pi}^{\pi} \frac{d^4\hat{p}}{(2\pi)^4} \tilde{K}(\hat{p})\, e^{i\hat{p}(n-m)} \,, \qquad \text{and} \qquad \tilde{K}(\hat{p}) = 4\sum_\mu \sin^2 \frac{\hat{p}_\mu}{2} + \hat{m}^2 \,, \tag{IV.12}$$

with

$$\delta_{n,m} = \int_{-\pi}^{\pi} \frac{d^4\hat{p}}{(2\pi)^4} e^{i\hat{p}(n-m)}\,, \qquad \text{and} \qquad \sum_n e^{i\hat{p}n} = (2\pi)^4 \delta(\hat{p})\,. \tag{IV.13}$$

The momentum integration in (IV.12) is restricted to the Brillouin zone, $\hat{p}_\mu \in [-\pi\,,\,\pi]$, that is the dimensionful mo1mentum p runs from $-\pi/a$ to π/a, reflecting the UV cut-off introduced by the lattice spacing a. In turn, a finite lattice volume $V = L^4$ introduces an IR cut-off. In the present lattice formulation this leads to finite sums $\sum_{n_\mu^2 > N^2}$ and to discrete momenta $\hat{p}_\mu = 2\pi a/L$ in the Brillouin zone.

Remarks:

(1) The discrete lattice generating functional as well as correlations functions can be computed numerically:

   (a) Put the theory on a finite lattice with $|n_\mu a| \leq L$

   (b) Perform N^4 integrations with Monte-Carlo methods, where $N = L/a$. Common sizes for lattice QCD simulations with dynamical fermions are $16^4, 32^4$. At finite temperature the temporal extend ranges from 4 to 16 lattice points.

   (c) Interaction term

$$S_{\text{int}}[\hat{\phi}] = \frac{\hat{\lambda}}{4!} \sum_n \hat{\phi}^4(n) \tag{IV.14}$$

(2) Continuum limit with correlation length ξ:

(a)

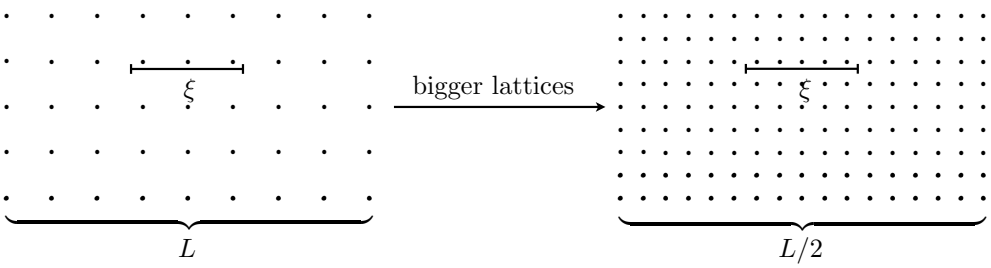

FIG. 13: Continuum limit at fixed lattice volume by increasing the number of lattice points.

(b)

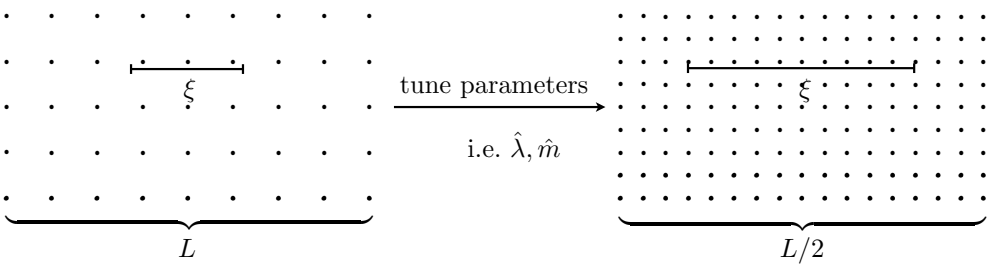

FIG. 14: Continuum limit at fixed number of lattice points by decreasing the lattice distance.

B. Non-Abelian gauge fields on the lattice

In the previous section we have disucss how to put scalar fields on the lattice. This involved in particular the use of discrete derivatives on the lattice that couple next and next-to-next neighbour sites. This already entails that the implementation of gauge transformations and gauge invariance requires gauge field variables that connect neighbouring sites, in other words they live on the links between the sites.

For the construction, as in the continuum, we start by introducing gauge transformations for the complex matter fields $\hat{\phi}$ (in the fundamental representation),

$$\hat{\phi}_n \to g(n)\hat{\phi}(n)\,, \qquad \text{with} \qquad g(n) \in SU(N)\,. \tag{IV.15}$$

In order to achieve gauge invariance for the classical action (IV.1) we have to ensure gauge invariance for e.g.

$$\hat{\phi}_n^\dagger \hat{\phi}_{n+\hat{\mu}}\,, \tag{IV.16}$$

via the introduction of the lattice analogue of the gauge field (connection). Eq.(IV.16) and the transformation law (IV.15) entails that we have to (parallel) transport the group element $g\,\dagger\,(n)$ from the lattice site n to the site $n+\hat{\mu}$. We define the link variable $U_\mu(n)$ with the transformation law

$$U_\mu(n) \to g(n)U_\mu(n)g^\dagger(n+\hat{\mu})\,. \tag{IV.17}$$

With the transformation properties (IV.17) the link variable U_μ has the following properties:

(1) $U_\mu(n)$ 'lives' on the link between n and $n+\hat{\mu}$:

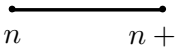

FIG. 15: link between two sites

(2) The term

$$\hat{\phi}_n^\dagger U_\mu(n)\hat{\phi}_{n+\hat{\mu}} \to \hat{\phi}_n^\dagger g^\dagger(n)g(n)U_\mu(n)g(n+\hat{\mu})\,\dagger\,(n)g(n+\hat{\mu})\hat{\phi}_{n+\hat{\mu}} = \hat{\phi}_n^\dagger U_\mu(n)\hat{\phi}_{n+\hat{\mu}} \tag{IV.18}$$

is gauge invariant. This also holds for the other terms in (IV.1), if modfied accordingly with the link variables U_μ. We are led to the gauge invariant action

$$S[\hat{\phi},U] = -\sum_{n,\mu}\left(\hat{\phi}_n^\dagger U_\mu^\dagger(n-\hat{\mu})\hat{\phi}_{n-\hat{\mu}} + \hat{\phi}_n^\dagger U_\mu(n)\hat{\phi}_{n+\hat{\mu}}\right) + (8+\hat{m}^2)\sum \hat{\phi}_n^\dagger\phi_n\,. \tag{IV.19}$$

(3) Continuum limit: We parameterise

$$U_\mu(n) = e^{ig_0 aA_\mu(n)}\,, \tag{IV.20}$$

with bare gauge coupling g_0 and gauge field $A_\mu(n)$ in the algebra. This expression is by no means unique and A_μ also lives on the link. Possible definitions of the gauge field differ by terms of order a^2. Now we expand the expression (IV.20) in powers of the lattice spacing a and arrive at

$$S[\hat{\phi},U] \overset{a\to 0}{\to} -\sum_{n,m}\hat{\phi}^\dagger K_{nm}\hat{\phi}_m - \sum_{n,\mu}\hat{\phi}_n^\dagger\left[-iag_0A_\mu(n-\hat{\mu})\hat{\phi}_{n-\hat{\mu}} + iag_0A_\mu(n)\hat{\phi}_{n+\hat{\mu}}\right]$$

$$+\hat{m}^2\sum_n\hat{\phi}_n^\dagger\phi_n - \sum_n[iag_0A_\mu(n)]^2\hat{\phi}_n^\dagger\hat{\phi}_n + O(a^2)\,. \tag{IV.21}$$

The second term on the right hand side of (IV.21) can be rewritten as

$$iag_0\hat{\phi}_n^\dagger\Big[\underbrace{(A_\mu(n)-A_\mu(n-\hat{\mu}))}_{\hat{\partial}_\mu^L A_\mu(n-\hat{\mu})}\hat{\phi}_n + A_\mu(n)\underbrace{\left(\hat{\phi}_{n+\hat{\mu}}-\hat{\phi}_{n-\hat{\mu}}\right)}_{2\hat{\partial}_\mu^S\hat{\phi}}\Big]\,. \tag{IV.22}$$

Using the above limites we arrive at the limit

$$S[\hat{\phi},U]\overset{a\to 0}{\to}\int_x \phi^\dagger(x)\left[-D_\mu^2+m^2\right]\phi(x)+O(a^2)\,, \tag{IV.23}$$

the standard gauge invariant action of a complex scalar field coupled to a (non-Abelian) gauge field.

It is left to define the lattice analogue of the Yang-Mills action in terms of the link variable. To that end we remind ourselves that the fieldstrength $F_{\mu\nu}$ is nothing but the curvature tensor, see (**??**). The product of covariant derivatives $D_\mu D_\nu$ just are infinitesimal (covariant) shifts or parallel transports at the space-time point x first in ν and then in μ-direction. Put differently, the local curvature is measure by a parallel transport on a closed line (where the length of the line goes to zero). On the lattice such a minimal closed path is around a plaquette, see Fig. 16,

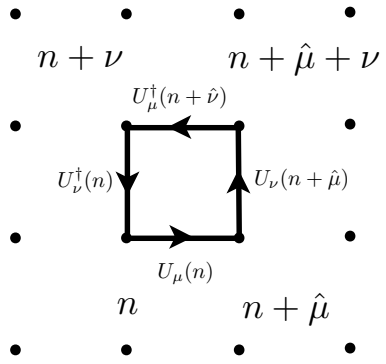

FIG. 16: Plaquette action

and the according infinitesimal shifts (parallel transports) are done by the link variables U_μ. On the lattice, this also implies shifts from e.g. $x\to x+\hat{\mu}$. Putting everything together we are led to

$$U_{\mu\nu}(n)=U_\mu(n)\,U_\nu(n+\hat{\mu})\,U_\mu^\dagger(n+\hat{\nu})\,U_\nu^\dagger(n)\,, \tag{IV.24}$$

with the plaquette variable $U_{\rm P}(n)=U_{\mu\nu}(n)$. The plaquette $U_{\rm P}$ is path ordered. In analogy to the lattice definition of the gauge field in (IV.20) we define

$$U_{\mu\nu}(n)=e^{ig_0a^2\mathcal{F}_{\mu\nu}(n)}\,, \tag{IV.25}$$

with the lattice fieldstrength tensor $\mathcal{F}_{\mu\nu}(n)$. As for the gauge field this definition is not unique, and different definitions differ at higher orders of a. For QED we derived from (IV.20), (IV.24), (IV.25) that

$$\mathcal{F}_{\mu\nu}(n)=\frac{1}{a}\left(\underbrace{A_\nu(n+\hat{\mu})-A_\nu(n)}\hat{\partial}_\mu^R A_\nu-\underbrace{A_\mu(n+\hat{\nu})-A_\mu(n)}\hat{\partial}_\nu^R A_\mu\right)\,, \tag{IV.26}$$

which in the continuum limit, $a\to 0$, tends towards the fieldstrength. In the non-Abelian case of QCD we use the Baker-Campbell-Haussdorff formula,

$$e^A\,e^B=e^{A+B+\frac{1}{2}[A\,,B]+\cdots}\,. \tag{IV.27}$$

and arrive at

$$\mathcal{F}_{\mu\nu}(n) = \frac{1}{a}\left(\hat{\partial}^R_\mu A_\nu(n) - \hat{\partial}^R_\nu A_\mu(n) + i\, g_0 a[A_\mu(n)\,,\, A_\nu(n)] + O(a^2)\right)\,, \tag{IV.28}$$

which tends towards to non-Abelian fieldstrength in the continuum limit, up to sub-leading terms. We conclude that the plaquette $U_{\mu\nu}$ has the continuum limit

$$U_{\mu\nu}(n) \to \mathbb{1} + ig_0 a\mathcal{F}_{\mu\nu}(n) - \frac{g_0^2 a^2}{2}\mathcal{F}_{\mu\nu}(n)^2 + O(a^3)\,, \qquad \to \qquad U_{\mu\nu}(n) + U^\dagger_{\mu\nu}(n) = 2 - g_0^2 a^2 \mathcal{F}_{\mu\nu}(n)^2 + O(a^3)\,. \tag{IV.29}$$

This allows us to derive a lattice analogue of the classical action of Yang-Mills (pure glue) theory,

$$S_{\rm W}[A_\mu] = \beta \sum_{n,\mu>\nu}\left(1 - \frac{1}{2N_c}{\rm tr}_{\rm f}\left[U_{\mu\nu}(n) + U^\dagger_{\mu\nu}(n)\right]\right)\,, \qquad \text{with} \qquad \beta = \frac{2N_c}{g_0^2}\,. \tag{IV.30}$$

In the continuum limit the first term on the right hand side of (IV.29), inserted in the trace in (IV.30), cancels with unity due to ${\rm tr}_{\rm f}\mathbb{1} = N_c$, the $\mathcal{F}_{\mu\nu}(n)^2$-term is the only surviving term and reduces to the standard Yang-Mills action given in (I.9).

The lattice generating functional can now be formulated in terms of the link variable U_μ and the Haar measure already discussed in Section I A. We define

$$Z \simeq \int \mathcal{D}U\, e^{-S_{\rm W}[U_\mu]}\,, \qquad \text{and} \qquad \langle U^{a_1 b_2}_{\mu_1}\cdots U^{a_m b_m}_{\mu_m}\rangle = \frac{1}{Z}\int \mathcal{D}U\, U^{a_1 b_2}_{\mu_1}\cdots U^{a_m b_m}_{\mu_m}\, e^{-S_{\rm W}[U_\mu]}\,. \tag{IV.31}$$

Here the path integral measure $\mathcal{D}U$ simply consists of a finite product of Haar measures (on a finite lattice), see e.g. [21–24]

$$\mathcal{D}U = \prod_{\text{links } l} dU_l\,, \qquad \text{with} \qquad \int dU^V = \int dU = 1\,, \quad \text{where} \qquad U^V = V\,U\,V^\dagger \quad \text{for} V \in SU(N_c)\,, \tag{IV.32}$$

and we have for $SU(3)$,

$$\begin{aligned}
\int dU\, U^{ab} &= 0\,,\\
\int dU\, U^{ab}U^{cd} &= 0\,,\\
\int dU\, U^{ab}(U^\dagger)^{cd} &= \frac{1}{3}\delta^{ad}\delta^{bc}\,,\\
\int dU\, U^{a_1 b_1}U^{a_2 b_2}\,U^{a_3 b_3} &= \frac{1}{3!}\epsilon^{a_1 a_2 a_3}\epsilon^{b_1 b_2 b_3}\,.
\end{aligned} \tag{IV.33}$$

Note that the factor 1/3 in (IV.33) follows with $\delta^{ad} = \int dU\,\delta^{ad} = \int dU\, U^{ab}\,(U^\dagger)^{bd}$. The above rules (and their extensions) allow to compute the path integrals in (IV.31) in a very simple manner.

C. The Wegner-Wilson loop & the static quark potential

In summary we conclude that the expectation value of a static quark–anti-quark pair $q\bar{q}$ discussed in chapter **??** is given by

$$W[L,T] = \frac{1}{Z}\int dA\, \mathcal{W}_{\mathcal{C}}(A)\, e^{-S_{\rm YM}[A]}\,, \qquad \text{with} \qquad \mathcal{W}_{\mathcal{C}}[A] = {\rm tr}_{\rm f} U_{\mathcal{C}}\,. \tag{IV.34}$$

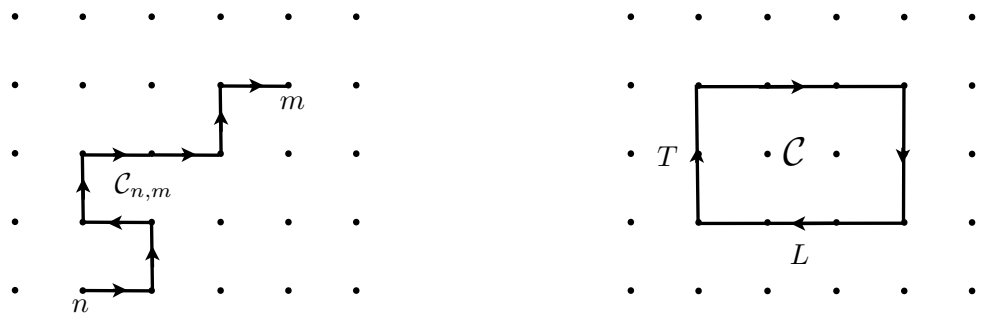

FIG. 17: Open and closed paths on the lattice

Due to its definition in terms of links variables in the continuum this correlation function is directly translated to the lattice. The paths $\mathcal{C}$ on the lattice begin end end at lattice points n and m respectively and go along the links. This is illustrated in Fig. 17. The Wilson loop is then defined as

$$W[L,T] = \frac{1}{Z}\int \mathcal{D}U\, \mathcal{W}_{\mathcal{C}}[U]\, e^{-S_{\rm w}[U]}\,, \qquad \text{with} \qquad \mathcal{W}_{\mathcal{C}}(A) \tag{IV.35}$$

where

$$\mathcal{W}_{\mathcal{C}}[U] = \mathrm{tr}_{\rm f}\, U_{\mathcal{C}} \qquad \text{with} \qquad U_{\mathcal{C}_{n,m}} = \prod_{l\in\mathcal{C}_{n,m}} U_l\,. \tag{IV.36}$$

We proceed by computing the quark–anti-quark potential, (**??**) in the strong coupling expansion on the lattice, that is

$$\beta = \frac{2N_c}{g_0^2} \to 0\,, \qquad \longleftrightarrow \qquad g_0 \to \infty\,. \tag{IV.37}$$

Within this limit the bare lattice coupling, g_0, tends fowards infinity. Note, however, that due to the RG-running of the coupling discussed earlier in the Sections I, II A, the bare coupling has to scale with a (since $\Lambda \propto 1/a$ is the ultraviolet cut-off) in order to keep the renormalised coupling finite. Envoking the one-loop running, (I.38), we deduce that the bare coupling indeed has to vanish with $1/\log a/a_0$ for $a \to 0$ with a reference lattice spacing a_0. The lattice RG and its consequences shall be discussed in the next Section IV D.

For now we concentrate on the limit (IV.37) and use it to compute

$$W[L,T] := \langle \mathcal{W}_{\mathcal{C}[L,T]}\rangle = \frac{\int \mathcal{D}U\, \mathcal{W}_{\mathcal{C}[L,T]}[U] e^{\beta\sum_P S_P}}{\int \mathcal{D}U\, e^{\beta\sum_P S_P}}\,, \qquad \text{where} \qquad S_P = \frac{1}{2N_c}\mathrm{tr}_{\rm f}\left(U_P + U_P^\dagger\right)\,. \tag{IV.38}$$

In (IV.38) we have dropped the volume factor in the Wilson action (IV.30) arising from the first term as it appears both in the numerator and the denominator. In the strong coupling limit (IV.37) we expand the action exponential as

$$e^{\beta\sum_P S_P} = \prod_P e^{\beta S_P} = \prod_P \sum_m \frac{\beta^m}{m!} S_P^m\,. \tag{IV.39}$$

Now we use the inegration rules for the Haar measure reported in (IV.32), (IV.33) to get the leading order result for (IV.38) in an expansion in β.

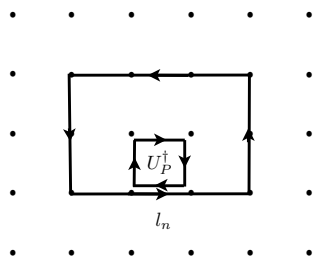

FIG. 18: Plaquette insertion in the Wegner-Wilson loop

(1) Expanding the denominator of (IV.38) in powers of β leads to

$$\int \mathcal{D}U\, e^{\beta \sum_P S_P} = \int \mathcal{D}U + O(\beta)\,, \tag{IV.40}$$

in leading order.

(2) The link variables U_l along the Wegner-Wilson loop have to be matched by $U_l^\dagger$, as the group integration $\int dU_L\, U_l$ vanishes. All other non-vanishing terms are of higher order in β. Hence a plaquette variable $U_P^\dagger$ from the expansion of the action exponential is required, see also Fig. 18 Evidently, inserting an $U_P^\dagger$ from the expansion machtes the link variable U_{l_n}, but also creates three free links $U_P^\dagger$, which have to be matched. Hence, the smallest number of plaquettes with all links matched simply covers the area bounded by the path $\mathcal{C}[L,T]$, see Fig. 19.

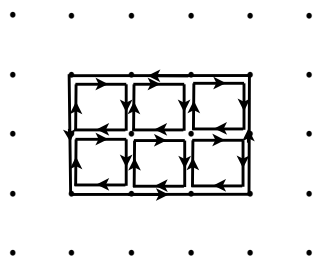

FIG. 19: Paving with plaquettes the area bounded by $\mathcal{C}[L,T]$.

In conclusion the loop is paved with

$$\frac{T}{a}\cdot\frac{L}{a} = \frac{\mathcal{A}}{a^2} = \hat{\mathcal{A}}\,, \tag{IV.41}$$

plaquettes. Thus, in leading order in the strong coupling expansion, the Wilson loop expectation value reduces to

$$W[L,T] = \prod_{l\in\mathcal{C}[L,T]} \int dU_l\, U_l^{a_l b_l} (U_l^\dagger)^{c_l d_l} \left(\frac{\beta}{6}\right)^{\hat{\mathcal{A}}} + O\left(\beta^{\hat{\mathcal{A}}+1}\right)\,, \tag{IV.42}$$

where the denominator, $6 = 2N_c$, relates to the gauge group. The group integrations and traces provide factors

$$\left(\frac{1}{3}\right)^{2\hat{\mathcal{A}}+\hat{L}+\hat{T}}, \qquad 3^{\underbrace{(\hat{L}+1)(\hat{T}+1)}_{\#\text{ lattice sites}}}, \qquad \hat{L}=\frac{L}{a}, \quad \hat{T}=\frac{T}{a}. \tag{IV.43}$$

Putting everything together we are finally led to

$$W[L,T] = 3\left(\frac{\beta}{18}\right)^{\hat{\mathcal{A}}} + O\left(\beta^{\hat{\mathcal{A}}+1}\right), \tag{IV.44}$$

leading to a static quark–anti-quark potential

$$\hat{V}[\hat{L}] = -\lim_{\hat{T}\to\infty}\frac{1}{\hat{T}}\langle \mathcal{W}_{\mathcal{C}[L,T]}[U]\rangle = \hat{\sigma}(g_0)\hat{L}, \qquad \text{with} \qquad \hat{\sigma} = -\log\beta/18, \tag{IV.45}$$

with string tension $\hat{\sigma}$. We close with final remarks:

(1) The computation leading to (IV.44) also goes through for $U(1)$. Accordingly, compact $U(1)$ has a confining phase on the lattice. It also has a Coulomb phase ($1/r$-potential).

(2) The above already raises the question about the continuum limit. As discussed in the beginning of this Section IV C, we have to finetune the lattice coupling $g_0(a)$ for approaching the continuum limit. This is discussed in the next sextion.

D. Continuum limit of lattice Yang-Mills theory

In the continuum limit of a lattice theory we kepp the physical mass m fixed (smalles physical momentum scale). This implies

$$\hat{m} = m\cdot a \to 0, \qquad \text{and} \qquad \hat{\xi} = \frac{1}{\hat{m}} \to \infty, \tag{IV.46}$$

the lattice correlation length $\hat{\xi}$ diverges. An infinite correlation length is the signature of a 2^{nd} order phase transition. A this point in parameter space the lattice has infinite many points inside a physical distance.

In lattice Yang-Mills the only tuning parameter at hand is the bare coupling g_0:

$$\hat{\xi}(g_0) \overset{g_0\to g_*}{\longrightarrow} \infty. \tag{IV.47}$$

Applying this limit to an observable $\mathcal{O}$ we have

$$\mathcal{O}(g_0,a) = \left(\frac{1}{a}\right)^{d_\mathcal{O}} \hat{\mathcal{O}}(g_0), \tag{IV.48}$$

where $d_\mathcal{O}$ is the momentum dimension of the operator $\mathcal{O}$. In the continuum limit we are led to

$$\mathcal{O}(g_0\to g_*, a\to 0) = \mathcal{O}_{\text{phys}}. \tag{IV.49}$$

We conclude that if we know the functional dependence of $\mathcal{O}$ on g_0, we know $g_0(a)$ with

$$\mathcal{O}(g_0(a),a) = O_{\text{phys}}. \tag{IV.50}$$

Note that the above argument seems to imply that $g_0(a)$ depends on the choice of $\mathcal{O}$. However, it turns out that for sufficiently small a, $g_0(a)$ is universal up to sub-leading terms ($\leftarrow$ renormalisation group equations).

Let us now take as $\mathcal{O}$ the static $q\bar{q}$ potential $V_{q\bar{q}}$ and we are led to

$$V(L,g_0,a) = \frac{1}{a}\hat{V}(\hat{L},g_0). \tag{IV.51}$$

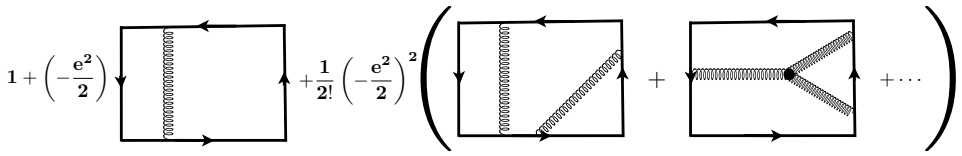

FIG. 20: Diagrams up to order g_0^4 contributing to the Wilson loop expextation value $W[L,T]$.

Now, keeping $V(L,g_0,a)$ fixed at its physics value $V_{\rm phys}$ while taking the limit $a\to 0$ implies

$$\left(a\frac{\partial}{\partial a}-\beta(g_0)\frac{\partial}{\partial g_0}\right)V(L,g_0,a)=0\,,\qquad\text{with}\qquad \beta(g_0)=-a\frac{\partial g_0}{\partial a}\,. \tag{IV.52}$$

As the ultraviolet cut-off $\Lambda_{\rm UV}=\pi/a$, (IV.52) can be simply read as the RG-equation for the static quark–anti-quark potential $V_{q\bar q}$. The contributing diagrams up to order g_0^4 are depicted in Fig. 20.

Then the potential is computed as

$$V(L)=-\frac{g_0(a)^2}{4\pi L}C_F\left[1+g_0(a)^2\frac{11N_c}{24\pi^2}\ln\hat L+\text{const.}\right]\,, \tag{IV.53}$$

with the second Casimir C_F in the fundamental representation, see (**??**). Inserting (IV.53) in (IV.52) yields

$$\beta(g_0)=-\frac{g_0^3}{16\pi^2}\frac{11}{3}N_c=\beta_0 g_0^3\,, \tag{IV.54}$$

the one-loop β-function of Yang-Mills theory whis has been already computed before. It should not be confused with $\beta=2N_c/g_0^2$ which unfortunately is labeld the same. Since we have $\beta(g_0)<0$ which signals asymptotic freedom, the bare lattice coupling g_0 is driven to zero in the continuum limit with $a\to 0$,

$$a=\frac{1}{\Lambda_L}e^{\frac{1}{2\beta_0 g_0^2}}\,,\qquad\text{with}\qquad \hat L(g_0)=L\,\Lambda_L e^{-\frac{1}{2\beta_0 g_0^2}}\,, \tag{IV.55}$$

where $\Lambda_L(\simeq 1/L)$ is a (physical) reference scale. Let us now rewrite the RG-equation (IV.52) in terms of pyhsical scales,

$$\left(L\partial_L+\beta(g_0)\frac{\partial}{\partial g_0}\right)V(L,g_0,a)=-V(L,g_0,a)\,, \tag{IV.56}$$

or

$$\left(L\partial_L+\beta(g_0)\frac{\partial}{\partial g_0}\right)\tilde V(L,g_0,a)=0\,,\qquad\text{with}\qquad \tilde V(L,g_0,a)=L\,V(L,g_0,a)\,. \tag{IV.57}$$

Eq.(IV.57) entails that a change of the physical distance L can be absorbed in a corresponding change of the bare coupling g_0. We write

$$\tilde V=\tilde V(L,\bar g(L),a)\,, \tag{IV.58}$$

where $\bar g(L)$ has the property $L\partial_L\bar g=-\beta(\bar g)$ and hence

$$\bar g^2(L)=\frac{\bar g_0^2}{1+\beta_0\bar g_0^2\log\hat L^2}\,. \tag{IV.59}$$

Using (IV.59) in $\tilde V$ leads to

$$V(L)=C\frac{\alpha_s(L)}{L}\,,\qquad\text{with}\qquad \alpha_s(L)=\frac{\bar g^2(L)}{4\pi}\,. \tag{IV.60}$$

This seemingly depends on a but with (IV.55) we arrive at

$$\alpha_s(L) = \frac{1}{4\pi} \frac{\bar{g}_0^2}{1 + \beta_0 \bar{g}_0^2 \log\left(L^2 \Lambda_L^2 e^{-\frac{1}{\beta_0 \bar{g}_0^2}}\right)} = \frac{1}{4\pi} \frac{1}{\beta_0 \log(L^2 \Lambda_L^2)} \,. \tag{IV.61}$$

This leaves us with a static quark–anti-quark potential potential $V(L)$, (IV.60) in terms of physical quantities. We add a few remarks:

(1) The coupling $\bar{g}_0^2/(4\pi)$ is the running coupling α_s at the scale $L = a$: $\alpha_s(a) = \bar{g}_0^2/(4\pi)$.

(2) The scale Λ_L is the momentum scale at which the (one-loop) coupling diverges: $\alpha_s(L \to 1/\Lambda_{L+}) \to \infty$.

(3) Λ_L is RG-invariant:

$$a\frac{d}{a}\Lambda_L = \left(a\frac{\partial}{\partial a} - \beta(g_0)\frac{\partial}{\partial g_0}\right)\left(\frac{1}{a} e^{\frac{1}{2\beta_0 \bar{g}_0^2}}\right) = 0 \,. \tag{IV.62}$$

The above analysis is by now means restricted to one loop, for the two loop extension see exercise.

We close the discussion on the static quark–anti-quark potential with a discussion of the asymptotic behaviour. We would like to know how close at a given lattice we are already to the continuum limit with a given observable $\hat{\mathcal{O}}$, see (IV.48). From (IV.49) and $a\partial_a O_{a\to 0} = 0$ we conclude that

$$\hat{O} \simeq \hat{C}_{\mathcal{O}} \left[\hat{L}(g_0)\right]^{d_C O} \,. \tag{IV.63}$$

The scaling behaviour in (IV.63) signals the continuum limit and is called 'asymptotic scaling'. It is not present in the following regimes:

(1) If g_0 and hence a get too small at a fixed numer of lattice points, the physical lattice volume shrinks and the physical scales will eventually exceed the lattice volume. This leads to finite size effects, and (IV.63) ceases to be valid.

(2) If g_0 gets to big, the lattice well get too coarse, and (IV.63) is not valid anymore.

In summary continuum physics is only seen in the (narrow) scaling window avoiding (1) & (2).

This allows us to (re-)evaluate our result on the string tension in the strong coupling limit derived in the last Section IV C, see (IV.45). In the continuum limit such a potential has the physical string tension

$$\sigma = \lim_{a\to 0} \frac{1}{a^2} \hat{\sigma}(g_0(a)) \,, \tag{IV.64}$$

and hence

$$\sigma \simeq \lim_{a\to 0} \frac{1}{a^2} \left[\hat{L}(g_0)\right]^2 \,. \tag{IV.65}$$

Note that $\hat{L}(g_0)$ is a non-perturbative scale and vanishes in any order of perturbation theory. These remarks on the continuum limit conclude our little lattice excursion.

V. PARTON DENSITIES

At the end of Section II B the discussion of different energy regimes for R experimentally makes sense — at an e^+e^- collider we can tune the energy of the initial state. At hadron colliders the situation is very different. The energy distribution of incoming quarks as parts of the colliding protons has to be taken into account. We first assume that quarks move collinearly with the surrounding proton such that at the LHC incoming partons have zero p_T. Under that condition we can define a probability distribution $f_i(x)$ for finding a parton i with a given fraction $x = 0 \cdots 1$ of the proton's longitudinal momentum, the so-called parton density function (pdf). In this section we will see how it is related to the splitting kernels describing the collinear and soft divergences of QCD parton splitting.

A pdf is not an observable, only a distribution in the mathematical sense: it has to produce reasonable results when we integrate it together with a test function. Different parton densities have very different behavior — for the valence

quarks (uud) they peak somewhere around $x \lesssim 1/3$, while the gluon pdf is small at $x \sim 1$ and grows very rapidly towards small x. For some typical part of the relevant parameter space ($x = 10^{-3} \cdots 10^{-1}$) the gluon density roughly scales like $f_g(x) \propto x^{-2}$. Towards smaller x values it becomes even steeper. This steep gluon distribution was initially not expected and means that for small enough x LHC processes will dominantly be gluon fusion processes.

While we cannot actually compute parton distribution functions $f_i(x)$ as a function of the momentum fraction x there are a few predictions we can make based on symmetries and properties of the hadrons, leading to to sum rules:

1. The parton distributions inside an antiproton are linked to those inside a proton through the CP symmetry, which is an exact symmetry of QCD. Therefore, we know that

$$f_q^{\bar{p}}(x) = f_{\bar{q}}(x) \qquad f_{\bar{q}}^{\bar{p}}(x) = f_q(x) \qquad f_g^{\bar{p}}(x) = f_g(x) \tag{V.1}$$

   for all values of x.

2. If the proton consists of three valence quarks uud, plus quantum fluctuations from the vacuum which can either involve gluons or quark–antiquark pairs, the contribution from the sea quarks has to be symmetric in quarks and antiquarks. The expectation values for the signed numbers of up and down quarks inside a proton have to fulfill

$$\langle N_u \rangle = \int_0^1 dx \; (f_u(x) - f_{\bar{u}}(x)) = 2 \qquad \langle N_d \rangle = \int_0^1 dx \; (f_d(x) - f_{\bar{d}}(x)) = 1 \; . \tag{V.2}$$

3. The total momentum of the proton has to consist of sum of all parton momenta. We can write this as the expectation value of $\sum x_i$

$$\left\langle \sum x_i \right\rangle = \int_0^1 dx \; x \left(\sum_q f_q(x) + \sum_{\bar{q}} f_{\bar{q}}(x) + f_g(x) \right) = 1 \tag{V.3}$$

   What makes this prediction interesting is that we can compute the same sum only taking into account the measured quark and antiquark parton densities. We find

$$\int_0^1 dx \; x \left(\sum_q f_q(x) + \sum_{\bar{q}} f_{\bar{q}}(x) \right) \approx \frac{1}{2} \; . \tag{V.4}$$

   Half of the proton momentum is then carried by gluons.

Given the correct definition and normalization of the pdf we can now compute the hadronic cross section from its partonic counterpart,

$$\boxed{\sigma_{\text{tot}} = \int_0^1 dx_1 \int_0^1 dx_2 \sum_{ij} f_i(x_1) \, f_j(x_2) \, \hat{\sigma}_{ij}(x_1 x_2 S)} \; , \tag{V.5}$$

where i, j are the incoming partons with the momentum factions $x_{i,j}$. The partonic energy of the scattering process is $s = x_1 x_2 S$ with the LHC proton energy of $\sqrt{S} = 13.6$ TeV. The partonic cross section $\hat{\sigma}$ includes all the necessary θ and δ functions for energy–momentum conservation. When we express a general n–particle cross section $\hat{\sigma}$ including the phase space integration, the x_i integrations and the phase space integrations can of course be interchanged, but Jacobians will make life hard.

A. DGLAP equation

We know that collinear parton splitting affects the incoming partons at hadron colliders. For example in $pp \to Z$ production incoming partons inside the protons transform into each other until they enter the Z production process as quarks. According to Eq.(II.62), the factorized phase space and splittings depend on the energy fraction z and the so-called virtuality t. The same has to be true for the parton densities, $f(x_n, -t_n)$. The additional parameter t is new compared to the purely probabilistic picture in Eq.(V.5).

More quantitatively, we start with a quark inside the proton with an energy fraction x_0, as it enters the hadronic phase space integral. As this quark is confined inside the proton, it can only have small transverse momentum, which

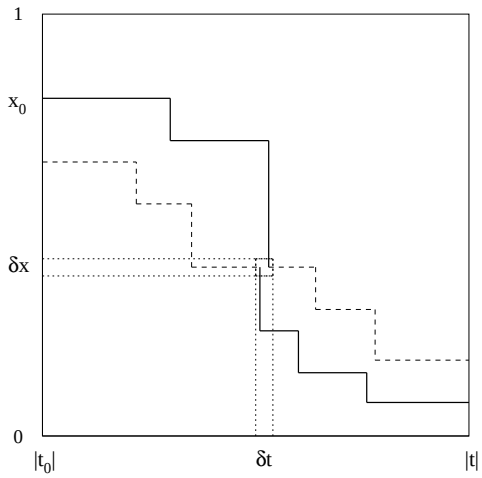

FIG. 21: Path of an incoming parton in the $(x-t)$ plane. Because we define t as a negative number its axis is labelled $|t|$.

means its four-momentum squared t_0 is negative and its absolute value $|t_0|$ is small. For the incoming partons which if on–shell have $p^2 = 0$ it gives the distance to the mass shell. Let us simplify our kinematic argument by assuming that there exists only one splitting, namely successive gluon radiation off an incoming quark, where the outgoing gluons are not relevant

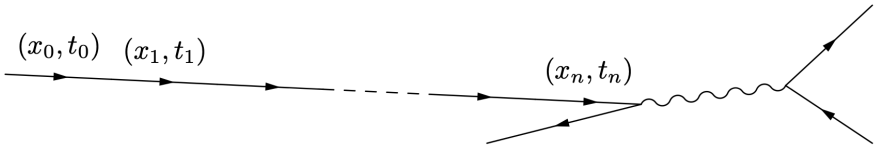

In that case each collinear gluon radiation will decrease the quark energy and increase its virtuality through recoil,

$$x_{j+1} < x_j \qquad \text{and} \qquad |t_{j+1}| = -t_{j+1} > -t_j = |t_j| \; . \tag{V.6}$$

We know what the successive splitting means in terms of splitting probabilities and can describe how the parton density $f(x,-t)$ evolves in the $(x-t)$ plane as depicted in Figure 21. The starting point (x_0, t_0) is, probabilistically, given by the energy and kinds of parton and hadron. We then interpret each branching as a step downward in $x_j \to x_{j+1}$ and assign to a increased virtuality $|t_{j+1}|$ after the branching. The actual splitting path in the $(x-t)$ plane is made of discrete points. The probability of a splitting to occur is given by Eq.(II.62),

$$\frac{\alpha_s}{2\pi} \, \hat{P}(z) \, \frac{dt}{t} \, dz \equiv \frac{\alpha_s}{2\pi} \, \hat{P}_{q \leftarrow q}(z) \, \frac{dt}{t} \, dz \; . \tag{V.7}$$

At the end of the path we will probe the evolved parton density at (x_n, t_n), entering the hard scattering process and its energy–momentum conservation.

To convert a partonic into a hadronic cross section, we probe the probability or the parton density $f(x,-t)$ over an infinitesimal square,

$$[x_j, x_j + \delta x] \qquad \text{and} \qquad [|t_j|, |t_j| + \delta t] \; . \tag{V.8}$$

Using our (x,t) plane we can compute the flows into this square and out of this square, which together define the net shift in f in the sense of a differential equation,

$$\delta f_{\text{in}} - \delta f_{\text{out}} = \delta f(x,-t) \; . \tag{V.9}$$

We compute the incoming and outgoing flows from the history of the (x,t) evolution. At this stage our picture becomes a little subtle; the way we define the path between two splittings in Figure 21 it can enter and leave the square either vertically or horizontally. Because we want to arrive at a differential equation in t we choose the vertical

drop, such that the area the incoming and outgoing flows see is given by δt. If we define a splitting as a vertical drop in x at the target value t_{j+1}, an incoming path hitting the square can come from any x-value above the square. Using this convention and following the fat solid lines in Figure 21 the vertical flow into (and out of) the square (x,t) square is proportional to δt as the size of the covered interval

$$\begin{aligned}
\delta f_{\text{in}}(-t) &= \delta t \left(\frac{\alpha_s \hat{P}}{2\pi t} \otimes f\right)(x,-t) \\
&= \frac{\delta t}{t}\int_x^1 \frac{dz}{z}\,\frac{\alpha_s}{2\pi}\,\hat{P}(z) f\left(\frac{x}{z},-t\right) \\
&\equiv \frac{\delta t}{t}\int_0^1 \frac{dz}{z}\,\frac{\alpha_s}{2\pi}\,\hat{P}(z) f\left(\frac{x}{z},-t\right) \qquad \text{assuming } f(x',-t)=0 \text{ for } x'>1\,. \qquad \text{(V.10)}
\end{aligned}$$

We use the definition of a convolution

$$(f\otimes g)(x) = \int_0^1 dx_1 dx_2 f(x_1) g(x_2)\,\delta(x-x_1x_2) = \int_0^1 \frac{dx_1}{x_1} f(x_1) g\left(\frac{x}{x_1}\right) = \int_0^1 \frac{dx_2}{x_2} f\left(\frac{x}{x_2}\right) g(x_2)\,. \qquad \text{(V.11)}$$

The outgoing flow we define as leaving the infinitesimal square vertically. Following the fat solid line in Figure 21 it is also proportional to δt

$$\delta f_{\text{out}}(-t) = \delta t \int_0^1 dy \frac{\alpha_s \hat{P}(y)}{2\pi t}\, f(x,-t) = \frac{\delta t}{t} f(x,-t)\int_0^1 dy\,\frac{\alpha_s}{2\pi}\,\hat{P}(y)\,. \qquad \text{(V.12)}$$

The y-integration is not a convolution, because we know the starting condition and integrate over all final configurations. Combining Eq.(V.10) and Eq.(V.12) we can compute the change in the quark pdf as

$$\begin{aligned}
\delta f(x,-t) &= \frac{\delta t}{t}\left[\int_0^1 \frac{dz}{z}\,\frac{\alpha_s}{2\pi}\,\hat{P}(z)\, f\left(\frac{x}{z},-t\right) - \int_0^1 dy\,\frac{\alpha_s}{2\pi}\,\hat{P}(y)\, f(x,-t)\right] \\
&= \frac{\delta t}{t}\int_0^1 \frac{dz}{z}\,\frac{\alpha_s}{2\pi}\left[\hat{P}(z) - \delta(1-z)\int_0^1 dy \hat{P}(y)\right] f\left(\frac{x}{z},-t\right) \\
&\equiv \frac{\delta t}{t}\int_x^1 \frac{dz}{z}\,\frac{\alpha_s}{2\pi}\,\hat{P}(z)_+\, f\left(\frac{x}{z},-t\right) \\
\Leftrightarrow \qquad \frac{\delta f(x,-t)}{\delta(-t)} &= \frac{1}{(-t)}\int_x^1 \frac{dz}{z}\,\frac{\alpha_s}{2\pi}\,\hat{P}(z)_+\, f\left(\frac{x}{z},-t\right) \qquad \text{(V.13)}
\end{aligned}$$

Strictly speaking, we require α_s to only depend on t and introduce the so-defined plus subtraction

$$F(z)_+ \equiv F(z) - \delta(1-z)\int_0^1 dy\, F(y) \qquad \text{or} \qquad \int_0^1 dz\,\frac{f(z)}{(1-z)_+} = \int_0^1 dz\left(\frac{f(z)}{1-z} - \frac{f(1)}{1-z}\right)\,. \qquad \text{(V.14)}$$

For the second definition we choose $F(z) = 1/(1-z)$, multiply it with an arbitrary test function $f(z)$ and integrate over z.

The plus–subtracted integral is by definition finite in the limit $z\to 1$, where some of the splitting kernels diverge. At this stage the plus prescription is simply a convenient way of writing a complicated combination of splitting kernels, but we will see that it also has a physics meaning. We can check that the plus prescription indeed acts as a regularization. Obviously, the integral over $f(z)/(1-z)$ is divergent at the boundary $z\to 1$, which we know we can cure using dimensional regularization. For $f(z)=1$ we illustrates the relation between the two regularization techniques,

$$\int_0^1 dz\,\frac{1}{(1-z)^{1-\epsilon}} = \int_0^1 dz\,\frac{1}{z^{1-\epsilon}} = \left.\frac{z^\epsilon}{\epsilon}\right|_0^1 = \frac{1}{\epsilon} \qquad \text{with } \epsilon>0\,, \qquad \text{(V.15)}$$

corresponding to $4+2\epsilon$ dimensions. This change in sign avoids the analytic continuation of the usual value $n=4-2\epsilon$

to $\epsilon < 0$. We can relate the dimensionally regularized integral to the plus subtraction as

$$\begin{aligned}
\int_0^1 dz\, \frac{f(z)}{(1-z)^{1-\epsilon}} &= \int_0^1 dz\, \frac{f(z)-f(1)}{(1-z)^{1-\epsilon}} + f(1) \int_0^1 dz\, \frac{1}{(1-z)^{1-\epsilon}} \\
&= \int_0^1 dz\, \frac{f(z)-f(1)}{1-z}\,(1+\mathcal{O}(\epsilon)) + \frac{f(1)}{\epsilon} \\
&= \int_0^1 dz\, \frac{f(z)}{(1-z)_+}\,(1+\mathcal{O}(\epsilon)) + \frac{f(1)}{\epsilon} \qquad \text{by definition} \\
\Leftrightarrow \qquad \int_0^1 dz\, \frac{f(z)}{(1-z)^{1-\epsilon}} - \frac{f(1)}{\epsilon} &= \int_0^1 dz\, \frac{f(z)}{(1-z)_+}\,(1+\mathcal{O}(\epsilon)) \; . \qquad \text{(V.16)}
\end{aligned}$$

The dimensionally regularized integral minus the pole, *i.e.* the finite part of the dimensionally regularized integral, is the same as the plus–subtracted integral modulo terms of the order ϵ. The third line in Eq.(V.16) shows that the difference between a dimensionally regularized splitting kernel and a plus–subtracted splitting kernel manifests itself as terms proportional to $\delta(1-z)$. Physically, they represent contributions to a soft–radiation phase space integral.

Finally, we turn to our splitting kernel $\hat{P}_{q\leftarrow q}$ in Eq.(II.59). If the plus prescription regularizes the pole at $z \to 1$, what is the effect of the numerator of the regularized quark splitting kernel? The finite difference between the two subtracted kernels is

$$\begin{aligned}
\left(\frac{1+z^2}{1-z}\right)_+ - (1+z^2)\,\left(\frac{1}{1-z}\right)_+ &= \frac{1+z^2}{1-z} - \delta(1-z)\int_0^1 dy\, \frac{1+y^2}{1-y} - \frac{1+z^2}{1-z} + \delta(1-z)\int_0^1 dy\, \frac{1+z^2}{1-y} \\
&= -\delta(1-z)\int_0^1 dy\, \left(\frac{1+y^2}{1-y} - \frac{2}{1-y}\right) \\
&= \delta(1-z)\int_0^1 dy\, \frac{y^2-1}{y-1} = \delta(1-z)\int_0^1 dy\,(y+1) = \frac{3}{2}\delta(1-z)\; . \qquad \text{(V.17)}
\end{aligned}$$

This means we can write the quark splitting kernel in two equivalent ways

$$P_{q\leftarrow q}(z) \equiv C_F \left(\frac{1+z^2}{1-z}\right)_+ = C_F \left[\frac{1+z^2}{(1-z)_+} + \frac{3}{2}\delta(1-z)\right] \; . \qquad \text{(V.18)}$$

Going back to our differential equation, the infinitesimal Eq.(V.13) is the Dokshitzer–Gribov–Lipatov–Altarelli–Parisi or DGLAP equation. It describes the virtuality or scale dependence of the quark parton density. Quarks do not only appear in $q \to q$ splitting, but also in gluon splitting. Therefore, we generalize Eq.(V.13) to include quarks and gluons. This generalization implies a sum over all allowed splittings and the plus–subtracted splitting kernels. For the quark density on the left hand side it is

$$\boxed{\frac{df_q(x,-t)}{d\log(-t)} = -t\,\frac{df_q(x,-t)}{d(-t)} = \sum_{j=q,g} \int_x^1 \frac{dz}{z}\,\frac{\alpha_s}{2\pi}\,P_{q\leftarrow j}(z)\,f_j\left(\frac{x}{z},-t\right)} \qquad \text{with} \quad P_{q\leftarrow j}(z) \equiv \hat{P}_{q\leftarrow j}(z)_+ \; . \qquad \text{(V.19)}$$

Going back to Eq.(V.13) the relevant splittings in that form give us

$$\begin{aligned}
\delta f_q(x,-t) = \frac{\delta t}{t}\,\left[\int_0^1 \frac{dz}{z}\,\frac{\alpha_s}{2\pi}\,\hat{P}_{q\leftarrow q}(z)\,f_q\left(\frac{x}{z},-t\right) + \int_0^1 \frac{dz}{z}\,\frac{\alpha_s}{2\pi}\,\hat{P}_{q\leftarrow g}(z)\,f_g\left(\frac{x}{z},-t\right)\right. \\
\left. - \int_0^1 dy\,\frac{\alpha_s}{2\pi}\,\hat{P}_{q\leftarrow q}(y)\,f_q(x,-t)\right] \; . \qquad \text{(V.20)}
\end{aligned}$$

Of the three terms on the right hand side the first and the third together define the plus–subtracted splitting kernel $P_{q\leftarrow q}(z)$, just following the argument above. The second term is a convolution proportional to the gluon pdf. Quarks can be produced in gluon splitting but cannot vanish into it. Therefore, the second term in Eq.(V.20) includes $P_{q\leftarrow g}$, without a plus–regulator

$$P_{q\leftarrow g}(z) \equiv \hat{P}_{q\leftarrow g}(z) = T_R\left[z^2 + (1-z)^2\right] \; . \qquad \text{(V.21)}$$

In the functional form of this kernel we are indeed missing the soft-radiation divergence for $z \to 1$ from $P_{q\leftarrow q}(z)$.

The second QCD parton density we have to study is the gluon density. The incoming contribution to the infinitesimal square is given by the sum of four splitting scenarios each leading to a gluon with virtuality $-t_{j+1}$

$$\begin{aligned}\delta f_{\text{in}}(-t) &= \frac{\delta t}{t}\int_0^1 \frac{dz}{z}\,\frac{\alpha_s}{2\pi}\left[\hat{P}_{g\leftarrow g}(z)\left(f_g\left(\frac{x}{z},-t\right)+f_g\left(\frac{x}{1-z},-t\right)\right)+\hat{P}_{g\leftarrow q}(z)\left(f_q\left(\frac{x}{z},-t\right)+f_{\bar{q}}\left(\frac{x}{z},-t\right)\right)\right] \\ &= \frac{\delta t}{t}\int_0^1 \frac{dz}{z}\,\frac{\alpha_s}{2\pi}\left[2\hat{P}_{g\leftarrow g}(z) f_g\left(\frac{x}{z},-t\right)+\hat{P}_{g\leftarrow q}(z)\left(f_q\left(\frac{x}{z},-t\right)+f_{\bar{q}}\left(\frac{x}{z},-t\right)\right)\right]\,, \end{aligned} \tag{V.22}$$

using $P_{g\leftarrow\bar{q}} = P_{g\leftarrow q}$ in the first line and $P_{g\leftarrow g}(1-z) = P_{g\leftarrow g}(z)$ in the second. To leave the volume element in (x,t)-space a gluon can either split into two gluons or radiate one of n_f light-quark flavors. Combining the incoming and outgoing flows we find

$$\begin{aligned}\delta f_g(x,-t) =& \frac{\delta t}{t}\int_0^1 \frac{dz}{z}\,\frac{\alpha_s}{2\pi}\left[2\hat{P}_{g\leftarrow g}(z) f_g\left(\frac{x}{z},-t\right)+\hat{P}_{g\leftarrow q}(z)\left(f_q\left(\frac{x}{z},-t\right)+f_{\bar{q}}\left(\frac{x}{z},-t\right)\right)\right] \\ &-\frac{\delta t}{t}\int_0^1 dy\,\frac{\alpha_s}{2\pi}\left[\hat{P}_{g\leftarrow g}(y)+n_f\hat{P}_{q\leftarrow g}(y)\right] f_g(x,-t)\end{aligned} \tag{V.23}$$

Unlike in the quark case these terms do not immediately correspond to regularizing the diagonal splitting kernel using the plus prescription.

First, the contribution to δf_{in} proportional to f_q or $f_{\bar{q}}$ which is not matched by the outgoing flow. From the quark case we already know how to deal with it. The corresponding splitting kernel does not need any regularization, so we define

$$P_{g\leftarrow q}(z) \equiv \hat{P}_{g\leftarrow q}(z) = C_F\frac{1+(1-z)^2}{z}\,. \tag{V.24}$$

We see that the structure of the DGLAP equation implies that the two off-diagonal splitting kernels do not include any plus prescription $\hat{P}_{i\leftarrow j} = P_{i\leftarrow j}$. We could have expected these kernels are finite in the soft limit, $z\to 1$.

Next, we can compute the y-integral describing the gluon splitting into a quark pair directly,

$$\begin{aligned}-\int_0^1 dy\,\frac{\alpha_s}{2\pi}\,n_f\,\hat{P}_{q\leftarrow g}(y) &= -\frac{\alpha_s}{2\pi}\,n_f\,T_R\int_0^1 dy\,\left[1-2y+2y^2\right] \qquad \text{using Eq.(V.21)} \\ &= -\frac{\alpha_s}{2\pi}\,n_f\,T_R\left[y-y^2+\frac{2y^3}{3}\right]_0^1 \\ &= -\frac{2}{3}\,\frac{\alpha_s}{2\pi}\,n_f\,T_R\,.\end{aligned} \tag{V.25}$$

Finally, the two terms proportional to the pure gluon splitting $P_{g\leftarrow g}$ in Eq.(V.23) require some work. The y-integral from the outgoing flow has to consist of a finite term and a term we can use to define the plus prescription for $\hat{P}_{g\leftarrow g}$. The integral gives

$$\begin{aligned}-\int_0^1 dy\,\frac{\alpha_s}{2\pi}\,\hat{P}_{g\leftarrow g}(y) &= -\frac{\alpha_s}{2\pi}\,C_A\int_0^1 dy\,\left[\frac{y}{1-y}+\frac{1-y}{y}+y(1-y)\right] \qquad \text{using Eq.(II.55)} \\ &= -\frac{\alpha_s}{2\pi}\,C_A\int_0^1 dy\,\left[\frac{2y}{1-y}+y(1-y)\right] \\ &= -\frac{\alpha_s}{2\pi}\,C_A\int_0^1 dy\,\left[\frac{2(y-1)}{1-y}+y(1-y)\right]-\frac{\alpha_s}{2\pi}\,C_A\int_0^1 dy\,\frac{2}{1-y} \\ &= -\frac{\alpha_s}{2\pi}\,C_A\int_0^1 dy\,\left[-2+y-y^2\right]-\frac{\alpha_s}{2\pi}\,2C_A\int_0^1 dz\,\frac{1}{1-z} \\ &= -\frac{\alpha_s}{2\pi}\,C_A\left[-2+\frac{1}{2}-\frac{1}{3}\right]-\frac{\alpha_s}{2\pi}\,2C_A\int_0^1 dz\,\frac{1}{1-z} \\ &= \frac{\alpha_s}{2\pi}\,\frac{11}{6}\,C_A\,-\frac{\alpha_s}{2\pi}\,2C_A\int_0^1 dz\,\frac{1}{1-z}\,.\end{aligned} \tag{V.26}$$

The second term in this result is what we need to replace the first term in the splitting kernel of Eq.(II.55) proportional to $1/(1-z)$ by $1/(1-z)_+$. We can see this using $f(z) = z$ and correspondingly $f(1) = 1$ in Eq.(V.14). The two finite terms in Eq.(V.25) and Eq.(V.26) are included in the definition of $\hat{P}_{g\leftarrow g}$ ad hoc. Because the regularized splitting kernel appears in a convolution, the two finite terms require an explicit factor $\delta(1-z)$. Collecting all of them we arrive at

$$P_{g\leftarrow g}(z) = 2C_A \left(\frac{z}{(1-z)_+} + \frac{1-z}{z} + z(1-z) \right) + \frac{11}{6} C_A \, \delta(1-z) - \frac{2}{3} \, n_f \, T_R \, \delta(1-z) \, . \tag{V.27}$$

This result concludes our computation of all four regularized splitting functions which appear in the DGLAP equation Eq.(V.19).

Before discussing and solving the DGLAP equation, let us briefly recapitulate: for the full quark and gluon particle content of QCD we have derived the DGLAP equation which describes a factorization scale dependence of the quark and gluon parton densities. The universality of the splitting kernels is obvious from the way we derive them — no information on the n-particle process ever enters the derivation.

The DGLAP equation is formulated in terms of four splitting kernels of gluons and quarks which are linked to the splitting probabilities, but which for the DGLAP equation have to be regularized. With the help of a plus–subtraction all kernels $P_{i\leftarrow j}(z)$ become finite, including in the soft limit $z \to 1$. However, splitting kernels are only regularized when needed, so the finite off-diagonal quark–gluon and gluon–quark splittings are unchanged. This means the plus prescription really acts as an infrared renormalization, moving universal infrared divergences into the definition of the parton densities. The original collinear divergence has vanished as well.

The only approximation we make in the computation of the splitting kernels is that in the y-integrals the running coupling α_s does not depend on the momentum fraction. In its standard form and in terms of the factorization scale $\mu_F^2 \equiv -t$ the DGLAP equation reads

$$\boxed{\frac{df_i(x,\mu_F)}{d\log\mu_F^2} = \sum_j \int_x^1 \frac{dz}{z} \frac{\alpha_s}{2\pi} P_{i\leftarrow j}(z) \, f_j\left(\frac{x}{z},\mu_F\right) = \frac{\alpha_s}{2\pi} \sum_j \left(P_{i\leftarrow j} \otimes f_j\right)(x,\mu_F)} \, . \tag{V.28}$$

B. Solving the DGLAP equation

Solving the integro-differential DGLAP equation Eq.(V.28) for the parton densities is clearly beyond the scope of this writeup. Nevertheless, we will sketch how we would approach this. This will give us some information on the structure of its solutions which we need to understand the physics of the DGLAP equation.

One simplification we can make is to postulate eigenvalues in parton space and solve the equation for them. This gets rid of the sum over partons on the right hand side. One such parton density is the non–singlet parton density, defined as the difference of two parton densities

$$f_q^{\text{NS}} = (f_q - f_{\bar{q}}) \, . \tag{V.29}$$

Since gluons cannot distinguish between quarks and antiquarks, the gluon contribution to their evolution cancels, at least in the massless limit, at arbitrary loop order. The corresponding DGLAP equation with leading order splitting kernels is

$$\frac{df_q^{\text{NS}}(x,\mu_F)}{d\log\mu_F^2} = \int_x^1 \frac{dz}{z} \frac{\alpha_s}{2\pi} P_{q\leftarrow q}(z) \, f_q^{\text{NS}}\left(\frac{x}{z},\mu_F\right) \, . \tag{V.30}$$

To solve it we need a transformation which simplifies a convolution, leading us to the Mellin transform. Starting from a function $f(x)$ of a real variable x we define the Mellin transform into moment space m

$$\mathcal{M}[f](m) \equiv \int_0^1 dx \, x^{m-1} f(x) \qquad\qquad f(x) = \frac{1}{2\pi i} \int_{c-i\infty}^{c+i\infty} dm \, \frac{\mathcal{M}[f](m)}{x^m} \, , \tag{V.31}$$

where for the back transformation we choose an arbitrary appropriate constant $c > 0$, such that the integration contour for the inverse transformation lies to the right of all singularities of the analytic continuation of $\mathcal{M}[f](m)$. The important property for us is that the Mellin transform of a convolution is the product of the two Mellin transforms,

which gives us the transformed DGLAP equation

$$\begin{aligned}\frac{d\mathcal{M}[f_q^{\rm NS}](m,\mu_F)}{d\log\mu_F^2} &= \frac{\alpha_s}{2\pi}\,\mathcal{M}\left[\int_0^1 \frac{dz}{z} P_{q\leftarrow q}\left(\frac{x}{z}\right) f_q^{\rm NS}(z)\right](m) \\ &= \frac{\alpha_s}{2\pi}\,\mathcal{M}[P_{q\leftarrow q}\otimes f_q^{\rm NS}](m) \\ &= \frac{\alpha_s}{2\pi}\,\mathcal{M}[P_{q\leftarrow q}](m)\quad \mathcal{M}[f_q^{\rm NS}](m,\mu_F)\,, \end{aligned} \tag{V.32}$$

with the simple solution

$$\begin{aligned}\mathcal{M}[f_q^{\rm NS}](m,\mu_F) &= \mathcal{M}[f_q^{\rm NS}](m,\mu_{F,0})\,\exp\left(\frac{\alpha_s}{2\pi}\,\mathcal{M}[P_{q\leftarrow q}](m)\log\frac{\mu_F^2}{\mu_{F,0}^2}\right) \\ &= \mathcal{M}[f_q^{\rm NS}](m,\mu_{F,0})\,\left(\frac{\mu_F^2}{\mu_{F,0}^2}\right)^{\frac{\alpha_s}{2\pi}\mathcal{M}[P_{q\leftarrow q}](m)} \\ &\equiv \mathcal{M}[f_q^{\rm NS}](m,\mu_{F,0})\,\left(\frac{\mu_F^2}{\mu_{F,0}^2}\right)^{\frac{\alpha_s}{2\pi}\gamma(m)}\,, \end{aligned} \tag{V.33}$$

defining $\gamma(m) = \mathcal{M}[P](m)$.

This solution still includes μ_F and α_s as two free parameters. To simplify this form we can include $\alpha_s(\mu_R^2)$ in the running of the DGLAP equation and identify the renormalization scale μ_R of the strong coupling with the factorization scale

$$\mu_F \equiv \mu_R \equiv \mu\,. \tag{V.34}$$

Physically, this identification is clearly correct for all one-scale problems where we have no freedom to choose either of the two scales. In the DGLAP equation it allows us to replace $\log\mu^2$ by α_s as

$$\frac{d}{d\log\mu^2} = \frac{d\log\alpha_s}{d\log\mu^2}\,\frac{d}{d\log\alpha_s} = \frac{1}{\alpha_s}\,\frac{d\alpha_s}{d\log\mu^2}\,\frac{d}{d\log\alpha_s} = -\alpha_s b_0\,\frac{d}{d\log\alpha_s}\,. \tag{V.35}$$

The additional factor of α_s will cancel the factor α_s on the right hand side of the DGLAP equation Eq.(V.32)

$$\begin{aligned}\frac{d\mathcal{M}[f_q^{\rm NS}](m,\mu)}{d\log\alpha_s} &= -\frac{1}{2\pi b_0}\gamma(m)\,\mathcal{M}[f_q^{\rm NS}](m,\mu) \\ \mathcal{M}[f_q^{\rm NS}](m,\mu) &= \mathcal{M}[f_q^{\rm NS}](m,\mu_0)\,\exp\left(-\frac{1}{2\pi b_0}\,\gamma(m)\log\frac{\alpha_s(\mu^2)}{\alpha_s(\mu_0^2)}\right) \\ &= \mathcal{M}[f_q^{\rm NS}](m,\mu_{F,0})\,\left(\frac{\alpha_s(\mu_0^2)}{\alpha_s(\mu^2)}\right)^{\frac{\gamma(m)}{2\pi b_0}}\,. \end{aligned} \tag{V.36}$$

Among other things, in this derivation we neglect that some splitting functions have singularities and therefore the Mellin transform is not obviously well defined. Our convolution is not really a convolution either, because we cut it off at Q_0^2 etc; but the final structure in Eq.(V.36) really holds.

Instead of the non-singlet parton densities we find the same kind of solution in pure Yang–Mills theory, *i.e.* in QCD without quarks. Looking at the different color factors in QCD this limit can also be derived as the leading terms in N_c. In that case there also exists only one splitting kernel defining an anomalous dimension γ. We find in complete analogy to Eq.(V.36)

$$\mathcal{M}[f_g](m,\mu) = \mathcal{M}[f_g](m,\mu_0)\,\left(\frac{\alpha_s(\mu_0^2)}{\alpha_s(\mu^2)}\right)^{\frac{\gamma(m)}{2\pi b_0}}\,. \tag{V.37}$$

The solutions to the DGLAP equation are not completely determined, because it an integration constant in terms of μ_0. The DGLAP equation does not determine parton densities, it only describes their evolution from one scale μ_F to another, just like a renormalization group equation for the strong coupling.

Remembering how we arrive at the DGLAP equation we notice an analogy to the case of ultraviolet divergences

and the running coupling. We start from universal infrared divergences. We describe them in terms of splitting functions which we regularize using the plus prescription. The DGLAP equation plays the role of a renormalization group equation for example for the running coupling. It links parton densities evaluated at different scales μ_F. In analogy to the scaling logarithms considered in Section II A 3 we should test if we can point to a type of logarithm the DGLAP equation resums by reorganizing our perturbative series of parton splitting.

C. Resumming collinear logarithms

In our discussion of the DGLAP equation and its solution we for instance encounter the splitting probability in the exponent. To make sense of such a structure we remind ourselves that such ratios of α_s values to some power can appear as a result of a resummed series. Such a series would need to include powers of $(\mathcal{M}[\hat{P}])^n$ summed over n which corresponds to a sum over splittings with a varying number of partons in the final state. Parton densities cannot be formulated in terms of a fixed final state because they include effects from any number of collinear partons summed over the number of such partons. For the processes we can evaluate using parton densities fulfilling the DGLAP equation this means that they always have the form

$$\boxed{pp \to \mu^+\mu^- + X} \qquad \text{where } X \text{ includes any number of collinear jets.} \tag{V.38}$$

The same argument leads us towards the logarithms the running parton densities re-sum. To identify them we build a physical model based on collinear splitting, but without using the DGLAP equation. We then solve it to see the resulting structure of the solutions and compare it to the structure of the DGLAP solutions in Eq.(V.37).

We start from the basic equation defining the physical picture of parton splitting in Eq.(II.54). Only taking into account gluons in pure Yang–Mills theory the starting point of our discussion was a factorization, schematically written as

$$\sigma_{n+1} = \int dz \frac{dt}{t} \frac{\alpha_s}{2\pi} \hat{P}_{g\leftarrow g}(z) \sigma_n \; . \tag{V.39}$$

For a moment, we forget about the parton densities and assume that they are part of the hadronic cross section σ_n.

To treat initial state splittings, we need a definition of the virtuality t. If we remember that $t = p_b^2 < 0$ we can follow Eq.(II.61) and introduce a positive transverse momentum variable $\vec{p}_T^{\,2}$ in the usual Sudakov decomposition, such that

$$-t = -\frac{p_T^2}{1-z} = \frac{\vec{p}_T^{\,2}}{1-z} > 0 \qquad \Rightarrow \qquad \frac{dt}{t} = \frac{dp_T^2}{p_T^2} = \frac{d\vec{p}_T^{\,2}}{\vec{p}_T^{\,2}} \; . \tag{V.40}$$

From the definition of p_T in Eq.(II.44) we see that $\vec{p}_T^{\,2}$ is really the transverse three-momentum of of the parton pair after splitting. The factorized form in Eq.(V.39) becomes a convolution in the collinear limit,

$$\sigma_{n+1}(x,\mu_F) = \int_{x_0}^1 \frac{dx_n}{x_n} \, P_{g\leftarrow g}\left(\frac{x}{x_n}\right) \sigma_n(x_n,\mu_0) \int_{\mu_0^2}^{\mu_F^2} \frac{d\vec{p}_{T,n}^{\,2}}{\vec{p}_{T,n}^{\,2}} \frac{\alpha_s(\mu_R^2)}{2\pi} \; . \tag{V.41}$$

Because the splitting kernel is infrared divergent we cut off the convolution integral at x_0. Similarly, the transverse momentum integral is bounded by an infrared cutoff μ_0 and the physical external scale μ_F. This is the range in which an additional collinear radiation is included in σ_{n+1}.

For splitting the two integrals in Eq.(V.41) it is crucial that μ_0 is the only scale the matrix element σ_n depends on. The other integration variable, the transverse momentum, does not feature in σ_n because collinear factorization is defined in the limit $\vec{p}_T^{\,2} \to 0$. All through the argument of this subsection we should keep in mind that we are looking for assumptions which allow us to solve Eq.(V.41) and compare the result to the solution of the DGLAP equation. To develop this physics picture of the DGLAP equation we make three assumptions:

1. If μ_F is the global upper boundary of the transverse momentum integration for collinear splitting, we can apply

the recursion formula in Eq.(V.41) iteratively

$$\sigma_{n+1}(x,\mu_F) \sim \int_{x_0}^1 \frac{dx_n}{x_n}\, P_{g\leftarrow g}\left(\frac{x}{x_n}\right) \cdots \int_{x_0}^1 \frac{dx_1}{x_1}\, P_{g\leftarrow g}\left(\frac{x_2}{x_1}\right)\, \sigma_1(x_1,\mu_0) \times \int_{\mu_0}^{\mu_F} \frac{d\vec{p}_{T,n}^{\,2}}{\vec{p}_{T,n}^{\,2}} \frac{\alpha_s(\mu_R^2)}{2\pi} \cdots \int_{\mu_0} \frac{d\vec{p}_{T,1}^{\,2}}{\vec{p}_{T,1}^{\,2}} \frac{\alpha_s(\mu_R^2)}{2\pi} \,. \tag{V.42}$$

2. We identify the scale of the strong coupling α_s with the transverse momentum scale of the splitting,

$$\mu_R^2 = \vec{p}_T^{\,2} \,. \tag{V.43}$$

This way we can fully integrate $\alpha_s/(2\pi)$ and link the final result to the global boundary μ_F.

3. Finally, we assume strongly ordered splittings in the transverse momentum. If the ordering of the splitting is fixed externally by the chain of momentum fractions x_j, this means

$$\mu_0^2 < \vec{p}_{T,1}^{\,2} < \vec{p}_{T,2}^{\,2} < \cdots < \mu_F^2 \tag{V.44}$$

We will study motivations for this *ad hoc* assumptions in Section VI B.

Under these three assumptions the transverse momentum integrals in Eq.(V.42) become

$$\begin{aligned}
&\int_{\mu_0}^{\mu_F} \frac{d\vec{p}_{T,n}^{\,2}}{\vec{p}_{T,n}^{\,2}} \frac{\alpha_s(\vec{p}_{T,n}^{\,2})}{2\pi} \cdots \int_{\mu_0}^{p_{T,3}} \frac{d\vec{p}_{T,2}^{\,2}}{\vec{p}_{T,2}^{\,2}} \frac{\alpha_s(\vec{p}_{T,2}^{\,2})}{2\pi} \int_{\mu_0}^{p_{T,2}} \frac{d\vec{p}_{T,1}^{\,2}}{\vec{p}_{T,1}^{\,2}} \frac{\alpha_s(\vec{p}_{T,1}^{\,2})}{2\pi} \\
=&\int_{\mu_0}^{\mu_F} \frac{d\vec{p}_{T,n}^{\,2}}{\vec{p}_{T,n}^{\,2}} \frac{1}{2\pi b_0 \log \dfrac{\vec{p}_{T,n}^{\,2}}{\Lambda_{\text{QCD}}^2}} \cdots \int_{\mu_0}^{p_{T,3}} \frac{d\vec{p}_{T,2}^{\,2}}{\vec{p}_{T,2}^{\,2}} \frac{1}{2\pi b_0 \log \dfrac{\vec{p}_{T,2}^{\,2}}{\Lambda_{\text{QCD}}^2}} \int_{\mu_0}^{p_{T,2}} \frac{d\vec{p}_{T,1}^{\,2}}{\vec{p}_{T,1}^{\,2}} \frac{1}{2\pi b_0 \log \dfrac{\vec{p}_{T,1}^{\,2}}{\Lambda_{\text{QCD}}^2}} \\
=&\frac{1}{(2\pi b_0)^n} \int_{\mu_0}^{\mu_F} \frac{d\vec{p}_{T,n}^{\,2}}{\vec{p}_{T,n}^{\,2}} \frac{1}{\log \dfrac{\vec{p}_{T,n}^{\,2}}{\Lambda_{\text{QCD}}^2}} \cdots \int_{\mu_0}^{p_{T,3}} \frac{d\vec{p}_{T,2}^{\,2}}{\vec{p}_{T,2}^{\,2}} \frac{1}{\log \dfrac{\vec{p}_{T,2}^{\,2}}{\Lambda_{\text{QCD}}^2}} \int_{\mu_0}^{p_{T,2}} \frac{d\vec{p}_{T,1}^{\,2}}{\vec{p}_{T,1}^{\,2}} \frac{1}{\log \dfrac{\vec{p}_{T,1}^{\,2}}{\Lambda_{\text{QCD}}^2}} \,.
\end{aligned} \tag{V.45}$$

We can solve the individual integrals by switching variables, for example in the last integral

$$\begin{aligned}
\int_{\mu_0}^{p_{T,2}} \frac{d\vec{p}_{T,1}^{\,2}}{\vec{p}_{T,1}^{\,2}} \frac{1}{\log \dfrac{\vec{p}_{T,1}^{\,2}}{\Lambda_{\text{QCD}}^2}} &= \int_{\log\log \mu_0^2/\Lambda^2}^{\log\log p_{T,2}^2/\Lambda^2} d\log\log \frac{\vec{p}_{T,1}^{\,2}}{\Lambda_{\text{QCD}}^2} \qquad \text{with} \qquad \frac{d(ax)}{(ax)\log x} = d\log\log x \\
&= \log \frac{\log \vec{p}_{T,2}^{\,2}/\Lambda_{\text{QCD}}^2}{\log \mu_0^2/\Lambda_{\text{QCD}}^2} \,.
\end{aligned} \tag{V.46}$$

This gives us for the chain of transverse momentum integrals, shifted to get rid of the lower boundaries,

$$\begin{aligned}
&\int^{p_{T,n}\equiv\mu_F} d\log \frac{\log \vec{p}_{T,n}^{\,2}/\Lambda_{\text{QCD}}^2}{\log \mu_0^2/\Lambda_{\text{QCD}}^2} \cdots \int^{p_{T,2}\equiv p_{T,3}} d\log \frac{\log \vec{p}_{T,2}^{\,2}/\Lambda_{\text{QCD}}^2}{\log \mu_0^2/\Lambda_{\text{QCD}}^2} \int^{p_{T,1}\equiv p_{T,2}} d\log \frac{\log \vec{p}_{T,1}^{\,2}/\Lambda_{\text{QCD}}^2}{\log \mu_0^2/\Lambda_{\text{QCD}}^2} \\
&= \int^{p_{T,n}\equiv\mu_F} d\log \frac{\log \vec{p}_{T,n}^{\,2}/\Lambda_{\text{QCD}}^2}{\log \mu_0^2/\Lambda_{\text{QCD}}^2} \cdots \int^{p_{T,2}\equiv p_{T,3}} d\log \frac{\log \vec{p}_{T,2}^{\,2}/\Lambda_{\text{QCD}}^2}{\log \mu_0^2/\Lambda_{\text{QCD}}^2} \left(\log \frac{\log \vec{p}_{T,2}^{\,2}/\Lambda_{\text{QCD}}^2}{\log \mu_0^2/\Lambda_{\text{QCD}}^2}\right) \\
&= \int^{p_{T,n}\equiv\mu_F} d\log \frac{\log \vec{p}_{T,n}^{\,2}/\Lambda_{\text{QCD}}^2}{\log \mu_0^2/\Lambda_{\text{QCD}}^2} \cdots \frac{1}{2}\left(\log \frac{\log \vec{p}_{T,3}^{\,2}/\Lambda_{\text{QCD}}^2}{\log \mu_0^2/\Lambda_{\text{QCD}}^2}\right)^2 \\
&= \int^{p_{T,n}\equiv\mu_F} d\log \frac{\log \vec{p}_{T,n}^{\,2}/\Lambda_{\text{QCD}}^2}{\log \mu_0^2/\Lambda_{\text{QCD}}^2} \left(\frac{1}{2}\cdots\frac{1}{n-1}\right)\left(\log \frac{\log \vec{p}_{T,n}^{\,2}/\Lambda_{\text{QCD}}^2}{\log \mu_0^2/\Lambda_{\text{QCD}}^2}\right)^{n-1} \\
&= \frac{1}{n!}\left(\log \frac{\log \mu_F^2/\Lambda_{\text{QCD}}^2}{\log \mu_0^2/\Lambda_{\text{QCD}}^2}\right)^n = \frac{1}{n!}\left(\log \frac{\alpha_s(\mu_0^2)}{\alpha_s(\mu_F^2)}\right)^n \,.
\end{aligned} \tag{V.47}$$

This is the final result for the chain of transverse momentum integrals in Eq.(V.42). After integrating over the transverse momenta, the strong coupling is evaluated at $\mu_R \equiv \mu_F$. This leaves us with the convolution integrals from Eq.(V.41),

$$\sigma_{n+1}(x,\mu) \sim \frac{1}{n!}\left(\frac{1}{2\pi b_0}\log\frac{\alpha_s(\mu_0^2)}{\alpha_s(\mu^2)}\right)^n \int_{x_0}^1 \frac{dx_n}{x_n}\, P_{g\leftarrow g}\left(\frac{x}{x_n}\right) \cdots \int_{x_0}^1 \frac{dx_1}{x_1}\, P_{g\leftarrow g}\left(\frac{x_2}{x_1}\right)\, \sigma_1(x_1,\mu_0)\,. \tag{V.48}$$

As before, we Mellin-transform the equation into moment space

$$\begin{aligned}
\mathcal{M}[\sigma_{n+1}](m,\mu) \sim& \frac{1}{n!}\left(\frac{1}{2\pi b_0}\log\frac{\alpha_s(\mu_0^2)}{\alpha_s(\mu^2)}\right)^n \mathcal{M}\left[\int_{x_0}^1 \frac{dx_n}{x_n}\, P_{g\leftarrow g}\left(\frac{x}{x_n}\right) \cdots \int_{x_0}^1 \frac{dx_1}{x_1}\, P_{g\leftarrow g}\left(\frac{x_2}{x_1}\right)\, \sigma_1(x_1,\mu_0)\right](m) \\
=& \frac{1}{n!}\left(\frac{1}{2\pi b_0}\log\frac{\alpha_s(\mu_0^2)}{\alpha_s(\mu^2)}\right)^n \gamma(m)^n\, \mathcal{M}[\sigma_1](m,\mu_0) \qquad \text{using } \gamma(m) \equiv \mathcal{M}[P](m) \\
=& \frac{1}{n!}\left(\frac{1}{2\pi b_0}\log\frac{\alpha_s(\mu_0^2)}{\alpha_s(\mu^2)}\,\gamma(m)\right)^n \mathcal{M}[\sigma_1](m,\mu_0)\,.
\end{aligned} \tag{V.49}$$

Finally, we sum the production cross sections for up to n collinear jets,

$$\begin{aligned}
\sum_{n=0}^\infty \mathcal{M}[\sigma_{n+1}](m,\mu) =& \mathcal{M}[\sigma_1](m,\mu_0) \sum_n \frac{1}{n!}\left(\frac{1}{2\pi b_0}\log\frac{\alpha_s(\mu_0^2)}{\alpha_s(\mu^2)}\,\gamma(m)\right)^n \\
=& \mathcal{M}[\sigma_1](m,\mu_0)\, \exp\left(\frac{\gamma(m)}{2\pi b_0}\,\log\frac{\alpha_s(\mu_0^2)}{\alpha_s(\mu^2)}\right) \\
=& \mathcal{M}[\sigma_1](m,\mu_0)\, \left(\frac{\alpha_s(\mu_0^2)}{\alpha_s(\mu^2)}\right)^{\frac{\gamma(m)}{2\pi b_0}}\,.
\end{aligned} \tag{V.50}$$

This is the same structure as the DGLAP equation's solution in Eq.(V.37). It means that we can understand the physics of the DGLAP equation using our model calculation of a successive gluon emission, including the generically variable number of collinear jets in the form of $pp \to \mu^+\mu^- + X$, as shown in Eq.(V.38). On the left hand side of Eq.(V.50) we have the sum over any number of additional collinear partons; on the right hand side we see fixed order Drell–Yan production without any additional partons, but with an exponentiated correction factor. Comparing this to the running parton densities we can draw the analogy that any process computed with a scale dependent parton density where the scale dependence is governed by the DGLAP equation includes any number of collinear partons.

We can also identify the logarithms which are resummed by scale dependent parton densities. Going back to Eq.(II.41) reminds us that we start from the divergent collinear logarithms $\log p_T^{\max}/p_T^{\min}$ arising from the collinear phase space integration. In our model for successive splitting we replace the upper boundary by μ_F. The collinear logarithm of successive initial–state parton splitting diverges for $\mu_0 \to 0$, but it gets absorbed into the parton densities and determines the structure of the DGLAP equation and its solutions. The upper boundary μ_F tells us to what extent we assume incoming quarks and gluons to be a coupled system of splitting partons and what the maximum

	renormalization scale μ_R	factorization scale μ_F
source	ultraviolet divergence	collinear (infrared) divergence
poles cancelled	counter terms (renormalization)	parton densities (mass factorization)
summation	resum self energy bubbles	resum parton splittings
parameter	running coupling $\alpha_s(\mu_R^2)$	running parton density $f_j(x,\mu_F)$
evolution	RGE for α_s	DGLAP equation
large scales	decrease of σ_{tot}	increase of σ_{tot} for gluons/sea quarks
theory background	renormalizability proven for gauge theories	factorization proven all orders for DIS proven order-by-order DY...

TABLE III: Comparison of renormalization and factorization scales appearing in LHC cross sections.

momentum scale of these splittings is. Transverse momenta $p_T > \mu_F$ generated by hard parton splitting are not covered by the DGLAP equation and hence not a feature of the incoming partons anymore. They belong to the hard process and have to be consistently simulated. While this scale can be chosen freely we have to make sure that it does not become too large, because at some point the collinear approximation $C \simeq$ constant in Eq.(II.41) ceases to hold.

VI. JET RADIATION

Jet vetos play a crucial role at the LHC, for instance when looking for Higgs production in weak boson fusion. If we add a virtual gluon exchange between the two quark lines in the leading order diagram, we find a vanishing color factor

$$\mathrm{tr} T^a \, \mathrm{tr} T^b \, \delta^{ab} = 0 \, . \tag{VI.1}$$

We also know that virtual gluon exchange and real gluon emission are very closely related. Radiating a gluon off any of the quarks in the weak boson fusion process will lead to a double infrared divergence, one because the gluon can be radiated at small angles and one because the gluon can be radiated with vanishing energy. The divergence at small angles is removed by redefining the quark densities in the proton. The soft, non–collinear divergence has to cancel between real gluon emission and virtual gluon exchange. However, if virtual gluon exchange does not appear, non–collinear soft gluon radiation cannot appear either. This means that additional QCD jet activity as part of the weak boson fusion process is limited to collinear radiation, *i.e.* radiation along the beam line or at least in the same direction as the far forward tagging jets. Gluon radiation into the central detector is suppressed by the color structure of the weak boson fusion process.

While it is not immediately clear how to quantify such a statement it is a very useful feature, for example looking at the top pair backgrounds. The $WWb\bar{b}$ final state as a background to $qqH, H \to WW$ searches includes two bottom jets which can mimic the signal's tagging jets. At the end, it turns out that it is much more likely that we will produce another jet through QCD jet radiation, *i.e.* $pp \to t\bar{t}$+jet, so only one of the two bottom jets from the top decays needs to be forward. One way to isolate the Higgs signal is to look at additional central jets. This strategy is referred to as central jet veto. Note that it has nothing to do with rapidity gaps at HERA or pomeron exchange, it is a QCD feature completely accounted for by standard perturbative QCD.

A. Jet ratios

If we assign a probability pattern to the radiation of jets from the core process we can compute the survival probability P_{pass} of such a jet veto. As an example we assume NNLO or two-loop precision for the Higgs production rate

$$\sigma = \sigma_0 + \alpha_s \sigma_1 + \alpha_s^2 \sigma_2 \, , \tag{VI.2}$$

where we omit the over–all factor α_s^2 in σ_0. Consequently, we define the cross section passing the jet veto

$$\sigma^{(\text{pass})} = P_{\text{pass}} \, \sigma = \sum_j \alpha_s^j \sigma_j^{(\text{pass})} \, . \tag{VI.3}$$

Because the leading order prediction only includes a Higgs in the final state we know that $\sigma_0^{(\text{pass})} = \sigma_0$. Solving this definition for the veto survival probability we can compute

$$P_{\text{pass}} = \frac{\sigma^{(\text{pass})}}{\sigma} = \frac{\sigma_0 + \alpha_s \sigma_1^{(\text{pass})} + \alpha_s^2 \sigma_2^{(\text{pass})}}{\sigma_0 + \alpha_s \sigma_1 + \alpha_s^2 \sigma_2} \, . \tag{VI.4}$$

One ansatz for the distribution of any number of radiated jets is motivated by soft photon emission off a hard electron. From quantum field theory we know that it gives us a Poisson distribution in the numbers of jet in the soft limit. In that case, the probability of observing exactly n jets given an expected $\bar{n}$ jets is

$$f(n;\bar{n}) = \frac{\bar{n}^n e^{-\bar{n}}}{n!} \qquad \Rightarrow \qquad \boxed{P_{\text{pass}} \equiv f(0;\bar{n}) = e^{-\bar{n}}} \, . \tag{VI.5}$$

Note that this probability links rates for exactly n jets, no at least n jets, *i.e.* it described the exclusive number of jets. The Poisson distribution defines the so-called exponentiation model when we fix the expectation value in terms of the inclusive cross sections producing at least zero or at least one jet,

$$\bar{n} = \frac{\sigma_1(p_T^{\min})}{\sigma_0} \qquad \Rightarrow \qquad P_{\text{pass}} = e^{-\sigma_1/\sigma_0} \; . \tag{VI.6}$$

Using this expectation value $\bar{n}$ in Eq.(VI.5) returns a veto survival probability of around 88% for the weak boson fusion signal and as 24% for the $t\bar{t}$ background.

An alternative model starts from a constant probability of radiating a jet, which in terms of the inclusive cross sections σ_n, *i.e.* the production rate for the radiation of at least n jets, reads

$$\frac{\sigma_{n+1}(p_T^{\min})}{\sigma_n(p_T^{\min})} = R^{(\text{incl})}_{(n+1)/n}(p_T^{\min}) = \text{const} \; . \tag{VI.7}$$

The expectation value for the number of jets, weighted with the respective cross sections, is then

$$\begin{aligned} \bar{n} &= \frac{1}{\sigma_0} \sum_{j=1} j(\sigma_j - \sigma_{j+1}) = \frac{1}{\sigma_0} \left(\sum_{j=1} j\sigma_j - \sum_{j=2} (j-1)\sigma_j \right) = \frac{1}{\sigma_0} \left[\sigma_1 + \sum_{j=2} \sigma_j \right] \\ &= \frac{\sigma_1}{\sigma_0} \sum_{j=0} (R^{(\text{incl})}_{(n+1)/n})^j = \frac{R^{(\text{incl})}_{(n+1)/n}}{1 - R^{(\text{incl})}_{(n+1)/n}} \; , \end{aligned} \tag{VI.8}$$

Radiating jets with such a constant probability has been observed at many experiments, including most recently the LHC, and is in the context of W+jets referred to as staircase scaling. Both, Poisson and staircase scaling can be derived from generating functionals. The former appears for large splitting probabilities and large scale ratios, while the latter is generated for democratic scales and smaller splitting probabilities. We can summarize the main properties of the n-jet rates in terms of the upper incomplete gamma function $\Gamma(n, \bar{n})$:

	staircase scaling	Poisson scaling
$\sigma_n^{(\text{excl})}$	$\sigma_0^{(\text{excl})} \; e^{-bn}$	$\sigma_0 \; \dfrac{e^{-\bar{n}} \bar{n}^n}{n!}$
$R_{(n+1)/n} = \dfrac{\sigma_{n+1}^{(\text{excl})}}{\sigma_n^{(\text{excl})}}$	e^{-b}	$\dfrac{\bar{n}}{n+1}$
$R^{(\text{incl})}_{(n+1)/n} = \dfrac{\sigma_{n+1}}{\sigma_n}$	e^{-b}	$\left(\dfrac{(n+1)\, e^{-\bar{n}}\, \bar{n}^{-(n+1)}}{\Gamma(n+1) - n\Gamma(n,\bar{n})} + 1 \right)^{-1}$
$\langle n \rangle$	$\dfrac{1}{2} \dfrac{1}{\cosh b - 1}$	$\bar{n}$
P_{pass}	$1 - e^{-b}$	$e^{-\bar{n}}$

B. Ordered emission

An interesting theory aspect is the postulated ordering of the splittings in Eq.(V.44). Our argument follows from the leading collinear approximation introduced in Section II B 1, so the strong p_T-ordering can in practice mean angular ordering or rapidity ordering, just applying a linear transformation.

For example the emission of a gluon off a hard quark line is governed by distinctive soft and collinear phase space regimes. When we exponentiate this gluon radiation we need to require multiple emission to be ordered by some parameter. In that case we can neglect interference terms when squaring the multiple-emission matrix element. These interference diagrams are called non–planar diagrams. The question is if we can justify to neglect them from first principles field theory and QCD. There are three reasons to do this.

First, an arguments for a strongly ordered gluon emission comes from the divergence structure of soft and collinear gluon emission. Two successively radiated gluons look like

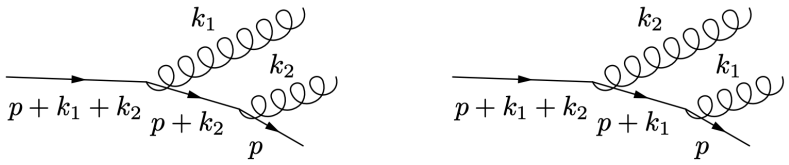

Single gluon radiation with momentum k off a hard quark with momentum p is described by the combination of a propatator and the polarization sum $(\epsilon p)(pk)$. For successive radiation the two Feynman diagrams give us the combined kinetic terms

$$\begin{aligned}
&\frac{(\epsilon_1 p)}{(p+k_1+k_2)^2-m^2}\frac{(\epsilon_2 p)}{(p+k_2)^2-m^2}+\frac{(\epsilon_2 p)}{(p+k_1+k_2)^2-m^2}\frac{(\epsilon_1 p)}{(p+k_1)^2-m^2} \\
&\quad=\frac{(\epsilon_1 p)}{2(pk_1)+2(pk_2)+(k_1+k_2)^2}\frac{(\epsilon_2 p)}{2(pk_2)}+\frac{(\epsilon_2 p)}{2(pk_1)+2(pk_2)+(k_1+k_2)^2}\frac{(\epsilon_1 p)}{2(pk_1)} \qquad k_1^2=0=k_2^2 \\
&\quad\simeq\frac{(\epsilon_1 p)}{2\max_j(pk_j)}\frac{(\epsilon_2 p)}{2(pk_2)}+\frac{(\epsilon_2 p)}{2\max_j(pk_j)}\frac{(\epsilon_1 p)}{2(pk_1)} \qquad (pk_j)\gg(k_1k_2) \text{ strongly ordered} \\
&\quad\simeq\begin{cases}\dfrac{(\epsilon_1 p)(\epsilon_2 p)}{2\max_j(pk_j)}\,\dfrac{1}{2(pk_2)} & (pk_2)\ll(pk_1)\ \ k_2 \text{ softer} \\ \dfrac{(\epsilon_1 p)(\epsilon_2 p)}{2\max_j(pk_j)}\,\dfrac{1}{2(pk_1)} & (pk_1)\ll(pk_2)\ \ k_1 \text{ softer}\,.\end{cases}
\end{aligned} \tag{VI.9}$$

Once one of the gluons is significantly softer, the Feynman diagram with the later soft emission dominates. After squaring the amplitude there will be no phase space regime where interference terms between the two diagrams are numerically relevant. The coherent sum over gluon radiation channels reduces to a incoherent sum, ordered by the softness of the gluon. Note that this argument is based on an ordering of the (pk_j). A small value of (pk_j) can as well point to a collinear divergence; every step of our argument still applies.

Second, we can derive ordered soft-gluon emission from the phase space integration in the eikonal approximation. There, gluon radiation is governed by the so-called radiation dipoles. For successive gluon radiation off a quark leg the question we are interested in is where the soft gluon k is radiated, for example in relation to the hard quark p_1 and the harder gluon p_2. The kinematics of this process is the same as the simpler soft gluon radiation off a quark–antiquark pair produced in an electroweak process. A well–defined process with all momenta defined as outgoing is

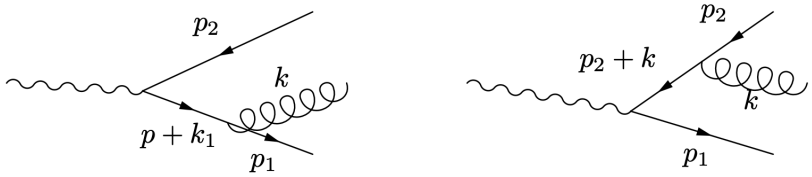

We start by symmetrizing the leading soft radiation dipole for zero masses with respect to the two hard momenta in a particular way,

$$\begin{aligned}
\frac{(p_1p_2)}{(p_1k)(p_2k)}&=\frac{1}{k_0^2}\frac{1-\cos\theta_{12}}{(1-\cos\theta_{1k})(1-\cos\theta_{2k})} \qquad \text{in terms of opening angles } \theta \\
&=\frac{1}{2k_0^2}\left(\frac{1-\cos\theta_{12}}{(1-\cos\theta_{1k})(1-\cos\theta_{2k})}+\frac{1}{1-\cos\theta_{1k}}-\frac{1}{1-\cos\theta_{2k}}\right)+(1\leftrightarrow 2) \\
&\equiv\frac{W_{12}^{[1]}+W_{12}^{[2]}}{k_0^2}\,.
\end{aligned} \tag{VI.10}$$

The last term is an implicit definition of the two terms $W_{12}^{[1]}$. The pre-factor $1/k_0^2$ is given by the leading soft divergence. In each of the two terms we need to integrate over the gluon's phase space, including the azimuthal angle ϕ_{1k}.

To compute the actual integral we express the three parton vectors in polar coordinates where the initial parton p_1 propagates into the x direction, the interference partner p_2 in the $(x-y)$ plane, and the soft gluon in the full three-dimensional space described by polar coordinates,

$$\begin{aligned}
\hat{p}_1 &= (1,0,0) && \text{hard parton} \\
\hat{p}_2 &= (\cos\theta_{12}, \sin\theta_{12}, 0) && \text{interference partner} \\
\hat{k} &= (\cos\theta_{1k}, \sin\theta_{1k}\cos\phi_{1k}, \sin\theta_{1k}\sin\phi_{1k}) && \text{soft gluon} \\
\Rightarrow \qquad \cos\theta_{2k} \equiv (\hat{p}_2\hat{k}) &= \cos\theta_{12}\cos\theta_{1k} + \sin\theta_{12}\sin\theta_{1k}\cos\phi_{1k}\,. && \text{(VI.11)}
\end{aligned}$$

From the scalar product between these four-vectors we see that of the terms appearing in Eq.(VI.10) only the opening angle θ_{2k} includes ϕ_{1k}, which for the azimuthal angle integration means

$$\begin{aligned}
\int_0^{2\pi} d\phi_{1k}\, W_{12}^{[1]} &= \frac{1}{2}\int_0^{2\pi} d\phi_{1k}\, \left(\frac{1-\cos\theta_{12}}{(1-\cos\theta_{1k})(1-\cos\theta_{2k})} + \frac{1}{1-\cos\theta_{1k}} - \frac{1}{1-\cos\theta_{2k}}\right)\,. \\
&= \frac{1}{2}\,\frac{1}{1-\cos\theta_{1k}}\int_0^{2\pi} d\phi_{1k}\, \left(\frac{1-\cos\theta_{12}}{1-\cos\theta_{2k}} + 1 - \frac{1-\cos\theta_{1k}}{1-\cos\theta_{2k}}\right) \\
&= \frac{1}{2}\,\frac{1}{1-\cos\theta_{1k}}\left(2\pi + (\cos\theta_{1k}-\cos\theta_{12})\int_0^{2\pi} d\phi_{1k}\,\frac{1}{1-\cos\theta_{2k}}\right)\,. \qquad \text{(VI.12)}
\end{aligned}$$

We can solve the azimuthal angle integral in this expression for $W_{12}^{[i]}$,

$$\begin{aligned}
\int_0^{2\pi} d\phi_{1k}\frac{1}{1-\cos\theta_{2k}} &= \int_0^{2\pi} d\phi_{1k}\frac{1}{1-\cos\theta_{12}\cos\theta_{1k}-\sin\theta_{12}\sin\theta_{1k}\cos\phi_{1k}} \\
&\equiv \int_0^{2\pi} d\phi_{1k}\frac{1}{a-b\cos\phi_{1k}} \\
&= \oint_{\text{unit circle}} dz\,\frac{1}{iz}\frac{1}{a-b\dfrac{z+1/z}{2}} && \text{with} \quad z = e^{i\phi_{1k}},\ \cos\phi_{1k} = \frac{z+1/z}{2} \\
&= \frac{2}{i}\oint dz\,\frac{1}{2az-b-bz^2} \\
&= \frac{2i}{b}\oint \frac{dz}{(z-z_-)(z-z_+)} && \text{with} \quad z_\pm = \frac{a}{b} \pm \sqrt{\frac{a^2}{b^2}-1}\,. \qquad \text{(VI.13)}
\end{aligned}$$

This integral is related to the sum of all residues of poles inside the closed integration contour. Of the two poles z_- is the one which typically lies within the unit circle, so we find

$$\int_0^{2\pi} d\phi_{1k}\frac{1}{1-\cos\theta_{2k}} = \frac{2i}{b}\,2\pi i\frac{1}{z_- - z_+} = \frac{2\pi}{\sqrt{a^2-b^2}} \qquad \text{(VI.14)}$$

We can use the above definitions of a and b to compute

$$\begin{aligned}
a^2-b^2 &= (1-\cos\theta_{12}\cos\theta_{1k})^2 - \sin\theta_{12}^2\sin\theta_{1k}^2 \\
&= 1 - 2\cos\theta_{12}\cos\theta_{1k} + \cos^2\theta_{12}\cos^2\theta_{1k} - (1-\cos^2\theta_{1k}-\cos^2\theta_{12}+\cos^2\theta_{12}\cos^2\theta_{1k}) \\
&= (\cos\theta_{1k}+\cos\theta_{12})^2\,, \qquad \text{(VI.15)}
\end{aligned}$$

and find for the azimuthal angle integral

$$\int_0^{2\pi} d\phi_{1k}\frac{1}{1-\cos\theta_{2k}} = \frac{2\pi}{\sqrt{(\cos\theta_{1k}-\cos\theta_{12})^2}} = \frac{2\pi}{|\cos\theta_{1k}-\cos\theta_{12}|}\,. \qquad \text{(VI.16)}$$

The entire integral in Eq.(VI.12) then becomes

$$\begin{aligned}\int_0^{2\pi} d\phi_{1k}\, W_{12}^{[1]} &= \frac{1}{2}\,\frac{1}{1-\cos\theta_{1k}}\left(2\pi + (\cos\theta_{1k}-\cos\theta_{12})\;\frac{2\pi}{|\cos\theta_{1k}-\cos\theta_{12}|}\right)\\ &= \frac{\pi}{1-\cos\theta_{1k}}\,(1+\text{sign}(\cos\theta_{1k}-\cos\theta_{12})\\ &= \begin{cases}\dfrac{2\pi}{1-\cos\theta_{1k}} & \text{if} \quad \theta_{1k}<\theta_{12}\\ 0 & \text{else}\,.\end{cases}\end{aligned} \tag{VI.17}$$

The soft gluon is only radiated at angles between zero and the opening angle of the initial parton p_1 and its hard interference partner or spectator p_2. The same integral over $W_{12}^{[2]}$ gives the same result, with switched roles of p_1 and p_2. The soft gluon is always radiated within a cone centered around one of the hard partons and with a radius given by the distance between the two hard partons. Again, the coherent sum of diagrams reduces to an incoherent sum. This derivation angular ordering is exact in the soft limit.

The third argument for ordered emission comes from color factors. Crossed successive splittings or interference terms between different orderings are color suppressed. For example in the squared diagram for three jet production in e^+e^- collisions the additional gluon contributes a color factor

$$\text{tr}(T^aT^a) = \frac{N_c^2-1}{2} = N_cC_F \tag{VI.18}$$

When we consider the successive radiation of two gluons the ordering matters. As long as the gluon legs do not cross each other we find the color factor

$$\begin{aligned}\text{tr}(T^aT^aT^bT^b) &= (T^aT^a)_{il}(T^bT^b)_{li}\\ &= \frac{1}{4}\left(\delta_{il}\delta_{jj}-\frac{\delta_{ij}\delta_{jl}}{N_c}\right)\left(\delta_{il}\delta_{jj}-\frac{\delta_{ij}\delta_{jl}}{N_c}\right) \qquad \text{using} \quad T^a_{ij}T^a_{kl} = \frac{1}{2}\left(\delta_{il}\delta_{jk}-\frac{\delta_{ij}\delta_{kl}}{N_c}\right)\\ &= \frac{1}{4}\left(\delta_{il}N_c-\frac{\delta_{il}}{N_c}\right)\left(\delta_{il}N_c-\frac{\delta_{il}}{N_c}\right)\\ &= N_c\left(\frac{N_c^2-1}{2N_c}\right)^2 = N_cC_F^2 = \frac{16}{3}\end{aligned} \tag{VI.19}$$

Similarly, we can compute the color factor when the two gluon lines cross. We find

$$\text{tr}(T^aT^bT^aT^b) = -\frac{N_c^2-1}{4N_c} = -\frac{C_F}{2} = -\frac{2}{3}\,. \tag{VI.20}$$

Numerically, this color factor is suppressed compared to 16/3. This kind of behavior is usually quoted in powers of N_c where we assume N_c to be large. In those terms non–planar diagrams are suppressed by a factor $1/N_c^2$ compared to the planar diagrams.

We can also try the argument for a purely gluonic theory. The color factor for single gluon emission after squaring is

$$f^{abc}f^{abc} = N_c\delta^{aa} = N_c(N_c^2-1) \sim N_c^3\,, \tag{VI.21}$$

using the large-N_c limit in the last step. For planar double gluon emission with the exchanged gluon indices b and f we find

$$f^{abd}f^{abe}f^{dfg}f^{efg} = N_c\delta^{de}\;N_c\delta^{de} = N_c^3\,. \tag{VI.22}$$

Splitting one radiated gluon into two gives

$$f^{abc}\;f^{cef}f^{def}\;f^{abd} = N_c\delta^{cd}\;N_c\delta^{cd} = N_c^3\,. \tag{VI.23}$$

This means that planar emission and successive splittings cannot be separated based on the color factor. We can use

the color factor argument only for abelian splittings to justify ordered gluon emission.

---

[1] W. Tung, *Group Theory in Physics* (World Scientific, 1985).
[2] L. Faddeev and V. Popov, Phys.Lett. **B25**, 29 (1967).
[3] S. Bethke, Progress in Particle and Nuclear Physics **58**, 351 (2007), arXiv:hep-ex/0606035.
[4] J. C. Collins, (1984).
[5] R. K. Ellis, W. J. Stirling, and B. R. Webber, Camb. Monogr. Part. Phys. Nucl. Phys. Cosmol. **8**, 1 (1996).
[6] R. Alkofer and L. von Smekal, Phys. Rept. **353**, 281 (2001), hep-ph/0007355.
[7] M. Buballa, Phys.Rept. **407**, 205 (2005), hep-ph/0402234.
[8] J. Braun, (2011), 1108.4449.
[9] A. K. Cyrol, M. Mitter, J. M. Pawlowski, and N. Strodthoff, (2017), 1706.06326.
[10] S. Klevansky, Rev.Mod.Phys. **64**, 649 (1992).
[11] F. J. Wegner and A. Houghton, Phys. Rev. **A8**, 401 (1973).
[12] K. Symanzik, Commun. Math. Phys. **18**, 227 (1970).
[13] C. G. Callan, Phys. Rev. D **2**, 1541 (1970).
[14] K. G. Wilson, Phys.Rev. **B4**, 3184 (1971).
[15] K. G. Wilson, Phys.Rev. **B4**, 3174 (1971).
[16] L. P. Kadanoff, Physics **2**, 263 (1966).
[17] E. C. G. Stueckelberg and A. Petermann, Helv. Phys. Acta **26**, 499 (1953).
[18] M. Gell-Mann and F. E. Low, Phys. Rev. **95**, 1300 (1954).
[19] Particle Data Group, C. Patrignani *et al.*, Chin. Phys. **C40**, 100001 (2016).
[20] J. R. Pelaez, Phys. Rept. **658**, 1 (2016), 1510.00653.
[21] M. Creutz, *Quarks, gluons and lattices* (Cambridge University Press, 1983).
[22] I. Montvay and G. Münster, *Quantum fields on a lattice* (Cambridge University Press, Cambridge, 1994), Cambridge, UK: Univ. Pr. (1994) 491 p. (Cambridge monographs on mathematical physics).
[23] H. J. Rothe, *Lattice gauge theories: An Introduction* (World Sci. Lect. Notes Phys., 2005).
[24] C. Gattringer and C. B. Lang, *Quantum chromodynamics on the lattice* (Lect. Notes Phys., 2010).